Fall 2014

Methodology for Trace and Ultratrace Analysis of Primary Amines

Sean Christopher Pawlowski

METHODOLOGY FOR TRACE AND ULTRATRACE ANALYSIS OF PRIMARY AMINES

A Dissertation

Submitted to the Bayer School of Natural and Environmental Sciences

Duquesne University

In partial fulfillment of the requirements for

the degree of Doctor of Philosophy

By

Sean C. Pawlowski

December 2014

METHODOLOGY FOR TRACE AND ULTRATRACE

ANALYSIS OF PRIMARY AMINES

By

Sean C. Pawlowski

Approved November 13, 2014

_____ Partha Basu Professor of Chemistry (Committee Chair)	_____ Bruce Beaver Professor of Chemistry (Committee Member)
_____ Michael Cascio Associate Professor of Chemistry (Committee Member)	_____ David Gallaher, Jr. Associate Professor of Chemistry (Committee Member)
_____ Phillip Reeder Dean, Bayer School of Natural and Environmental Sciences	_____ Ralph Wheeler Chair, Department of Chemistry and Biochemistry Professor of Chemistry

ABSTRACT

METHODOLOGY FOR TRACE AND ULTRATRACE

ANALYSIS OF PRIMARY AMINES

By

Sean C. Pawlowski

December 2014

Dissertation supervised by the late Mitchell E. Johnson and subsequently by Partha Basu

In the study of lipids, or "lipidomics," methods for the separation and identification of specific trace compounds are highly sought. Microdroplet techniques have allowed for the ability to handle and detect these trace amounts. The use of low volumes allows for a decrease of the effective mean free path allowing chemical reactions to be carried out efficiently at lower concentrations by performing the reactions in microdroplets as opposed to bulk containers. Microdroplets created on microfluidic devices as segmented flow plugs have the advantage of efficient mixing and minimal dilution or dispersion relative to other nanoliter scale capillary reaction methods. The most sensitive detection techniques are needed for ultratrace analyses. Laser induced fluorescence (LIF) is the most attractive choice for ultratrace analysis. We show two methods for the derivatization and detection of primary amines with 3-(2-

furoyl)quinoline-2-carboxaldehyde (FQCA) and with naphthalene-2,3-dicarboxaldehyde (NDA). The method has shown to be successful down to the sub-picomolar level in bulk solutions using an HPLC coupled with a fluorescence detector. The method has been transferred to microfluidic chips to explore the reaction and detection limits of the derivatized amines. Laser induced fluorescence (LIF) by a solid state blue violet laser was used as the detection method for the microfluidic platform. Successful usage of this methodology would allow for ultratrace detection of bioactive amines from small samples.

.

DEDICATION

This is dedicated to MEJ, the guiding light behind all of this.

ACKNOWLEDGEMENT

"The best time to do science is when everything works. The second best time to do science is when nothing works." These were the words that I was first told upon starting at Duquesne by my late advisor, Dr. Mitch Johnson. I never thought I would take it as seriously and to heart as much as I have. I have to thank Mitch for taking me in and mentoring me. Allowing me to bounce seemingly crazy ideas off of him during our Monday morning meetings and then go try them, as long as I finished what he wanted me to do as well. Mitch would answer any question you needed him to; as long as you listened the first time he answered it. He guided our work from its conception and still guides it through what he had taught his students. Thank you Mitch for all that you did for us, thank you for making us not only better scientists but better people as well.

I want to thank the undergraduates who tested so many of the initial experiments that made up this work. From Dan Watsula and Jeff Chmiel on the initial FQCA works to the Integrated Lab students testing the microfluidic chip fabrication and solid phase extraction. You all were excellent to work with and made my life a little better.

A special thank you though to two undergraduates that worked with me. Firstly, to Angela Jovanovich, thank you for the hard work you put in working on the microfluidic chip mixing with me. I know I wasn't always fun to work with but it is because I saw the promise in you. I truly wish you the best in your career and life.

Secondly, Andrew Davic, who couldn't keep himself away after finishing his URP, thank you for the hard work, tireless hours, and excellent conversations over the many years. I

am proud to see the scientist you've grown into and can't wait to see you finish your Ph.D. working on the continuation of some of these efforts.

Thank you to Dr. Erin Divito, for the many years of assistance and entertainment in the lab. Your sense of humor and your intelligence always made lab work and group meeting a whole new level of enjoyment. Thank you also for the analytical work you performed to assist this project, from the Prep LC to the TQMS, your hard work was and is appreciated.

Thank you to Dr. Kristin Kroniser for your guidance, humor, and knowledge through the years. You were an excellent example for all of us (especially when it came to fire extinguisher training).

Thank you to Dr. John Williams for your guidance, snark, and coffee breaks. Your grounded attitude helped through even the most stressful days of my first year.

Thank you to the rest of the Johnson Group for your constant source of stories and entertainment that I would hold definitely dear for the rest of my time.

Thank you to Dr. Dave Gallaher who stepped up the summer Mitch became ill and took his sabbatical time to help the lab and make sure we kept on task. Thank you also for being my outside reader and providing a sounding board for me during my time at Duquesne.

Thank you to my committee members, Drs. Bruce Beaver, Tomislav Pintauer, and Michael Cascio. You helped make it possible for me to write this and I cannot thank you all enough for it.

Thank you to Dr. Partha Basu, who was the best committee chair a student could ask for. You were patient with me but still knew when to kick my butt. Thank you for sticking

with me and making sure I finished this work. We may have come down to the end of the third period on this one but I truly believe without your guidance and assistance it would have been for naught.

A special thank you to my family, who (not-so) patiently supported me through the years. From the constant, "When are you finishing" to the questions about, "Did you write today?" your pushing me to finish did help and I cannot tell you how much I appreciate it. I am overjoyed to share this achievement with all of you; Mom, Dad, Josh, Nikki, and the rest of my family this is for you as much as this is for me.

To all of my Alpha Chi Sigma brothers, you were the source of needed mental respite that I needed after long days in the lab or teaching. The many life-long friendships made through Alpha Chi Sigma I still hold today were made during my time working on this and I thank you for keeping me sane enough to finish.

To the rest of the graduate students who were sounding boards or provided the moment of respite that may have been needed during a stressful day, thank you. Rachelle, Becky, Lekse, Chris, Will, Nate, and Greg, thank you for the incredible memories I will have the rest of my life.

To anyone I may have forgotten to thank, it was not intentional, so thank you to you as well.

TABLE OF CONTENTS

Page

LIST OF FIGURES

TABLE OF SCHEMES

LIST OF TABLES

Chapter 1: A Review on Bioactive Lipids and High Sensitivity Detection "Lipidomics" and Separation Methods

Lipids are an important biochemical subspecies that are involved in many different areas of mammalian biology. Biological lipids are a chemically diverse group of compounds, the common and defining feature of which is the extent of their solubility in water.[2] Lipids are bioorganic hydrocarbon based molecules that are soluble in nonpolar solvents but are almost insoluble in water. This is mainly due to a lipid makeup consisting generally of polar head groups with long carbon chain tails. The various biochemical duties of lipids include energy storage (fats and sterols such as cholesterol), cell structure (phospholipids, cholesterol and its esters), and essential hormones (steroids and eicosanoids).[3]

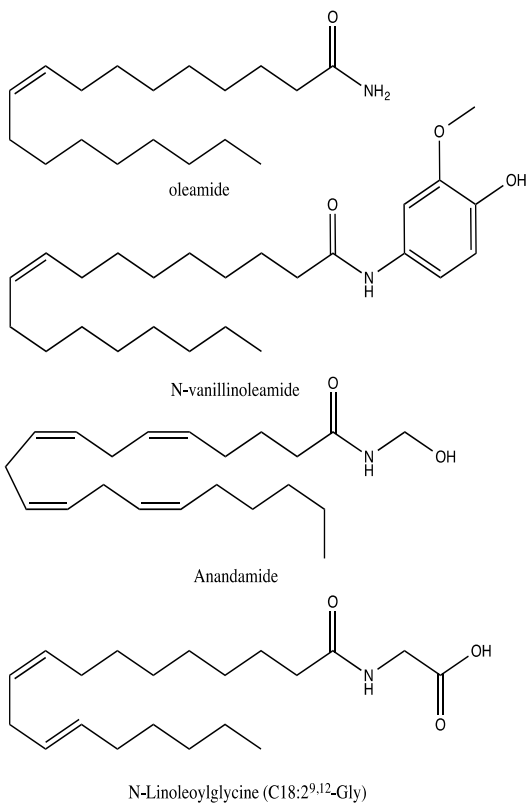

Figure 1.1 Examples of bioactive fatty acid amides.

The quantitative study of lipids, or 'lipidomics', is a burgeoning field in bioanalytical chemistry. With the report by Nagy *et al.* in 1971 a push for understanding these critical biomolecules sprung up. Methods for separations and quantification are the biggest area of chemical research in lipids. Separation methods such as chromatography (GC and HPLC), electrophoresis (capillary or gel), solid phase extraction (SPE), and thin layer chromatography (TLC) are used to

isolate specific lipid classes for identification and quantification.[4-6] Studies in the separation of lipid classes have shown the power of modern chromatographic techniques in isolating unique subgroups.

Lipids are an important biochemical subspecies that are involved in many different areas of biology. Lipids are bioorganic hydrocarbon based molecules that are soluble in nonpolar solvents but are almost insoluble in water. The reason lower detection limits are attractive to those studying lipids is that some are in trace (picomolar (10^{-12}M) – nanomolar (10^{-9} M)) and even ultra-trace (femtomolar (10^{-15}M) and below) concentrations in samples. Lipids can be defined as falling in to three major groups: storage, signaling, and membrane. Storage lipids lack a polar head group while membrane lipids have a polar head group attached to their lipid backbone. Storage lipids include traditional fats, such as triacylglycerols (TAGs), and water repellent lipids, such as waxes. TAGs make up 80% of the mass of adipocytes (fat cells). These fat cells makeup adipose tissue an important tissue type in humans. Adipose is responsible for 10-15% of the average male body mass and ≥20% of female body mass. TAGs are also found as metabolic fuels and as oils in many seeds and nuts. The hydrophobic property of waxes aids in keeping the skin water-resistant and it also slows down the evaporation of water. Due to its firm consistency it is extracted from animal and plants and used in the manufacturing industries for various purposes such as the manufacture of cosmetics or polishes.

Membrane lipids, also known as structural lipids, include phospholipids, sterols, and glycolipids. Membrane lipids make up 5-10% of the dry weight of cells. They are responsible for cell membrane and cell wall makeup. Other lipids, which may not be

categorized as the major types listed, are still very important and consist of messenger lipids. These include eicosanoids, free fatty acids, and primary fatty acid amides (PFAMs). Eicosanoids, a family of signaling lipids including prostaglandins and leukotrienes, have been shown at average levels of 0.9-2 ng/mL in rat heart and brain tissue[8,9] Figure 1.1 shows some representative examples.

The sample volumes are usually minute due to a limited total amount of tissue or fluid media; for example, there is only about 140 mL of cerebrospinal fluid (CSF) in the average human body. The CSF is mostly water and contains very little cells, hence its clear and colorless nature. In an early study by Nagai and Kanfer, the concentration of lipids in 100 mL of CSF was calculated.[6] Only 87.2 nanomoles of total organics were isolated. This 87.2 nmol was not just lipids, specifically cerebrosides, but also proteins and hexoses.[6] Lipids include many subgroups that are of intrigue, such as endocannabinoids like anandamide, are researched due to their drug effects and theoretical binding to natural cannabinoid receptors in the brain.[2-10] While the presence of these amides in biological systems has been reported over several decades[7-8], it is only recently that the survey abilities of tandem mass spectrometry have been brought to bear on a systematic search for novel fatty acid amides.[9-10] An area that is intriguing to us is primary fatty acid amides, or PFAMs. The PFAMs are a neutral lipid family that is part of the fatty acyl group and have been shown to be in the CSF of cats, mice, and humans, omentum samples and as slip additives in plastics.[11-20]

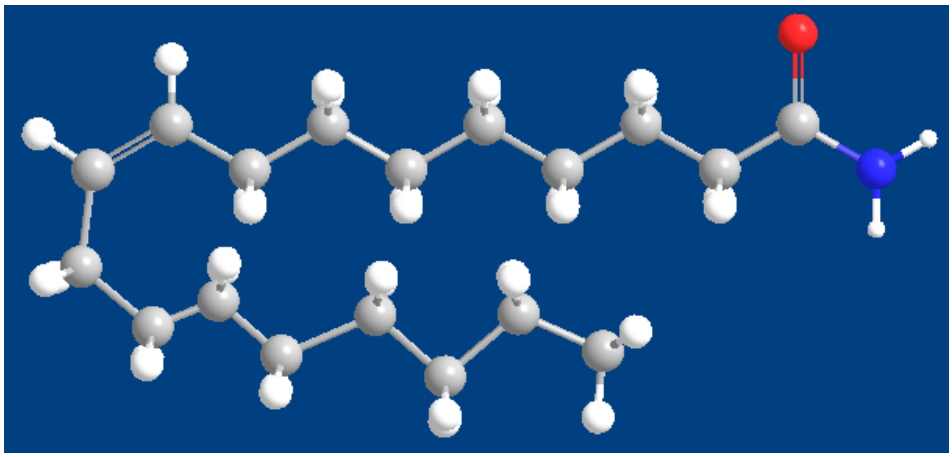

Figure 1.2 Oleamide, a long chain primary fatty acid amide with one point of unsaturation at the 9th carbon.

It has since been widely demonstrated that NAEs and related acylglycerols act as endocannabinoids and endovanilloids[1, 10, 11]. Their metabolic pathways have been (largely) established. Fatty acid amido-hydrolase, FAAH, the enzyme responsible for catabolism of NAEs to fatty acids, has been extensively characterized[12]. It is worth briefly reviewing some of the evidence that PFAMs are an important set of bioactive lipids. There is some evidence that erucamide (C22:1^{13}) is an angiogenic agent[14-16] and that it modulates water balance[17]. Erucamide was found with oleamide and other PFAMs in tear film[7]. Linoleamide (C18:2^{9,12}) was found with oleamide in sleep deprived cats, blocks erg (ether-à-go-go-related-gene) current (known for its link to the electrical activity of the heart)[18], and increases cytosolic Ca^{2+} levels in renal tubular cells[19] and bladder cancer cells[18]. Linoleamide can be enzymatically oxidized by lipoxygenase,[13] and the oxidized form is more resistant to hydrolysis. Arachidonamide was found to inhibit leukotriene biosynthesis[21], and some amides inhibit epoxide hydrolase.[22-23] Oleamide (C18:1^{9}) (Figure 1.2) is a primary amide that demonstrates a variety of physiological effects. Intraperitioneal administration of oleamide into rats induces sleep and

hypomotility and exhibits long-lasting hypothermic effects.[17] Oleamide has been found in human plasma and circulating levels of 35 nM and 56 nM have been reported in rat plasma as opposed to 156 nM in CSF.[12, 19, 21, 22] Oleamide has been linked to GABA inhibition and binding to dopamine and 5-hydroxytriptamine (5-HT) receptors.[14, 23-26] Recently, oleamide has been shown to inhibit voltage-gated Na+ channels at concentrations of 100 μM, concluding that oleamide acts similarly to anesthetics.[21, 25,27] Oleamide has been shown to be a potent regional vasodilator and a modifier of gap junction in the heart and endothelial cells with a half-maximal effective concentration of 1.2 μM.[25] Another study of oleamide derivatives showed their possibility as prototypes for anticancer drugs due to their ability to suppress spontaneous metastasis in the BL6 line of melanoma cells at 10 mg/kg.[25, 28-29] There are scattered reports of other activities of oleamide, including memory modulation[30] and as a potential signaling molecule in the cardiovascular system[26]. The latter is intriguing, as it offers another link between oleamide and affective disorders through cardiovascular health.[31] There is some speculation that the ratio of acid to corresponding amide is important in disease versus normal function[7]. If true, it suggests that studies involving fatty acids and health (particularly mental health) should also involve fatty acid amides, and it also suggests that, in general, epidemiological studies would be more definitive if they included measurement of metabolically related species. The importance of PFAMs requires an analysis and detection scheme. The low concentration levels demand sensitive techniques at the trace and ultra-trace levels. If these molecules could be linked to a fluorescent tag or reacted with a fluorogen then the most sensitive detection scheme there is, fluorescence, would be perfect for their detection.

Fluorescence Detection

Traditionally GC or LC analysis followed by flame ionization (FID), electron ionization-mass spectrometry (EI/MS), or ultraviolet-visible absorbance (UV-Vis) is used for the analysis of lipids. These methods are well defined but lack the sensitivity for direct analysis of nanomolar and picoMolar analytes. Traditional studies usually relied on pre-concentration of a sample in order to analyze components that are present at concentrations below their limit of detection. In order to detect at trace and ultratrace levels a highly sensitive technique with low detection limits is needed. The identification technology most utilized in lipid studies is mass spectrometry (MS), specifically tandem mass spectrometry (MS/MS), which allows for the fragmentation of molecular ions for structural and component identification. However there are additional situations where laser induced fluorescence (LIF) detection is employed, specifically where its increased sensitivity and lower detection limits are necessary. Fluorescence is the excitation of an incident, or initial, photon and the subsequent emission of a photon that varies in wavelength from the incident/initial photon.

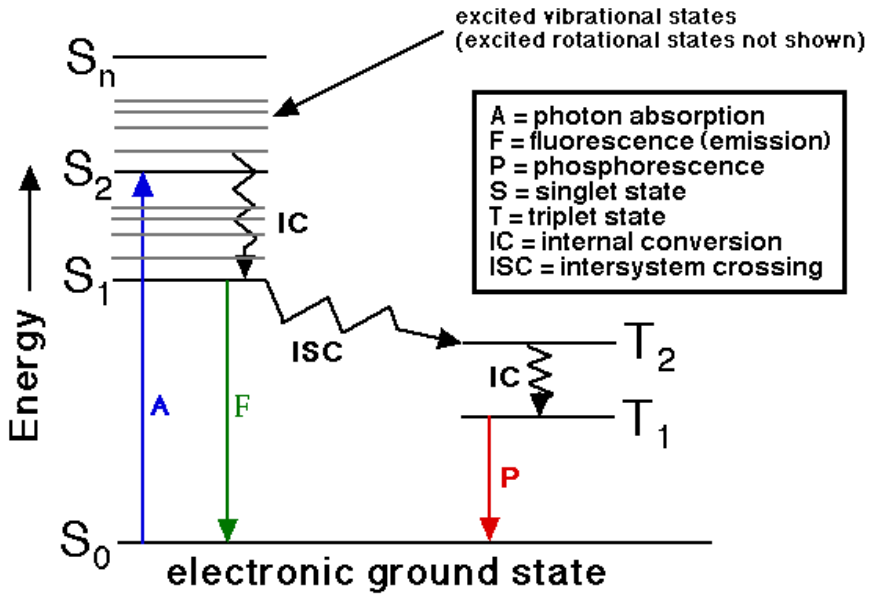

Figure 1.3 Scheme for fluorescence and phosphorescence showing energy transitions.[32]

Fluorescence is a resonant effect in that there is a resonance lifetime between the excitation to an excited electronic state, relaxation to a parallel vibrational state, the relaxation to its electronic excited state and then the emission of the shifted photon.[32] Fluorescence always deals with a Stokes, or red, shift.[33-36] One problem that accompanies fluorescence is noise in the form of scattering. There are two main types of scattering, Rayleigh and Raman. Rayleigh scattering is an elastic process where the scattered photon is of the same energy as the incident photon. Raman is an inelastic process, where the scattered photon is of a different wavelength than the incident photon. There are two different ways the photon can be scattered in Raman scattering, Stokes or Anti-Stokes. A Stokes shift occurs when the molecule being analyzed absorbs energy and the scattered photon is then shifted to a higher wavelength (lower energy), often called a red shift. Anti-Stokes is the opposite. The analyzed molecule emits energy and the scattered

photon is of lower wavelength (higher energy), often called a blue shift.[32] This is illustrated in Figure 1.4.

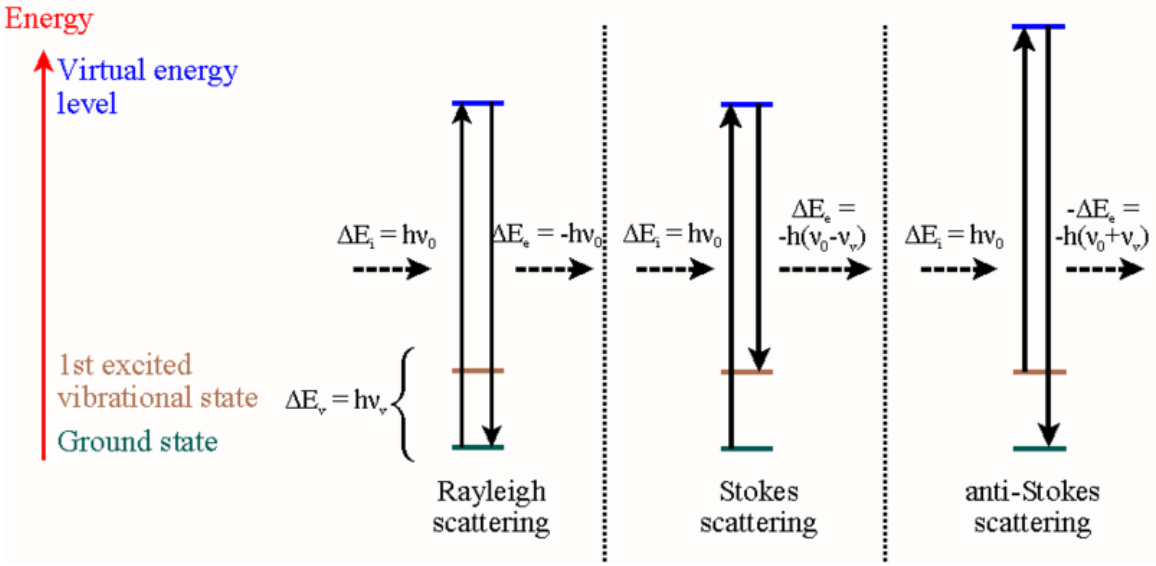

Figure 1.4 Diagram comparing Rayleigh and Raman scattering. Raman scattering can be described as either Stokes scattering or anti-Stokes scattering.[32]

Raman scattering is similar to fluorescence but a distinction must be drawn between the two. As stated above fluorescence is a resonant effect, fluorescence is also wavelength dependent. Raman scattering is not a resonant effect and is not dependent on the wavelength of light. LIF is made possible by "tagging" the lipid with a fluorophore or a fluorogen, both of which are fluorescing compounds, the main difference between the two fluorescent types is their natural fluorescence. Fluorophores have a natural fluorescence, while fluorogens only fluoresce when they are bound to a specific molecule type. These fluorescent molecules allow for several applications such as a tracer molecule for kinetic experiments, as a dye for cell staining, and for the tagging of non-fluorescent analytes of interest. Families of fluorophores have been created that are analyte specific, such as the DAPI family for nucleic acids.[37] Due to the prevalence of

amine groups in biochemistry, one of the most attractive families of fluorescent molecules are the amine-reactive molecules. Some of the tags that are used in amine studies include fluorescein isothiocyanate (FITC), 3-(2-Furoyl)-Quinoline-2-Carbaldehyde (FQCA), and naphthalene-2,3-dicarboxylic acid (NDA). Fluorescein, a typical fluorophore, is widely used in many areas of research.[38] It has a strong excitation maximum at 488 nm and an emission peak at 512 nm. It is naturally fluorescent and has a quantum yield of >80%, which is approaching unity, or when a fluorescent molecule release as many photons as it absorbs. FQCA, a fluorogen, reacts with amines to produce a highly fluorescent aromatic complex (Scheme 1.1) that excites at 480 nm and emits at 590 nm.

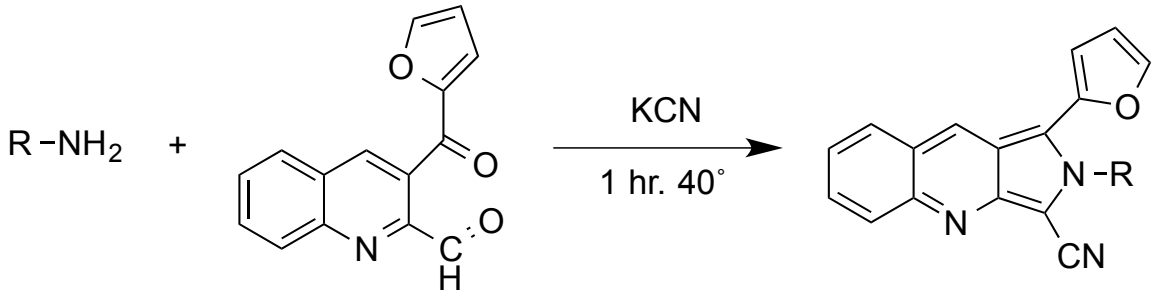

Scheme 1.1: Reaction of FQCA with primary amines yielding a fluorescent molecule.

The advantage of using FQCA is that, unlike FITC, it has a low natural fluorescence and a large Stokes shift meaning that there is an elimination of background fluorescence from unreacted tag. FQCA, can self-react and create a fluorescent dimer which can cause background noise.[39] The Stokes shift cuts down on the background scatter by detecting at a higher wavelength than the incident beam. This raises the signal to noise ratio, which allows for lower LOD. FQCA has been used for the analysis of amino acids and straight chain amines.[39-40] It has been used to achieve detection limits of

0.5 amol of oligosaccharides using on-column LIF.[39, 41] The tag has been shown to bind to amines and not amides, which are difficult to tag. A derivatization step would be required to take the amide to an amine.

Conversion of amides to amines

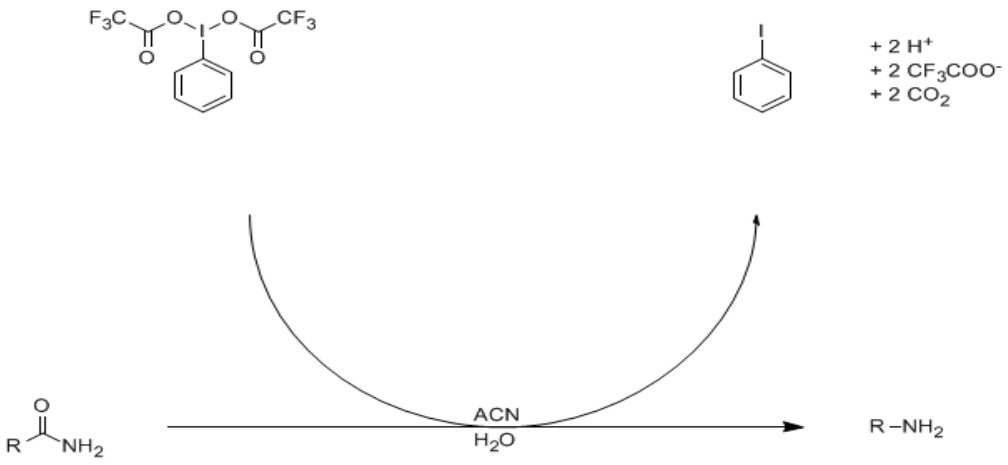

Scheme 1.2: Conversion of a primary amide (R-CONH$_2$) to a primary amine (R-NH$_2$) using PIFA

Unlike their primary amine chemical counterparts, such as amino acids, PFAMs are difficult to tag using conventional fluorophores. Previous work by Lei Feng has shown a method using PIFA ((bis-[trifluoro]-acetoxy) iodo benzene) for the conversion of amides to amines.[42-43] The reaction is a modified form of the Hofmann rearrangement. (Scheme 1.2) The rearrangement would allow for tagging of the amino group that is left with FQ, an uncharged fluorescent tag that can be used at trace levels for detection of the PFAMs. A method using a derivatized PFAM for HPLC separation coupled to fluorescence detection would prove beneficial and allow steps to be taken towards ultra-trace analysis of these PFAMs. A highly sensitive detection technique for detection of PFAMs would be the platform to tag the target molecules for fluorescence detection. The

major issue with respect to the development of a fluorescence method for ultratrace analysis is the ability to perform the reaction at low concentrations.

Microfluidic Applications

In the past fifteen to twenty years, a movement towards smaller analytical systems has emerged. These systems, often referred to as micro total analytical systems or simply *μTAS*, are diverse in their nature and their construction.[44-46] Cell culture, lysis and analysis are all very attractive areas for microchips.[44-47] However, most of these areas of research occur in systems using aqueous solvents. Due to the hydrophobicity of the lipids, nonaqueous solvents are needed for the separations. This brings a new area of microfluidics into consideration, their substrate: do you choose polymers or glass? The main advantage to using glass chips is the ability to use nonaqueous solvents with them; the main disadvantage, however, is the fabrication method.

A growing trend in chemistry is the use of low volume samples for organic reactions. This can be achieved using microreactors, segmented flow microfluidics, or nanovials.[48-55] Nanovials feature their own unique qualities. A vial is etched onto a substrate that has nanometer dimensions. Droplets of reactants and solvents can be added to the vial for a reaction to occur. The attractiveness of this method comes in the recirculating flow that occurs while the droplet evaporates. Not only does rapid mixing occur but also a preconcentration effect is observed. The preconcentration comes from the evaporation of the solvents leaving little solvent left with the reactants and products in the well. This is attractive because detection can be done in the well. Nanovials have been shown to assist in mixing of organic reactions in 15 nL and 30 pL wells.[48-50]

The ability to minimize sample size is an attractive aspect of microfluidics. With a decrease in sample size and concentration, trace and ultratrace analysis becomes more readily available. The advantage to this is scaling down to trace analysis from macroscale reactions involves multiple dilution steps, whereas when you start with trace amounts there are less steps between reaction and analysis.

Some unique issues arise from attempting reactions on microfluidic chips. One of the biggest problems is mixing. Due to low Reynolds and capillary numbers, dimensionless numbers that describe fluid mechanics, the flow is laminar in a microfluidic channel. The mixing that occurs between two streams in a laminar flow is simple diffusion, which is not ideal for mixing of two reactants. To combat this some ingenious applications have been used. The first to be used was the Baker's transformation.[56-58] A segmented flow version of this is shown in Figure 1.5.

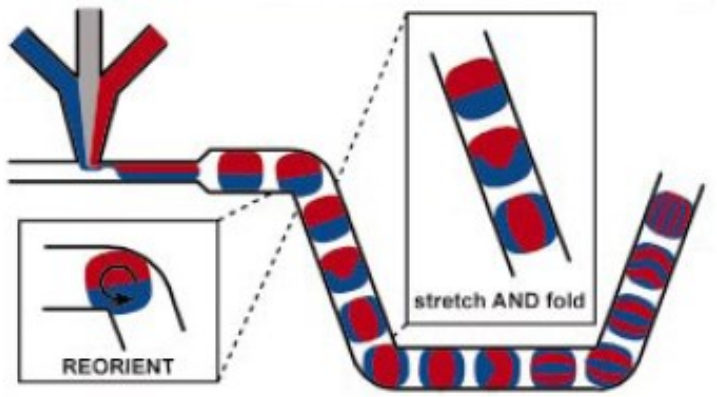

Figure 1.5 Schematic of a Baker's transformation. The stretching and folding of the plugs can be seen in the right inset. The reorientation of the droplets can be seen in left inset.[54]

The streams or plugs are 'stretched' and 'folded', breaking laminar flow, and thus mixing the reactants. Beebe and Ottino have both shown mixing of inorganic reactions using the Baker's transformation to attain and detect a fluorescent product.[56-58] While this shows

the capabilities of the transform, it does not give a clear method for organic reactions. A modification of the baker's transformation is using serpentine channels, which alters the internal recirculating flow as can be seen by the white arrows in Figure 1.6.

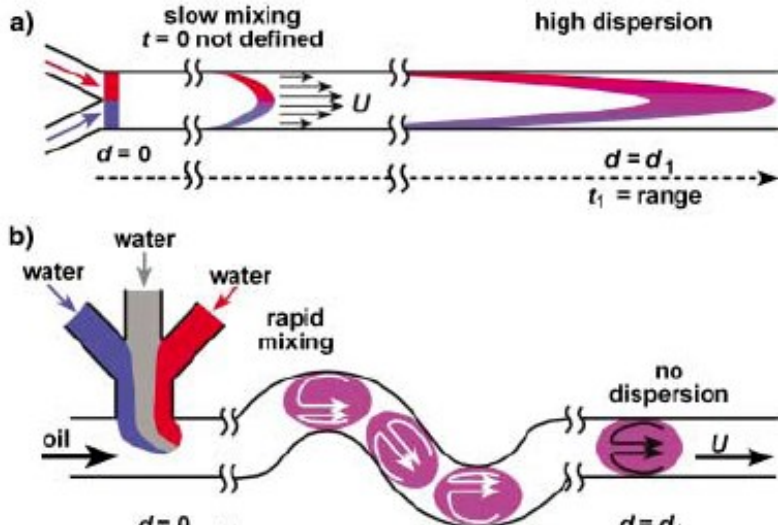

Figure 1.6 Laminar flow versus segmented flow droplets. A) laminar flow showing slow mixing and high dispersion of components. B) segmented flow droplets exhibiting rapid mixing due to internal recirculating flow from the serpentine channels and immiscible fluid interactions. Note the lack of dispersion in the segmented flow.[59]

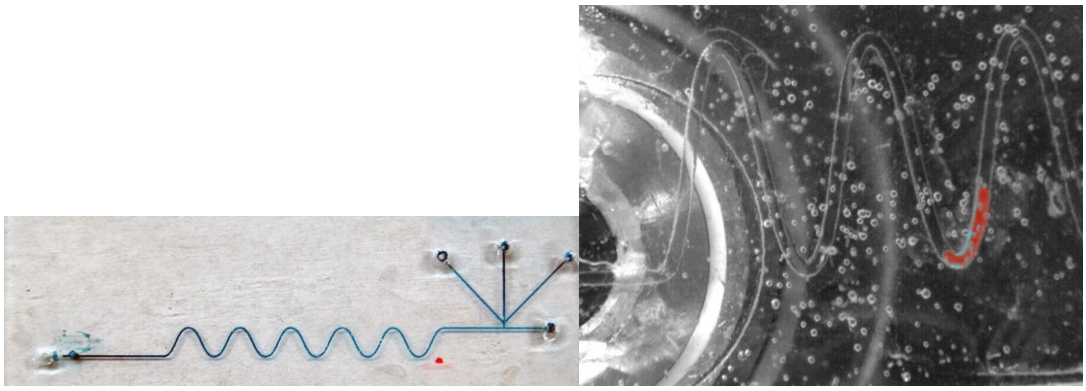

Figure 1.7 (Left) photograph of one prototype microdroplet manifold for derivatization. Channels are filled with food dye for visibility. (Right) false color fluorescence image (excitation at 488 nm, emission at 530±15 nm) of a FITC droplet traversing the mixing channel (different chip design) following dilution by 3X at the mixing inlet. At left is the image of the objective in the inverted epifluorescence microscope.

Song has shown not only inorganic reactions in the serpentine method but also organic reactions on a time scale of ~2 ms.[59] One report demonstrates the use of perfluorodecaline, PFD, as a carrier stream due to its immiscibility with not only water but also organic solvents. PFD is also compatible with a range of biological molecules due to its use as blood substitute in humans during surgeries. Song also showed that merging and separation of plugs were attainable on a chip. Merging involved splitting the plugs from the PFD at branching points. In order to achieve reliable separation the branching points were constricted, the plugs became long and narrow and behaved simply like laminar flows subjected to pressure gradients. The merging of plugs was used to combine multiple streams of plugs into one stream.[59]

The generation of microdroplets in microfluidic systems has formed the basis for a wide variety of research areas in recent years[59-61]. Microdroplets generated on a microfluidic platform (Figure 1.7) from convergent flow of immiscible fluids (water and PFD) have a number of unique properties that are relevant to performing chemical reactions, including derivatization with fluorescent reagents: droplets can be very small (pL to nL), so they can be used with very small amounts of reagent or analyte; they can be mixed very efficiently by chaotic advection[57], thus facilitating efficient chemical reaction [58,59]; they are non-dispersive, so droplets formed from (and reactions performed in) the eluent of a chromatograph will not increase extra-column band broadening; it is simple to add additional reagents, either directly to the eluent or downstream, without introducing additional band broadening or contamination[60,61]; and they can easily be manipulated by splitting, recombining, etc.[62], allowing for use in for a variety of other

functions, such as micro-extraction. In order to get highly mixed droplets, secondary flow must be induced in the droplets. The best way to induce secondary flow and to enhance turbulent mixing is to curve the channels[63]. The chip shown in Figure 1.7 has a series of wavy channels that induce secondary flow; higher degrees of curvature enhance the mixing[64]. As shown above Song and Ismagilov have reported mixing times on the order of milliseconds[54,65]. As the chromatographic eluent is not dispersed once it has been divided into droplets, the actual mixing time is not critical. However, the reaction is dependent on kinetics of the derivatization reaction and travel time from droplet creation to detection.

The major issue with respect to the development of coupling a fluorescence method for ultratrace analysis to the microfluidic chips is the ability to perform the reaction at low concentrations. Quite a number of derivatization reactions work quite well at high concentrations, but it is a significantly greater challenge to derivatize an analyte at very low concentrations. In the context described above, there is a need to tag lipids such as PFAMs that are in the picomolar concentration range. As discussed, detection by LIF can handle the picomolar concentration (yoctomole mass) range, provided attention is paid to the photophysical qualities of the tag and the optics of the detection system[62]. If a peak from a HPLC separation is contained in a 100 nL volume, dispersing the eluent into 100 pL droplets at constant droplet generation rate essentially oversamples the peak by about 5-fold in time. If the concentration in the peak is 1 pM, the number of molecules in an average droplet will be about 60 (100 ymol). This analysis is oversimplified, as it ignores issues of dilution on the column and the concentration distribution over the axially dispersed peak, but it serves to help understand the order of magnitude. In order to

generate such small droplets, we have to keep the capillary number small[63]: $Ca = \frac{u_x \eta}{\gamma}$, where u_x is the linear flow velocity, n is the viscosity, and y is the surface tension at the interface of the two solvents. The actual droplet size can be larger or smaller, depending on how well the reactions proceed and what kind of flow rates are finally produced in the coupled fluid handling system, whether it is direct infusion or a HPLC system. Droplet size and channel size are parameters that need to be optimized for low concentration reactions. For microdroplets, 5 – 10 nL sized droplets are targeted due to their ability to hold low concentrations and sample loads while still being big enough to measure multiple points during LIF.

The properties of microdroplets for chemical reactions – high mass and thermal transport, lack of dispersion, ease of manipulation – have been recognized for some time[64,69]. These properties have been put to excellent use for creating highly monodisperse polymers[65-67], performing highly exothermic reactions[69], and many other applications. A number of publications have demonstrated the potential of microdroplet platforms for screening reaction conditions for difficult chemical reactions.[70,71] In terms of enhancing the efficiency of chemical reactions, reactions whose rates are limited by mass transport, even in part, benefit from the highly efficient mixing and small volumes provided by microdroplets[64, 68]. It has also been suggested that confinement of the reaction to small volumes greatly facilitates chemical reactions by enhancing the collision frequency of the reactants[52, 69]. These properties of microdroplets ought to help in derivatizing reagents at low concentration by enhancing the reaction rate and by minimizing the waste byproducts. By dispersing the reaction into very small microdroplets, on the order of nanoliters or even picoliters, and by using more reactive

and smaller tags, it should be possible to perform chemical derivatization even for very dilute eluents from a capillary column. The following chapters explore the establishment and execution of an analysis and detection scheme for these reasons.

Conclusion

When studying low concentration substances it is imperative to have a highly sensitive analysis technique that allows for excellent reproducibility. Bioactive amines are an ideal target for this type of analysis. Their low *in-situ* concentrations require a system that can be used to derivatize and analyze these analytes. As part of the drive to establish an analytical technique for the detection of derivatized primary amines the following goals must be met:

- Construct a method for detecting fluorescent molecules at the trace and, ideally, ultratrace concentration levels. The detection scheme is an optimized laser-induced-fluorescence (LIF) setup that is built from scratch and to the needs of the chosen fluorophore.
- Build and optimize a method for fabricating microfluidic analysis systems for the on-chip derivatization of the analyte with a chosen fluorophore. This methodology will allow the bulk reaction method to be tested at trace analysis levels.
- Chose a fluorophore for the derivatization of primary amines that allows for minimization of impurities and background noise while maximizing the detection limit of the fluorescent products.

The ability to reproducibly and efficiently detect these trace molecules in a highly sensitive way allows for an added dimension for researchers to further their analysis into bioactive molecules.

Chapter 2: Design and Optimization of a Microfluidic Chip Fabrication System

Background

"Lipidomics" and Separation Methods

Biological lipids are a chemically diverse group of compounds, the common and defining feature of which is the extent of their hydrophobic nature.[2] The various biochemical duties of lipids include energy storage (fats and sterols such as cholesterol), cell structure (phospholipids, cholesterol and its esters), and essential hormones (steroids and eicosanoids).[3] The large-scale study of lipid pathways and signaling, or 'lipidomics', is a burgeoning field in bioanalytical chemistry. Methods for separations and quantification are one of the biggest areas of analytical chemistry research in lipids. Separation methods such as chromatography (GC and HPLC), electrophoresis (capillary or gel), solid phase extraction (SPE), and thin layer chromatography (TLC) are used to isolate specific lipid classes for identification and quantification.[5-6, 70] The most attractive identification technology utilized in lipid studies is mass spectrometry (MS) but laser induced fluorescence (LIF) detection is employed in situations where its increased sensitivity and lower detection limits are necessary.[71]

Microfluidic Applications

In the past fifteen to twenty years, a movement towards smaller analytical systems has emerged.[47, 72-82] These systems, often referred to as micro total analytical systems or simply *μTAS*, are diverse in their nature and their construction.[44, 46, 83] Cell culture, lysis,

and analysis are all very attractive areas for microchips.[44, 47, 83-84] However, most of these areas of research occur in systems using aqueous solvents. Due to the hydrophobicity of the lipids, nonaqueous solvents are needed for the separations. This brings a new area of microfluidics into consideration, substrates: polymers vs. glass. The main advantage to using glass chips is their compatibility with nonaqueous solvents; the main disadvantage, however, is the method of fabrication.[72-73, 85] The differences lie in the way that the template is imaged and then formed onto the chip.

Photolithography is the process of transferring an image from a photomask to a chemical substrate or photoresist, attained by exposing the substrate to UV light. There are two types of photoresist: positive and negative. Positive resist, when exposed to UV light, is made more soluble in developer. When the chip is placed in developing solution the area that was exposed to the UV light dissolves away. Negative resist works on the opposite tenet. Whatever is exposed on a negative resist also polymerizes, but is less soluble in the developing solution than the unpolymerized resist and therefore stays when the chip is processed.[86-88] Figure 2.1 shows an example of how the two different photoresists work.

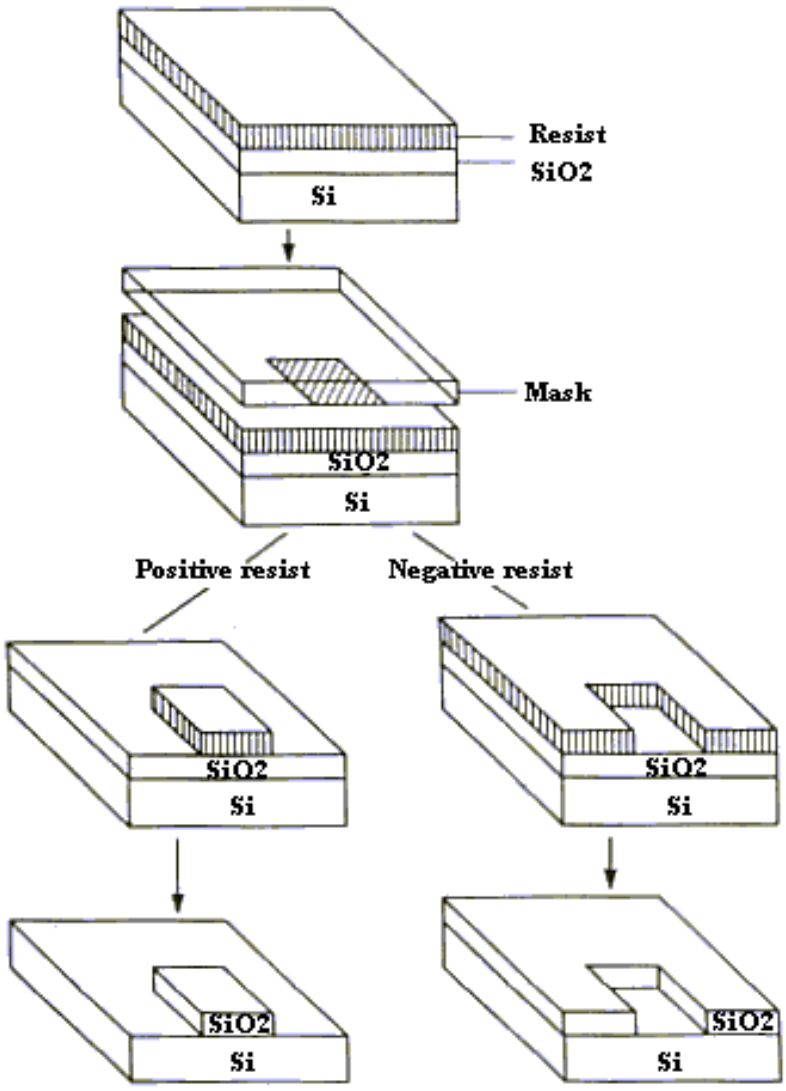

Figure 2.1 - Example of photolithography on positive vs. negative resists: Shaded area on mask covers the resist from the UV light.[88]

A growing trend in chemistry is the use of low volume samples for organic reactions. This can be achieved using microreactors, segmented flow microfluidics, or nanovials.[48-55] The ability to minimize sample size is an attractive aspect of microfluidics. With a decrease in sample size and concentration, trace and ultratrace analysis becomes more readily available. The advantage to this is scaling down to trace analysis from

macroscale reactions involves multiple dilution steps, whereas when starting with trace amounts there are less steps between reaction and analysis. Some unique issues arise from attempting reactions on microfluidic chips. One of the biggest problems is mixing of the reactants. Due to low Reynolds and capillary numbers, dimensionless numbers that describe fluid mechanics, the flow is laminar in a microfluidic channel. The mixing that occurs between two streams in a laminar flow is simple diffusion, which is not ideal for mixing of two reactants. To combat this some interesting engineering has been tested. The first to be used was the Baker's transformation.[56-58] A segmented flow version of this is shown in Figure 2.2.

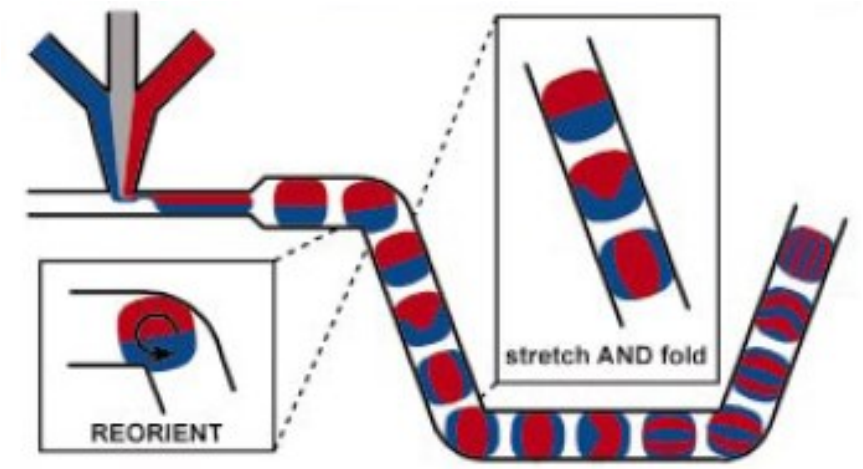

Figure 2.2 - Schematic of a Baker's transformation. The stretching and folding of the plugs can be seen in the right inset. The reorientation of the droplets can be seen in left inset.

The streams or plugs are 'stretched' and 'folded', breaking laminar flow, and thus mixing the reactants. Beebe and Ottino have both shown mixing of inorganic reactions using the Baker's transformation to attain and detect a fluorescent product.[56-58] While this shows the capabilities of the transform, it does not give a clear method for organic reactions. A modification of the baker's transformation is using serpentine channels,

which alters the internal recirculating flow as can be seen by the white arrows in Figure 2.3.

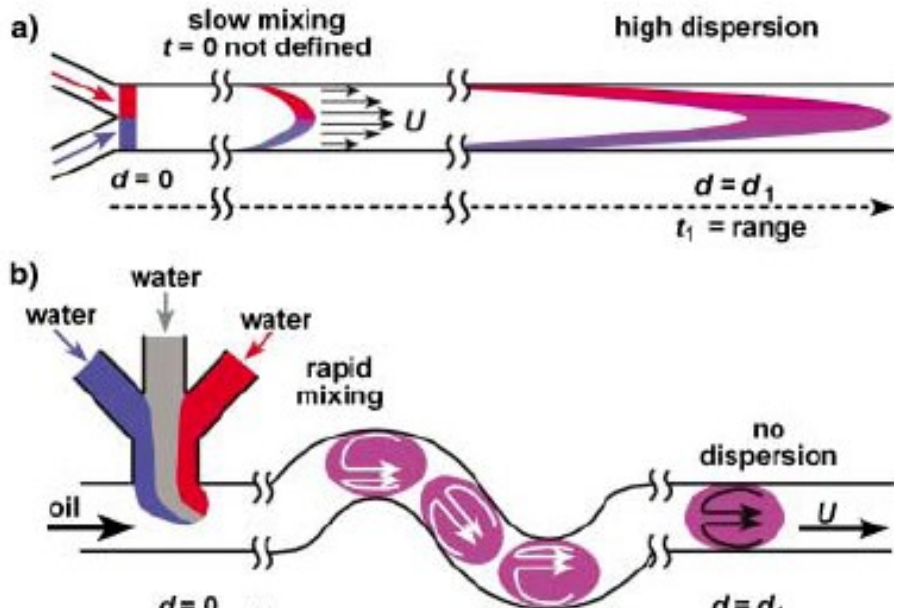

Figure 2.3 - Laminar flow versus segmented flow droplets. A) laminar flow showing slow mixing and high dispersion of components. B) segmented flow droplets exhibiting rapid mixing due to internal recirculating flow from the serpentine channels and immiscible fluid interactions. Note the lack of dispersion in the segmented flow.[59]

Song has shown not only inorganic reactions in the serpentine method but also organic reactions on a time scale of ~2 ms.[59] She reports the use of perfluorodecalin, PFD, as the carrier stream due to its immiscibility with not only water but also organic solvents. PFD is also compatible with a range of biological molecules shown by to its use as blood substitute in humans during surgeries. Song also showed that merging and separation of plugs were attainable on a chip. Merging involved splitting the plugs from the PFD at branching points. In order to achieve reliable separation the branching points were constricted, the plugs became long, narrow, and behaved simply like laminar flows

subjected to pressure gradients. The merging of plugs was used to combine multiple streams of plugs into one stream.[59]

If segmented flow does not deliver the results needed for our analysis then an alternate method for small scale reactions at the nanoliter and picoliter level is the use of nanovials.[48-50] Nanovials feature their own unique qualities. A vial is etched onto a substrate that has nanometer dimensions. Droplets of reactants and solvents can be added to the vial for a reaction to occur. The attractiveness of this method comes in the recirculating flow that occurs while the droplet evaporates. Not only does rapid mixing occur but also a preconcentration effect is observed. The preconcentration comes from the evaporation of the solvents leaving little solvent left with the reactants and products in the well. This is attractive because detection can be done in the well. Nanovials have been shown to assist in mixing of organic reactions in 15 nL and 30 pL wells.[48-50]

Experimental

In order to make glass microfluidic chips, the chip must go through a process of developing, etching, and stripping the chrome photomask into the pattern of the chip then etching the glass with hydrofluoric acid, then stripping the remainder of the photomask. However, a system needs setup to handle the fabrication of these microchips.
AZ 300 MIF chrome developer was obtained from AZ Electronic Materials and distributed through Mays Chemical (Indianapolis, IN). CR-9 chrome etch, RS-120 resist strip, and NanoStrip resist strip were obtained from Cyantek Corp. (Fremont, CA). HF was obtained from Fisher Scientific (Pittsburgh, PA). Microchip substrate blanks, pre-

coated with AZ-1517 positive photoresist, were obtained from Telic Corp. (Valencia, CA).

Indirect Exposure System

In order to develop the photomask, an ultraviolet light developing system is needed. These normally are expensive, costing well over $15,000 at the time, so a less expensive alternative was sought. In order to minimize the exposure during the warm-up time of the lamp (several minutes from power on), it was decided that a nontraditional system needed to be built. Blueprints for a shutter system were needed before fabrication and assembly could begin. (Figure 2.4)

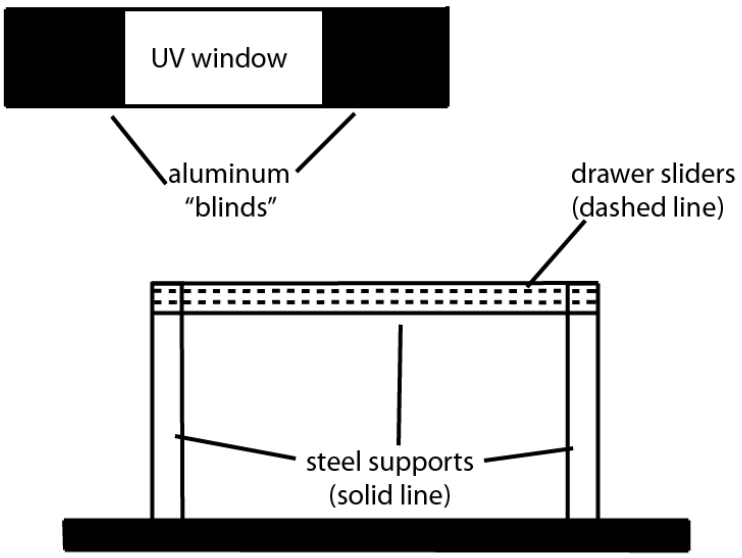

Figure 2.4 - Schematic of UV shutter: The top image is a top down view of the shutter showing the two 'blinds' and the exposure window. Bottom image is a side view of the shutter system on a breadboard. The supports (solid lines) and drawer sliders (dashed lines) complete the drawing. In operation, the shutter fits in the drawer sliders and is moved manually.

Once the rough sketch was completed, materials were purchased to build the shutter. The materials used were sheet metal, cabinet drawer roller mechanism, a bread

board and angled steel. Once completed, the shutter was fitted with the UV spot lamp and mirror system. (Figure 2.5)

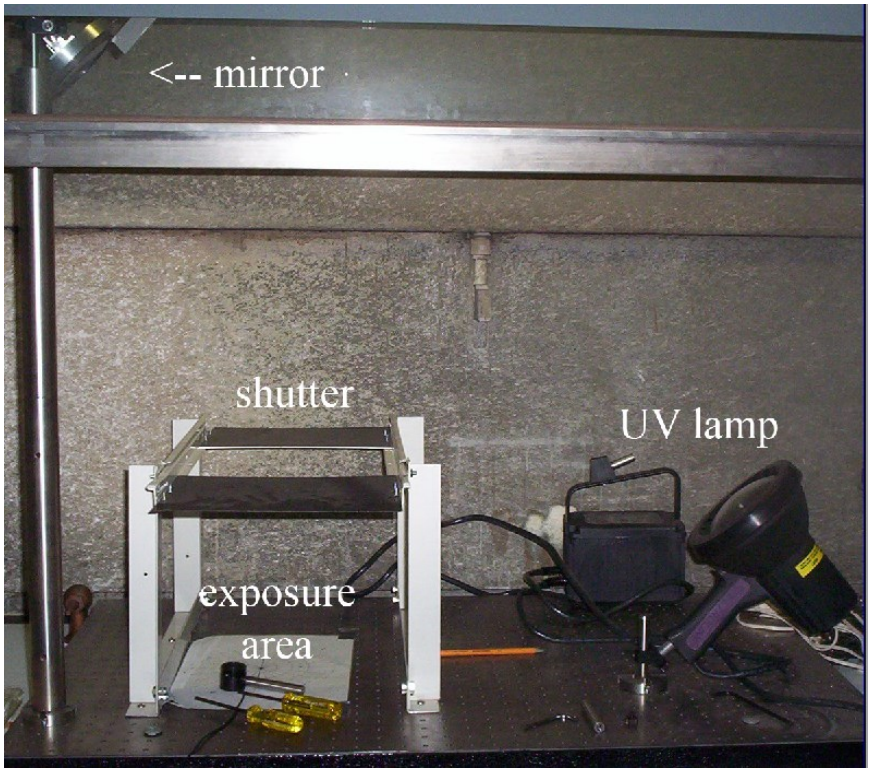

Figure 2.5 - Completed shutter system with UV lamp and mirror. Setup is located in a fume hood.

Irradiance was then measured using a digital multimeter fitted with an iris diaphragm, with the shutter on the diaphragm set to a diameter of 0.3 cm. The irradiance was detected in mW, converted to mW/cm^2, and then a plot was made using Igor Pro v. 6 (Wavemetrics, Inc., Lake Oswego, OR).

Direct Exposure System

Upon testing the indirect method it was decided to also test the direct method of exposure. The exposure system was modified as seen below (Figure 6) to accommodate the direct exposure system. The irradiance tests were repeated as described above and compared to the results of the indirect study to decide on the best exposure method.

Figure 2.6 Completed direct shutter system with UV lamp and mirror. Setup was still located in a fume hood

Fabrication and Design of Glass Microfluidic Chips

Adobe Illustrator Design

When making microfluidic chips, templates are needed of the designs to "guide" the photolithography. Chips were designed using Adobe Illustrator CS2 (Adobe Systems Inc.) in order to create vector-based drawings that would print true-to-measurement. All chip templates were made on a 2 cm x 3 cm outline and possessed uniform channel widths of 0.04 mm.

The primary testing for the glass chips involved adding separation channels to the chips. Weirs were added on the chips in order to allow for packing material for the separations. Weirs are areas of the channel where the opening is small enough that the packing will not overflow into the rest of the channel but large enough to allow the flow

of the mobile phase. These weirs were created by placing gaps in the photomask with a width of 0.120 mm for the top templates and 0.160 mm for the bottom templates. This allows for isocratic etching which will create the weir, shown in Figure 2.7.

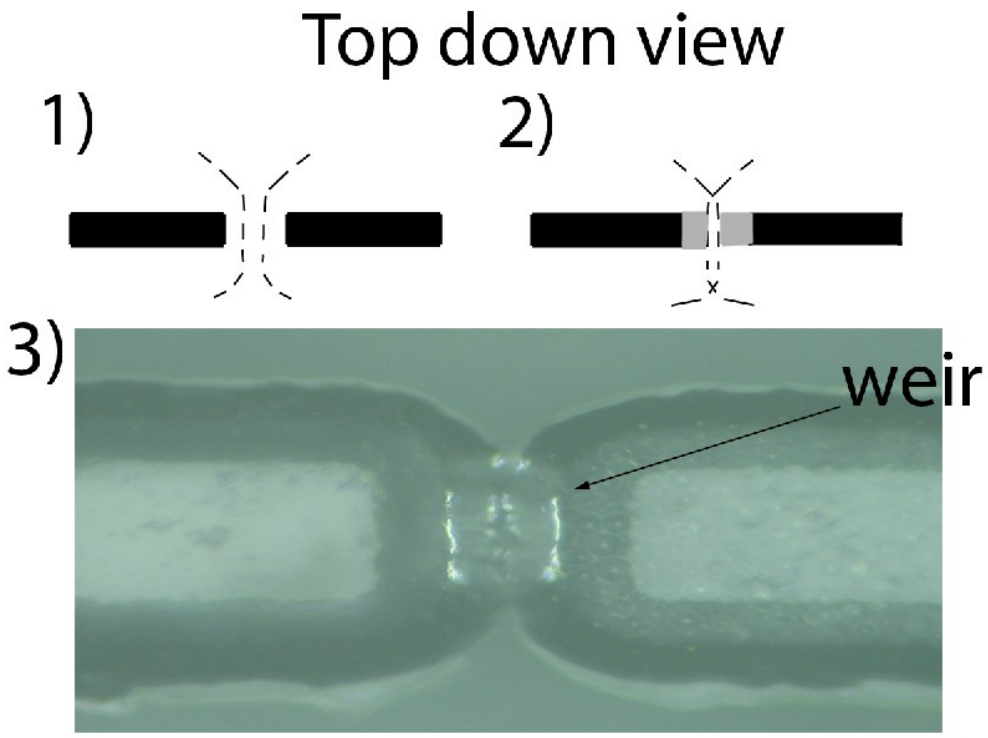

Figure 2.7 - Schematic for isocratic etching of weir systems. 1) Pre-etched channels are seen in black with post-etch seen as dashed lines. Weir width of 160 micrometers will cause the gap between the dashed lines. 2) Grey areas are the post-etch microchip from step 1, post-etch again is noted by dashed lines, note the overlap which will etch part of the gap between the channels. This is due to a gap width of 120 micrometers. 3) Microscopy picture of the etched weir system, note the "texture" in the right channel that is missing from the left, this is the packing (in this case C18).

A proper clean laboratory setup and safety preparations must be taken into account before chip making can begin. An AirClean 600 PCR Workstation (Raleigh, NC) with laminar flow capabilities was setup with a Cimarec Hot Plate and Lab Line Bi-Directional rotator both obtained from Barnstead (Dubuque, IA). A Lindberg/Blue Box

Furnace equipped with UP150 Program Temperature Controller (Asheville, NC) was installed for the baking and sintering steps in the microfluidic chip production.

Glass Fabrication

The production of glass microfluidic chips can be a dangerous process if proper safety procedures are not taken. Multiple steps and the use of corrosive chemicals make this an unattractive area in microfluidics. However, there are very few ways around the use of glass chips when dealing with non-aqueous solvents, which diffuse into PDMS and other polymer microfluidic chips. The fabrication process has been adapted from Telic Co., the makers of the glass blanks[89].

The glass blanks were coated with a layer of chrome and a thin-film AZ 1517 photoresist. After initial test proved that the spin coat was not uniform we decided to go with the pre-spun wafers available from Telic. We mounted the blanks with a template that was printed on transparent film. They were then exposed using the shutter system, described in above, for 7 seconds in order to polymerize the exposed regions of the chip. The chip then gets bathed in a sequence of different chemical baths. The chip was first submerged in AZ 312 MIF developer. This will develop the photoresist layer, solubilizing the exposed areas. The chip was then rinsed in doubly deionized (DDI) water for 40 seconds to remove all of the developer. The chip was then submerged in the CR-9 chrome etch for 60 seconds to remove the exposed chrome down to the glass layer of the chip. The chip was rinsed again with DDI water for 40 seconds to make sure all of the chrome was removed from the channels. At this point we began the HF etching of the glass.

The HF wet etch procedure was adapted from Roper's work at FSU.[90] A mixture of 14:20:66 (v:v:v) HNO_3:HF:H_2O was needed for the wet etch. In order to keep with a safe work environment, plastic dishes are recommended for all steps and protective clothing (coveralls, gloves and goggles) were mandatory due to the danger of the HF. The chip was then placed in the etching solution for an appropriate amount of time for the desired depth of the channel. Roper et al. have reported etching rates as 0.3 mm/min.[90] The etched chip was then be removed with plastic forceps and placed in a 1 L beaker of DDI H_2O to flush any remaining HF from the substrate. Once the chip is removed from the H_2O, the chip can be fully cleaned with a process adapted from Telic Co.[89] This is slightly different from the method described in Roper's SOP but was more manageable for the lab's smaller setup and gave cleaner chips for annealing.

After the HF etch and rinse, the chips were placed in Cyantek RS-120 resist strip at 50 °C for 5 minutes in order to strip away the remaining photoresist. Once all of the resist was removed, the chips were then rinsed with DI water and then submerged in the CR-9 chrome strip to remove the rest of the chrome layer. We performed one final rinse which preceded the submergence in Nanostrip for 3 minutes. The Nanostrip was used to destroy any organic compounds on the chip. The chips was once again rinsed well with DI water and then a glass slide was placed on top using capillary action to hold together the two pieces of glass. It was imperative that no particulates were allowed in between the two pieces of glass. The chip was then placed in an oven and the temperature was ramped to 640 °C at a gradient of 10 °C/min. This causes the glass surfaces that are in contact with each other to soften and bond. The chip was baked for 8 hours and then the temperature was ramped back down to room temperature at 10 °C/min. Chip bonding

was examined by use of a microscope and channels were examined for particulate matter, etch depth, and incomplete etching.

PDMS Fabrication

Once the microchip fabrication was examined and fully underway, it was decided to assemble a polydimethylsiloxane, or PDMS, based microfluidic chip manufacturing process. PDMS was attractive due to its inexpensive components and easier manufacturing. The downside was that PDMS chips must be treated before each usage with a fluorocarbon based oil so that non-aqueous solvents do not absorb into the plastic and cause destructive swelling. The manufacturing of the PDMS involves using the same UV irradiance setup as the glass chips but do not require any of the harsh chemicals that glass needs.

SU-8 Master Molding

The first step in manufacturing PDMS microchips was manufacturing a stamp, or reverse mold, that they will take the form of. This was the opposite of the way glass chips are made. First a SU-8 mold was created using a UV pattern and a clean 8" glass wafer. The SU-8 was spin coated onto the glass wafer. Once the coating was evenly spread across the wafer it was removed from the spin coater and placed on a hot plate for a soft-bake, which sets the SU-8. The UV pattern, which was printed onto a quartz glass blank, seen in the Figure below, was placed on top of the SU-8 and exposed to UV light. This polymerizes the exposed SU-8 allowing it to be washed away leaving the raised pattern of the channels and borders on the wafer.

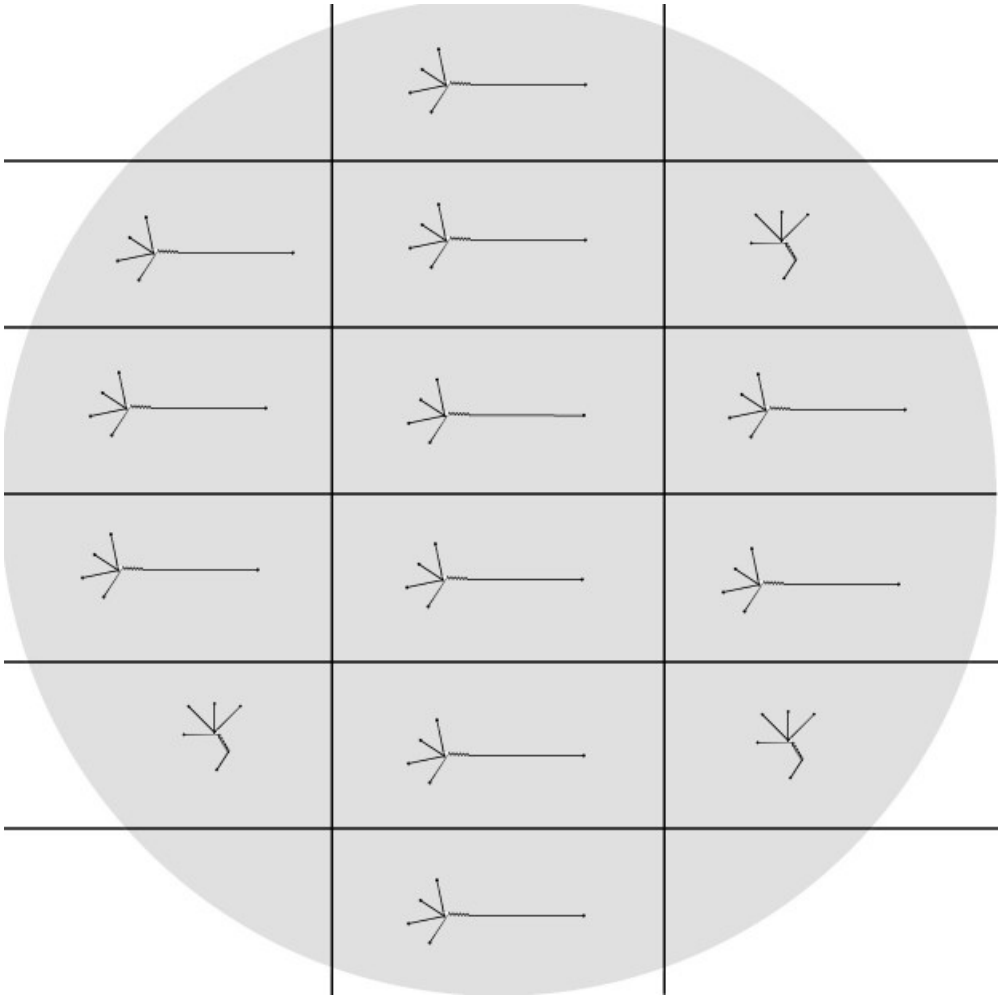

Figure 2.8 UV mask for SU-8 master mold fabrication

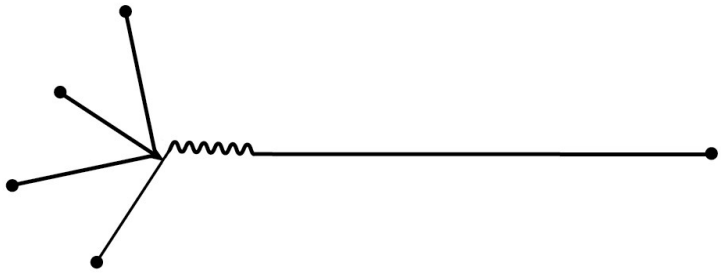

Figure 2.9 Close-up View of the Microchip Pattern

Micromolding polydimethylsiloxane (PDMS) microfluidic devices.[85]

In order to make the PDMS chips the polymer must be prepared. We poured pre-polymer and added a curing agent to it at a 10:1 ratio, which is then mixed. The mixture is then placed in a desiccator for approximately 45 minutes (or until most bubbles are gone). We placed the 3" SU-8 masters in Petri dishes, or flat-bottomed Pyrex glass dishes for the 6" diameter large masters, and poured PDMS mixture over each. The glass dishes were placed on a hotplate and set for 2.5 hours at 80 ºC. In order to maximize the efficiency and not crack the polymer by over-baking, we used an AUTO OFF feature that initiated a cool down mode. Once the PDMS was cured, we carefully removed the PDMS and wafer from the Petri. We then used the spatula to separate the PDMS from the Petri dish edges and then had to carefully pry the PDMS and wafer out. After cutting the wafer out of the PDMS by running an x-acto knife around the edge of the wafer we then very carefully peeled the PDMS off of the wafer, making sure it wouldn't tear. We verified none of the SU-8 remains in the channel imprints, and then proceeded to bonding. If SU-8 remained in the channels a sharp probe or x-acto knife can be used to remove it.

Bonding PDMS devices

We cleaned all the particulates and dust off of the bonding surface of the PDMS with a piece of Scotch tape or packing tape before proceeding. Once the individual halves were separated they were cleaned using DI water and methanol. An instrument air nozzle was fixed with a pulsing handle in order to deliver filtered instrument air at a high pressure to clear away particulates and liquid. PDMS can be reversibly or irreversibly bonded.

Reversible Bonding of PDMS Chips

We simply placed our PDMS molded chip half onto a glass slide or slide coverslip (making sure it was of optically flat glass) in a Petri dish, or macor plate depending on what was available. Glass surfaces needed to be cleaned with isopropyl alcohol (IPA) to improve adhesion. We let the sandwiched chip sit with a flat weight resting on top in order to create an even seal.

Irreversible Bonding of PDMS Chips

This method used a Plasma Cleaner in the laminar flow hood. We placed the unsandwiched PDMS and glass in the vacuum chamber, held the lid in place, and turned the vacuum pump on. We had to make sure the needle valve attached to the lid is fully closed (clockwise) and turned the plasma on to "HIGH". We slowly turned the needle value counterclockwise until the plasma became more intense (less than one revolution). If we kept turning the valve counterclockwise, the intensity would begin to decrease. At that visible maximum is where we set the cleaner. We treated the PDMS and glass for 20 seconds. After turning the plasma off and then turning the pump off, we held the lid so that it did not fall on the floor after the chamber purges. We removed the PDMS and glass from the chamber and pressed them together. After placing a weight on top to aid in adherence the chip was left to sit for a few hours to finalize bonding.

Results and Discussion

After measuring the irradiance using the digital multimeter as described above, we found that we were getting a very irregular, asymmetric, and weak irradiance pattern. Upon testing the irradiance from the reflected indirect setup it was found to be too weak and uneven. (Figure 2.10)

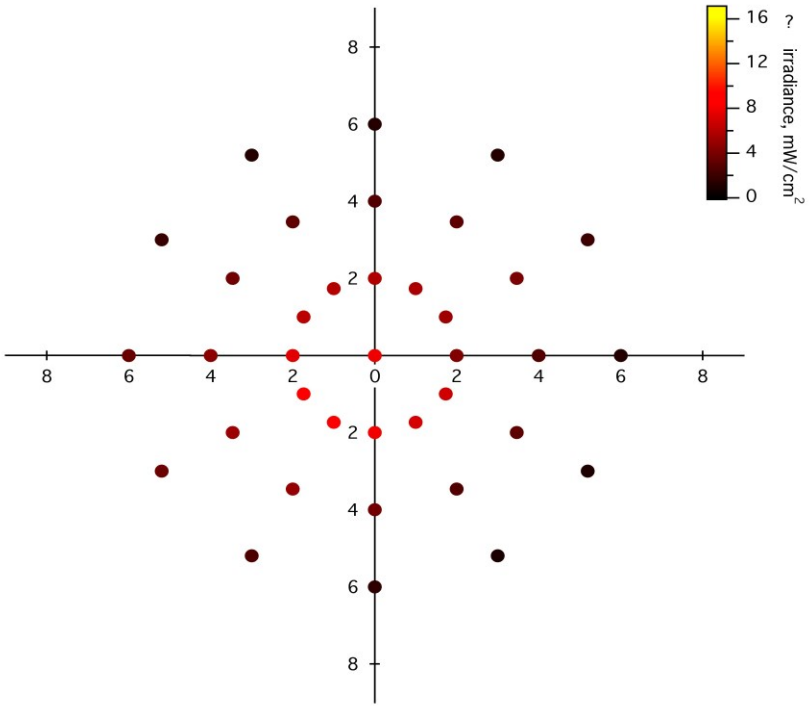

Figure 2.10 - Irradiance map of reflected UV light: The scale on the right is in mW/cm^2 with yellow being the most intense and black being the least intense.

The amount of power that is coming from the reflected light is not strong enough to polymerize either the SU-8 or PDMS. Since this was an initial concern in the setup of the lab, a direct illumination irradiance map was created and a comparison of the two irradiances can be seen in Figure 2.11.

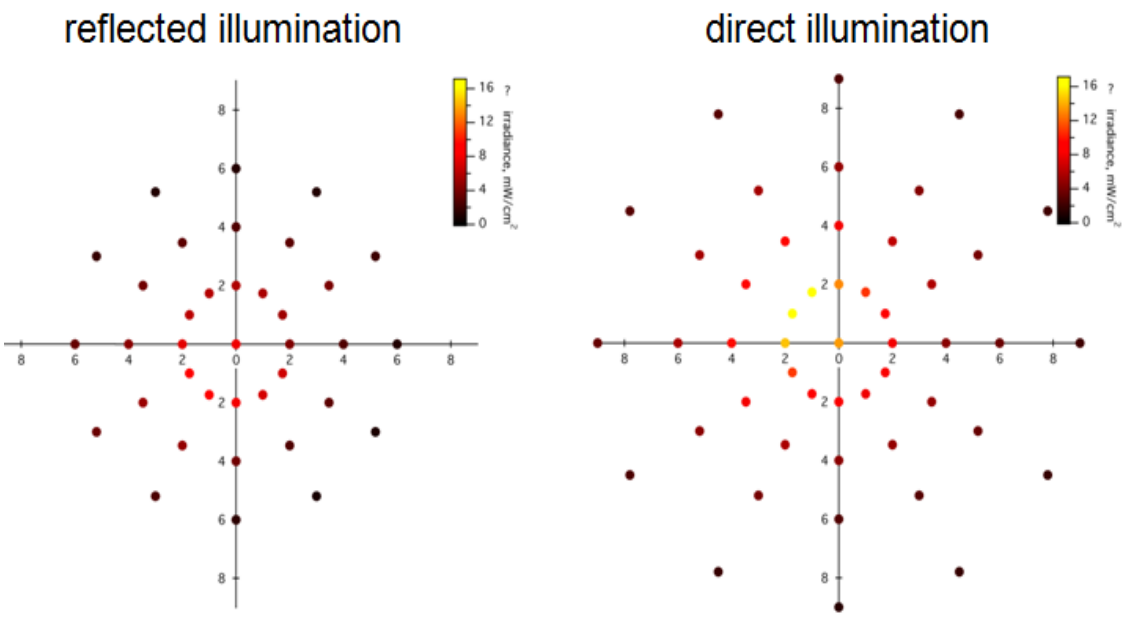

Figure 2.11 - Reflected vs. direct illumination: The irradiance is measured in mW/cm^2.

The direct illumination was initially thought to have too much light and have too uneven of an exposure pattern. An attempted filter was created using the inverse of the irradiance pattern as a guide, allowing for destructive interference to aid in correcting the illumination. This was thought to even out the irradiance giving a more uniform pattern. The shutter system was modified to allow the lamp to illuminate the exposure area directly. After testing the filter the exposure took too long to polymerize the SU-8 photoresist for the glass chips. The filter was abandoned and the bare exposure was used with the photoresist. The methodology was modified to rotate the chip every 7 seconds so that it was uniformly exposed. Eventually it was found that even this was unnecessary in the direct UV irradiance. The lab eventually upgraded to a Newport NUV Illumination system that has 4.29 W/cm2 irradiance in a symmetric and uniform illumination pattern

with self-correcting optics. This allowed for the chips to have a uniform irradiance and minimized any defects that had occurred using the old system.

Glass Microchip Fabrication

The initial usages for the glass microfluidic chips were for performing cell lysis and lipid capture. In the use of microchips for capture of lipids by SPE, trace clean-up and capture is desired in order to introduce trace analysis. Using Adobe Illustrator CS-2, a mask was created with features of 190-micron wide channels with a dual weir design. The design (Figure 10) was printed onto acetate transparencies to be used for chip making.

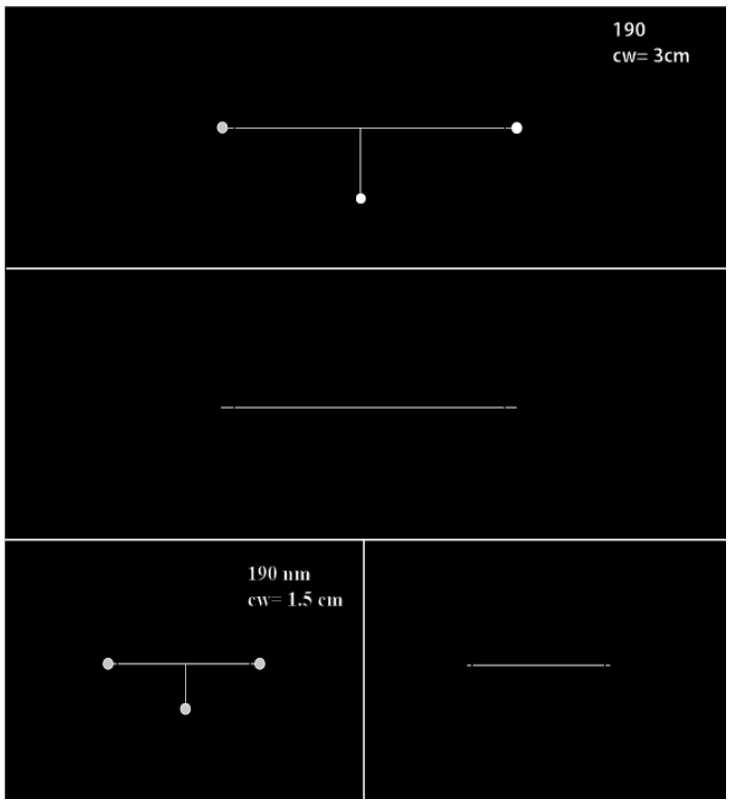

Figure 2.12: Photoresist design for microfluidic SPE chips

However, it was found that the design was not transferred to the photoresist. It is unknown why this happened, due to the lamp's exposure wavelength being at 365 nm,

which is transmitted by the transparency. It was decided to fabricate microfluidic chips using photographic emulsion photomasks created by Pixels (Charlottesville, VA). The first step was exposing the photoresist with the patterned photomask on top to UV light. The photomask used is seen in Figure 2.13.

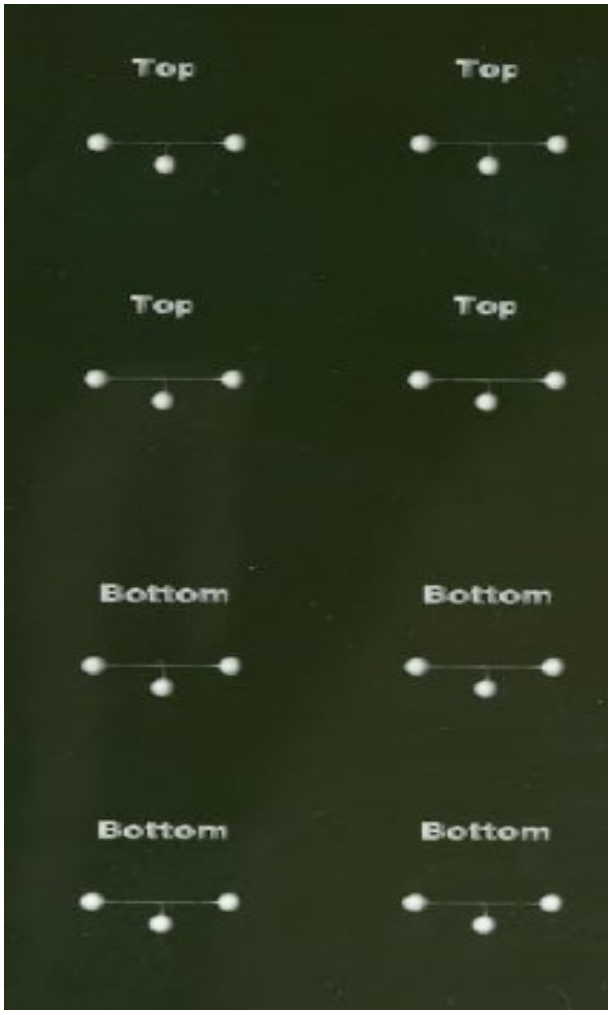

Figure 2.13 - Photoresist used to fabricate microfluidic SPE chips. Top and bottom labels can be seen for the chips.

Bonding, as described above, was performed by sandwiching the two sides of the chips and aligning the weirs, channels, and wells. The chip was then sandwiched between two Macor ceramic plates, a 400 g weight was placed on top after initial tests

showed that any lighter would cause incomplete annealing and heavier would cause the glass to anneal to the macor or fracture. The temperature ramp was taken from 25 °C to 600 °C at 10 °C per minute, held for 8.5 hours, then ramped back down at 10 °C per minute. Chips were then removed and examined under stereoscope to verify bonding. (Figure 2.14)

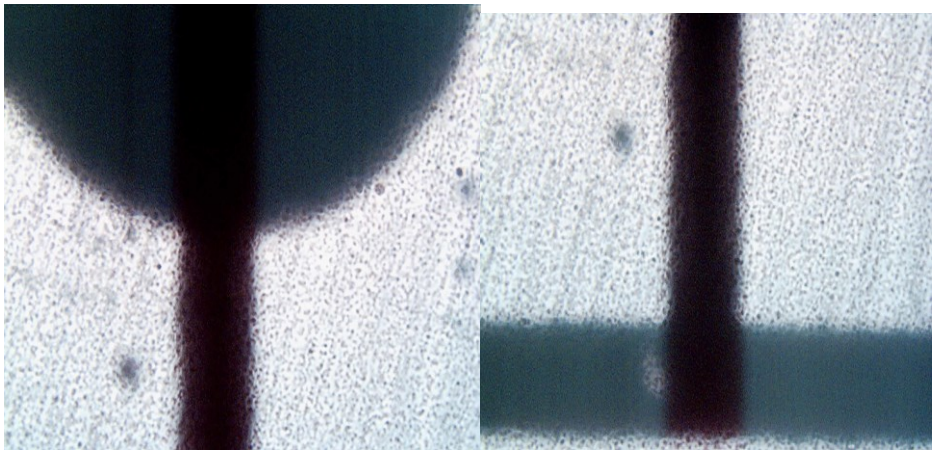

Figure 2.14: Stereoscopic images of fabricated microchips. Left: image of channel-well intersection Right: image of t-junction.

This project was successful enough that further scientific analysis of extracted lipids was attractive. After training on how to fabricate the chips themselves, the separation project was then transferred to Tao Sun to perform for his doctoral dissertation on μF/LC/MS of lipids. This allowed us to focus on more difficult projects and the microfluidic project moved onto microreactions where a new design was needed as seen in Figure 2.15. The pattern included 30 turns then a long transport channel before another 50 turns. Detection can be moved between the initial short turns and the secondary long turns.

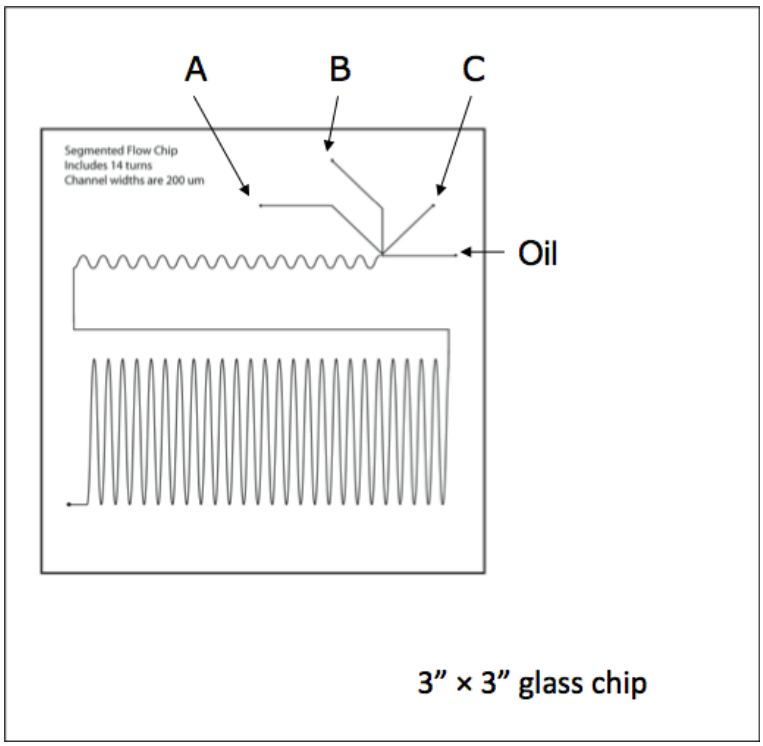

Figure 2.15 - Chip layout for fluorescence tagging of amines. Wells are labeled to define different reactants. For initial imaging and droplet measurements: A=H_2O, B=FITC, C=H_2O. For the mixing studies: A= H_2O, B=FITC, C=HCl. For the FQ/amine &NDA/amine tagging reaction: A=FQ/NDA, B=amine, C=KCN

This design was tested in several ways to verify that the design worked and would present a viable method to do tagging reactions at very small concentration for LIF detection. Once the chips were made, several tests were performed. For droplet verification and fluorescence imaging a 590DF40 filter was added to a Leica stereoscope fitted with a digital CCD camera. Rhodamine 6G, a fluorescent dye that absorbs at 488 nm and emits at 590 nm was used for the imaging. As can be seen in Figure 2.16 the rhodamine fluoresced brightly, illuminating the channels and showing the clear delineations between the perfluorodecalin oil and the rhodamine solution.

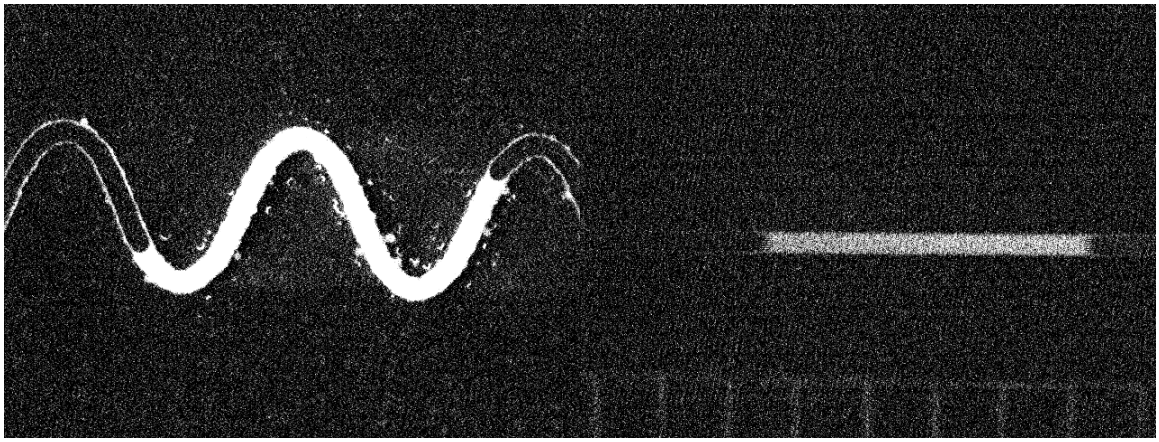

Figure 2.16 Rhodamine 6G droplets imaged in the channels of a glass micromixer chip

Once the rhodamine was imaged, mixing was tested using FITC, a well known pH sensitive fluorescent dye. Figure 2.17 depicts the droplet formation over time between FITC at pH = 10.4 and water. The same imaging setup was used as the Rhodamine tests with the only change being the changing of the filter from the 590DF40 to a 510DF20. One other change that occurred in this time was the switch from glass to PDMS chips primarily due to their ease of fabrication. The FITC is shown through every other turn on the newer chip (12 total turns vs. 80 on the old chip). FITC was clearly seen in each droplet throughout the whole chip.

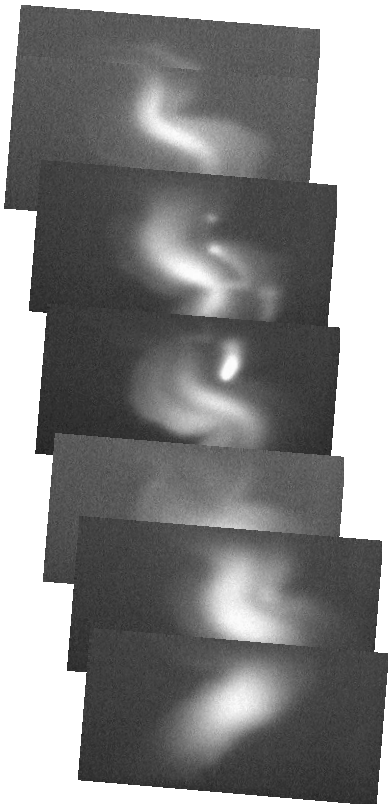

Figure 2.17 31.4 uM FITC at pH=10.4 in channel B, H_2O in channels B & C

Once the imaging was verified that we could see FITC throughout the chip; Channel C's reactant was swapped from H_2O to 10 mM hydrochloric acid. Due to FITC's sensitivity to pH conditions the HCl should quench the fluorescence quickly if the FITC mixes with it or slowly if the FITC and HCl mix by simple diffusion. We then would expect to see the fluorescence very slowly diminish if mixing is not seen on chip while if the droplet is mixing then the fluorescence would disappear.

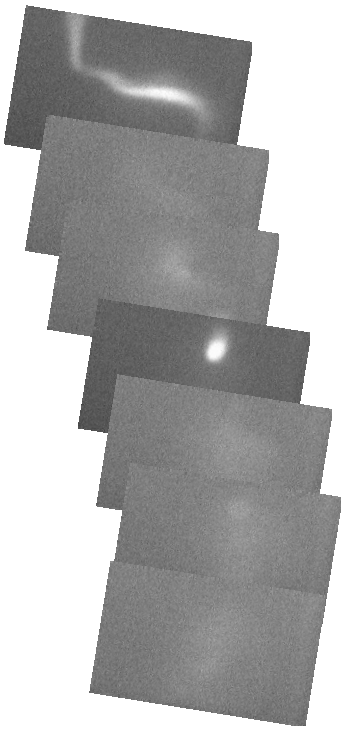

Figure 2.18 FITC as mixed with 10 mM HCl. Note that the fluorescence is quenched before the droplet goes through one full turn.

As Figure 2.18 demonstrates, the FITC was quenched quickly and efficiently, before the droplet goes through one full turn cycle, demonstrating the functionality of the micromixing within the droplets. We imaged further turns to verify that the fluorescence did actually get quenched and not that there was an issue with imaging. The fluorescence was fully quenched and gives incredible support to the microdroplets working for our needs.

What was incredibly exciting was that the proof of mixing allows for the system to be adapted for the mixing of a fluorogen with amines for their detection using LIF. A small-scale reaction setup was added to our toolbox.

Conclusion

The fabrication of microfluidic chips has allowed for the miniaturization of several processes within the lab. Chip based solutions for analyte extraction, reactions,

and fluorescence detection open up a suite of solutions that allow for the minimization of solvents, sample sizes, while also maximing the ability to multiplex analysis. Mixing in microdroplets has been shown, allowing for adaptation of a fluorogen and analyte mixing scheme to be used. The goal of this project was to create a platform that would eventually allow for the minimization of the reaction of FQ and, eventually, NDA with amines onto this platform. The results show that this platform is very attractive and flexible showing promise for the future studies.

The fluorescence was easily and vividly captured using the microfluidic platform and chosen optics. This allows the researcher to have confidence that their results will be well captured when building a complete laser induced fluorescence detection setup for the trace and ultratrace analysis of the amines.

One other aspect of these tests showed the possibilities of PDMS and glass based chips. The initial fabrication and the projects that eventually became the basis for Tao Sun's dissertation were all fabricated from glass-based substrates. As the project moved on the PDMS was tested, fabricated, and eventually won out. The move from glass to PDMS has allowed chips to be more readily produced and altered at a fraction of the time (1-3 hours fabrication time for PDMS versus 12-16 for glass) and cost (PDMS chips are $0.10 - $0.50 a chip whereas the glass plates alone are several dollars which doesn't include the chemical treatments).

Future Work

The microfluidics platform allowed for the miniaturization of several processes in the laboratory. Solid phase extraction, lipid-capture for cell profiling, and microreactions have all been shown using the setup established in this project.[91-92] Future work is

focusing on optimizing the fabrication process to maximize its efficiency and turnover. Another area that future work is attractive would be an integrated full analysis system, grouping the sample preparation, pre-concentration, tagging reaction, and detection schemes all in a 3 x 3” chip.

Chapter 3: Design and Optimization of a Laser Induced Fluorescence System

Introduction

Microfluidic chips have been described in a broad range of applications in the literature.[90, 93-101] One of these applications is the use of segmented flow. Segmented flow has been used for miniaturizing reaction schemes[60, 102], encapsulating cell profusion[103], and performing PCR.[104] One of the most attractive reasons for using segmented flow is the ability to detect analytes at ultratrace levels within the droplets with a minimization of band broadening and further dilution[61]. By encapsulating the target within a droplet, minimizing the diffusion and band broadening, enhanced detection sensitivity is achieved.[105-107] Detection methods for segmented flow devices are as varying as their uses and have included mass spectrometry,[61, 91, 108] electrochemical sensors,[109-111] and colorimetric assays.[98] Arguably the most sensitive detection scheme for microdroplets and microfluidics in general is fluorescence.[62, 112-113] However, fluorescence detection is only as sensitive as the detection setup.[62, 112-113] In this report we describe a method to optimize an epifluorescence detection setup originally described by Johnson et al.[62] for use with segmented flow microfluidic chips.

Experimental

Design Layout and Choosing Optical Components

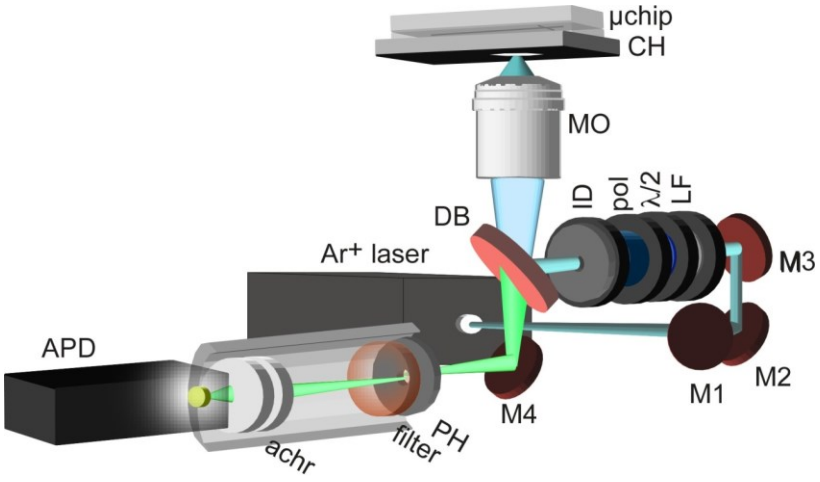

Figure 3.1 - LIF Setup: Inverse microscope setup for laser induced fluorescence on an optical table. Incoming, 488 nm, beam is in blue and fluorescence is in green. Abbreviations are described in the text.

The FQCA analysis, as discussed in chapter 4, requires a 488 nm excitation beam, which coincides with the main line of an Argon ion laser. This main line also is optimal for the FITC tests described in chapter 2, and the two sets of rhodamine 6G tests described in chapter 2 and this one as well. The NDA analysis, described in chapter 5, used a solid state diode laser that emitted at 405 nm.

Optical "front-end" and "back-end"

When building the setup, several optical elements are needed to get the beam of laser light to the sample.to excite it, often called the optical front-end. The optical back-end is therefore the set of optics used to get the emitted light from the sample to the detector. Both of our analyses used the following: A microscope stage, Chip holder (CH), which included micrometers for holder manipulation to align the laser with the sample channel.

Also included in the optical scheme were the following lenses. Some of the elements were only used in one of the setups and are noted as such:

- microscope objective (MO) – for magnifiying the sample channel to obtain as much photon detection as possible. This was normally a 40x objective, however a 10x and 30x were used in some tests.
- dichroic beamsplitter (DB) – The dichroic beamsplitter split the multiwavelength Argon ion beam into its principal components allowing for the usage of the 488nm line without the interferences of the other lines. This was used only with the Argon ion laser.
- iris diaphragm (ID) – The iris can be dialed in to a selected aperture size which allows for the selective sizing of the beam spot. This maximizes the uniformity of the laser beam on the sample.
- polarizer (pol) – Allows for polarized light to either be allowed through the system or selectively filtered out. Has two settings, horizontal and vertical.
- Interference filter (λ/2) – Causes reflected light entering the filter to be turned 180 degrees out of phase. This out of phase light interacts with the reflected light and cause destructive interference.
- Line filter (LF) – This creates a tight band of light that is allowed through. In the Argon ion laser a 488±15 line pass was used. The ±15 is the nm gap around 288 that is allowed through. In the SSDiode laser a 405±20 was used.
- Mirrors (M1-M4) – optical quality mirrors. They must completely reflect the laser light with minimal interference.

- Pinhole (PH) – The pinhole is part of the detector tube optics. It acts similar to the Iris by maximizing the uniformity of the detector spot while minimizing the reflected light into the tube optics.
- Bandpass filter (filter) – Similar to the LF but made for the emitted analyte fluorescence. The FQCA (and rhodamine) setup used a 590±35 filter while the NDA setup used a 488±15.
- Achromat lens (achr) – Used to magnify the spot size onto the CCD of the detector.
- Avalanche photodiode detector (APD) – detector similar in functionality to a faraday cup electron multiplier. A photon enters the CCD and causes a cascade of photons. These photons in turn cause their own cascade each until an "avalanche" of photons hit the diode detector plate.

Alignment of System

Optical Alignment

In order to test the system a full optical alignment needed to occur. This is very tedious work that requires the researcher to adjust each individual optical element until it reaches an optimal level and then move to the next element. Once that element is optimized the researcher must go back and optimize every element in front of it again to verify they are at their mutual optimization. A full description of these manipulations can be found in the appendices.

Signal Alignment

Once the optical elements are aligned a signal alignment takes place. This is where an active sample is added to the sample stage and the stage and detection scheme is manipulated to maximize the sensitivity of the analysis. The researcher simply manipulates the micrometers while monitoring the signal in the detection software until it hits a maximum signal-to-noise ratio. Once these alignments are performed the system then can go through the optimization tests.

Optimization Tests

Power Test

In order to optimize the detection of fluorescent molecules, the maximum power of the laser must be used that does not cause quenching of the fluorescent molecule. In order to do this the researcher must manually manipulate the power of the laser beam. The power of the excitation beam was varied from 10 mW to 25 μW, which is accomplished by adjusting the laser beams power output while verifying the power using a digital multimeter fitted with an iris diaphragm. The power was measured before the dichroic beam splitter due to the ability to control and measure the full beam power readily. The signal was measured in multiples of five readings and averaged to allow for the natural beam fluctuations that occur in laser light.

Polarization Test

Once the power tests were optimized, the next step was to hold the power constant at 10 mW and vary the polarization of the excitation beam. Polarized light can be a hindrance to signal-to-noise and low concentration detection. In order to verify, the

variance of the noise must be measured over the polarizers range. The polarization is adjusted by rotating the face of the polarizer holder in increments of 10 degrees. The polarization was measured over 360 degrees and then refined over 180 degrees. This variance monitors the change of the polarization from horizontal to vertical and back. Horizontal polarization allows polarized light to pass through the filter to the sample and is parallel to the optical table while Vertical polarization blocks the polarized light and is perpendicular to the optical table.

Pinhole Test

The final variable tested was the pinhole diameter. The highest intensity of the excitation light is at the focal point of the lens, but nonetheless, the other parts of the sample do get some of this light and they do fluoresce. This contributes to a background haze in the resulting image. Adding a pinhole solves this problem. The response was measured using six different pinholes. Polarization and power settings were kept at vertical polarization and 10 mW, respectively. The optimal pinhole will allow the most signal without allowing quenching of the sample.

Spectral Studies

The efficiency of the optical filters and a general evaluation of optical bandwidth were desired to verify that back reflectance wasn't increasing the noise in the system. The APD was removed and a 150 mm spectrograph was added to the inverted microscope setup to evaluate the spectra of the droplets. The visible light spectrum was scanned using the spectrograph and was plotted to verify that most of the laser light was being eliminated from the detection scheme.

Results and Discussion

Power Study

After measuring the fluorescence response at each power setting the data was averaged to give a data point of the average response with a standard deviation. Figure 1 shows the results of the beam intensity test. The maximum signal-to-noise ratio was found to be at 10 mW for the Argon ion laser. Surprisingly the laser power never hit its quenching maxima. One would expect that once the fluorescence intensity hits a maximum, if the laser power is pushed higher then fluorescent molecules would be quenched and the total signal would actually flat-line then fall. This was not seen with this particular fluorophor and laser.

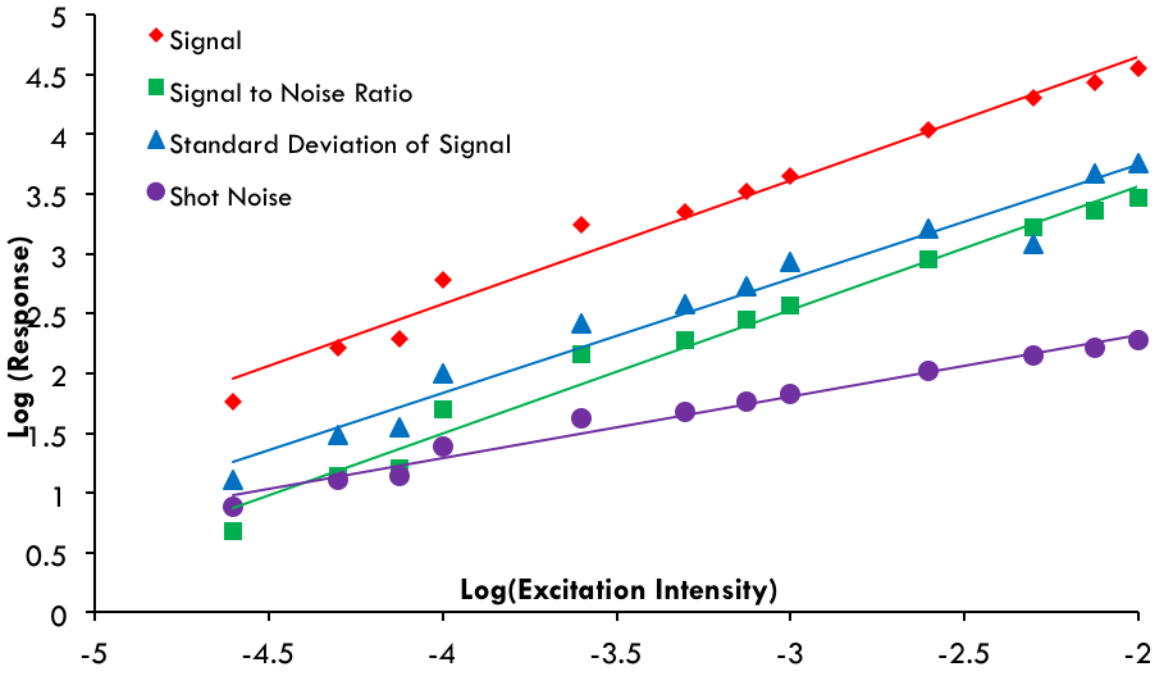

Figure 3.2 - Laser intensity test results. Each point is an average of the maximum signal to noise ratio was achieved using a 10 mW intensity setting

Polarization

After measuring fluorescence response at each polarization setting the data was averaged to give a data point of the average response with a standard deviation. Vertical polarization was found to maximize the signal to noise ratio by minimizing the variance of the noise. This would be the optimal setting for our analyses. This lends credence to the hypothesis that reflected and refracted light caused noise in the system and using the vertical polarization, which removes that reflected light, gave a cleaner signal.

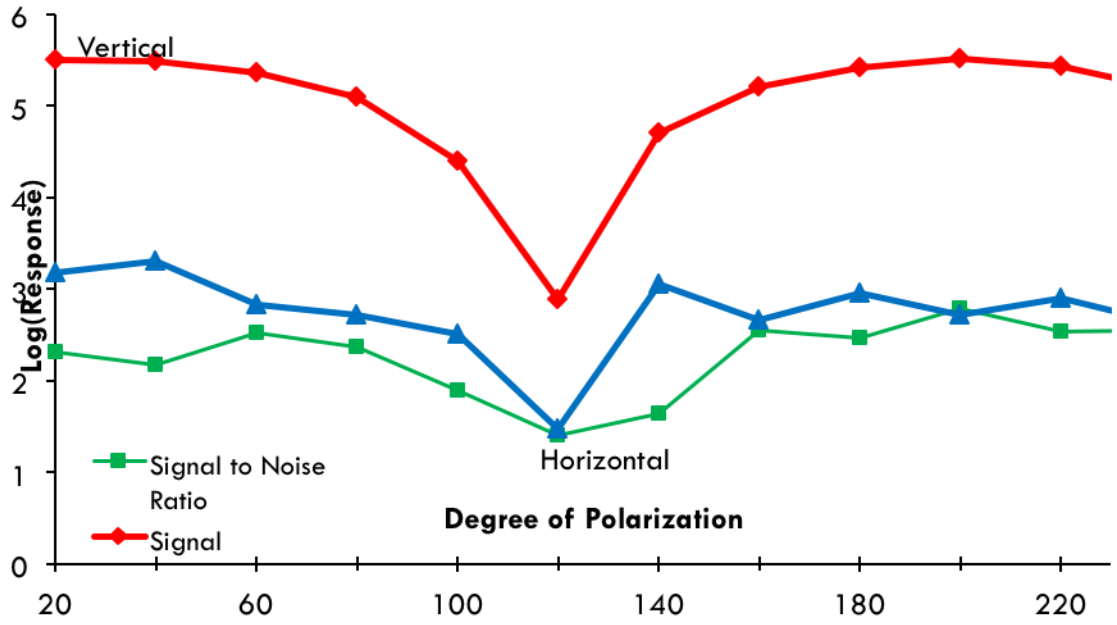

Figure 3.3 - Polarization test. The maximum signal-to-noise ratio was found to be at vertical polarization for the Argon ion laser.

Pinhole

After measuring fluorescence response at each pinhole setting the data was averaged to give a data point of the average response with a standard deviation. These

were then plotted to see if a plateau was found and whether that plateau ended with a pinhole size that allowed the quenching of the fluorescence (seen as a downward slope). From these studies an 800 µm pinhole was chosen for further analyses. As hypothesized, but not seen, with the power study, a pinhole that is too big would actually allow for too much laser light to be exposed to the analyte causing Joule heating and quenching. The slight down-turn of signal at 1000 µm pinhole shows this starting to happen.

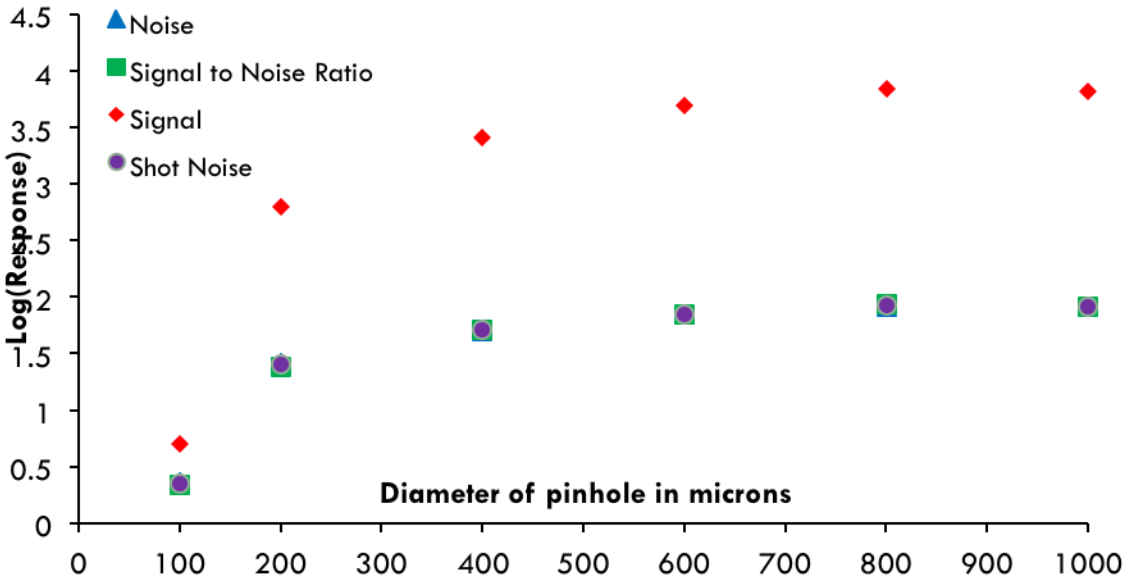

Figure 3.4 shows the results of the pinhole test. The maximum signal-to-noise ratio was found to be at 800 microns for the 40× MO

Spectral Studies

Using the optimized settings of 10 mW laser intensity, vertical polarization and an 800-µm pinhole, droplets were analyzed using a 150 mm spectrograph. The primary goal of the study was to evaluate the optical bandwidth and efficiency of the filters. As the spectrograph scanned across the wavelengths the signal would change based on the optical elements in the system. Ideally only one clear peak would be seen but impurities or misalignment would cause sharp peaks in the signal.

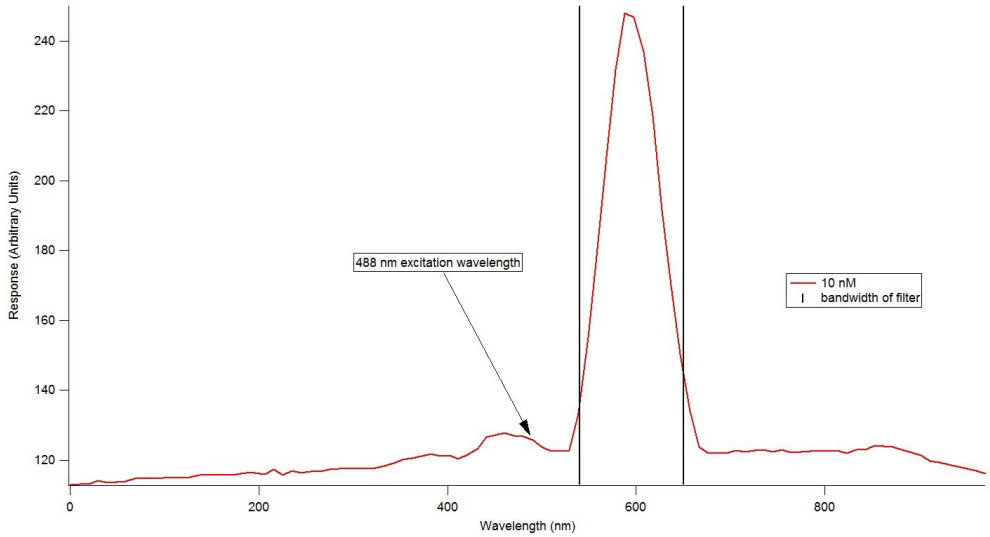

Figure 3.5 - Optical component efficiency. The black lines denote the bandwidth of the emission filter. The 488 nm laser line is noted on the spectra.

As Figure 3.5 shows the 6 cavity dichroic filter is very effective at removing excitation light while still allowing 95% of the emission band, the bandwidth of the filter is shown by the black window bars and the excitation wavelength is noted. The primary goal of the study was to evaluate the optical bandwidth and efficiency of the filters along with the alignment of the system. The 6 cavity dichroic filter is found to be effective at removing excitation light.

Detection Limits

Droplets of Rhodamine 6G in methanol were generated in the microfluidic device and the fluorescence was measured over several minutes. Droplets were generated from 0.5 minutes until 3.5 minutes. One thing noticed in the droplet spectra, especially at low concentrations was the pulse at the beginning of collected spectra due to the syringe pumps being turned on. After a settling time the droplets maintained minimal variability.

The leading and trailing baseline are due to a stream of the immiscible mobile phase, perfluorodecalin, before and after the aqueous channels were started.

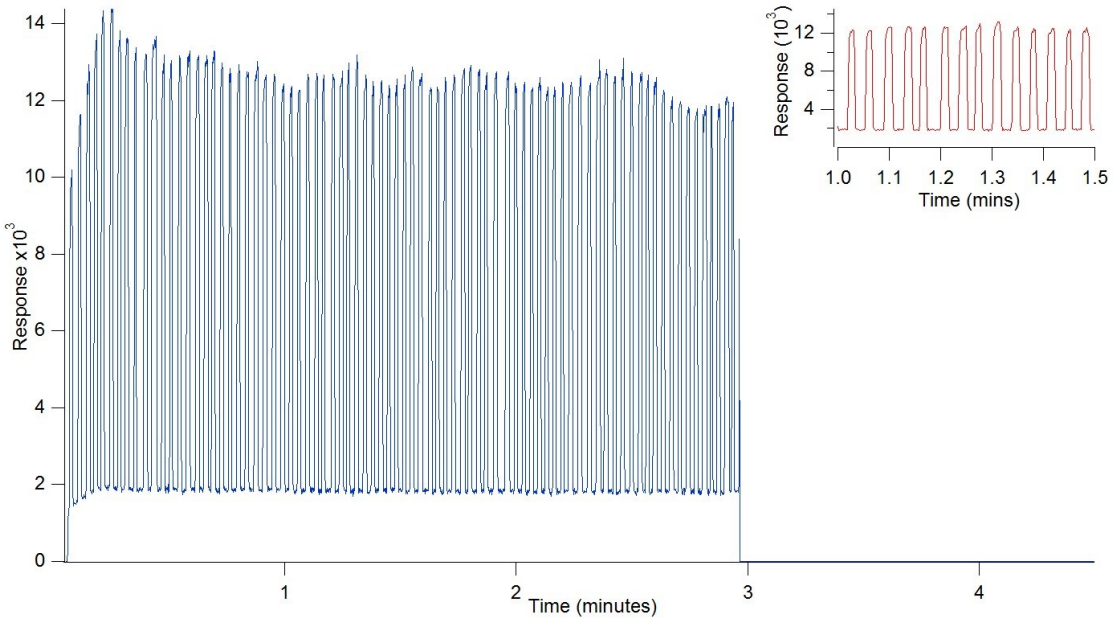

Figure 3.6 - Fluorescence chronogram of 33 nM rhodamine 6G.

Optimized settings were used to obtain a maximized signal-to-noise ratio of 164 for droplets with a peak height of 12,000 counts/second. The inset to Figure 6 shows peak shapes of individual droplets over a 30 second span. The droplets are reproducible and statistically consistent. The average sample load in droplets is 170 femtomoles of Rhodamine 6G. This was calculated using the 150 µm channel width, perfluorodecalin carrier phase flow rate of 4.8 µL/min, aqueous phase flow rate of 0.8 µL/min and that Rhodamine 6G is at a concentration of 10 nM. Rhodamine 6G was then diluted to 100 pM to test for detection of single digit femtomole loads. All other flow rates and settings stayed consistent.

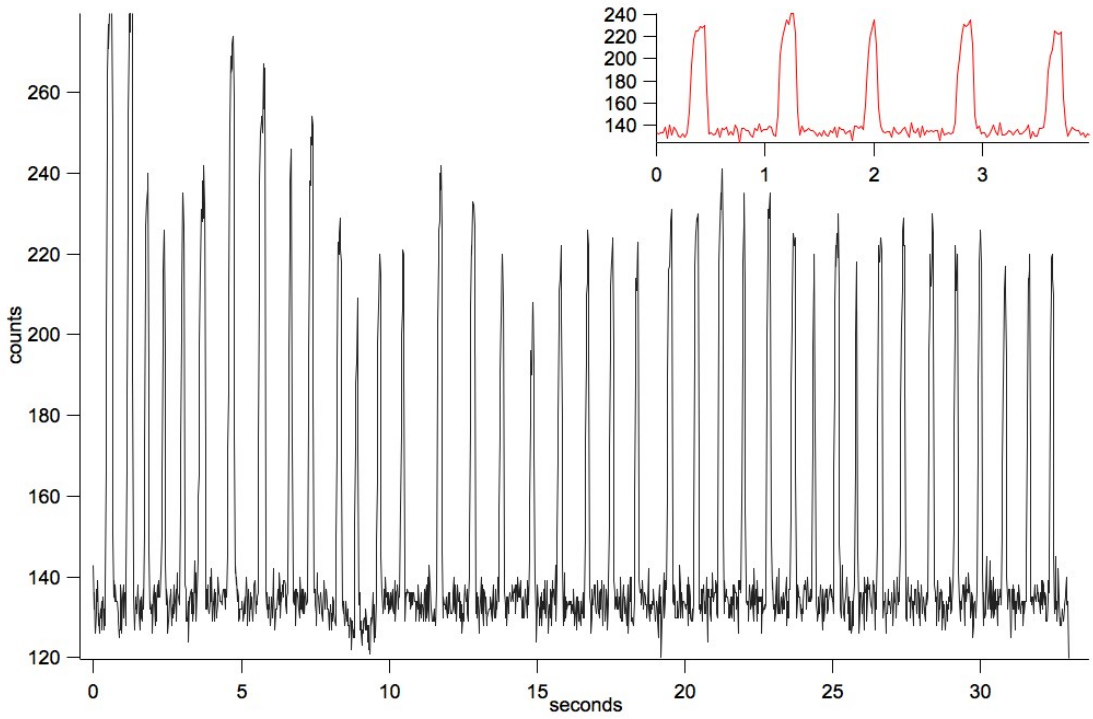

Figure 3.7 – Chronogram of rhodamine 6G at 100 pM concentration in droplets. Inset is to show peak detail and reproducibility.

Once these tests were found to have rather high signal-to-noise ratios (2000 for the 100 pM study), it was decided to try and push the absolute limits of the system by running a sample of 10 fM Rhodamine 6G, giving us sub-attomoles of fluorphor in the droplets.

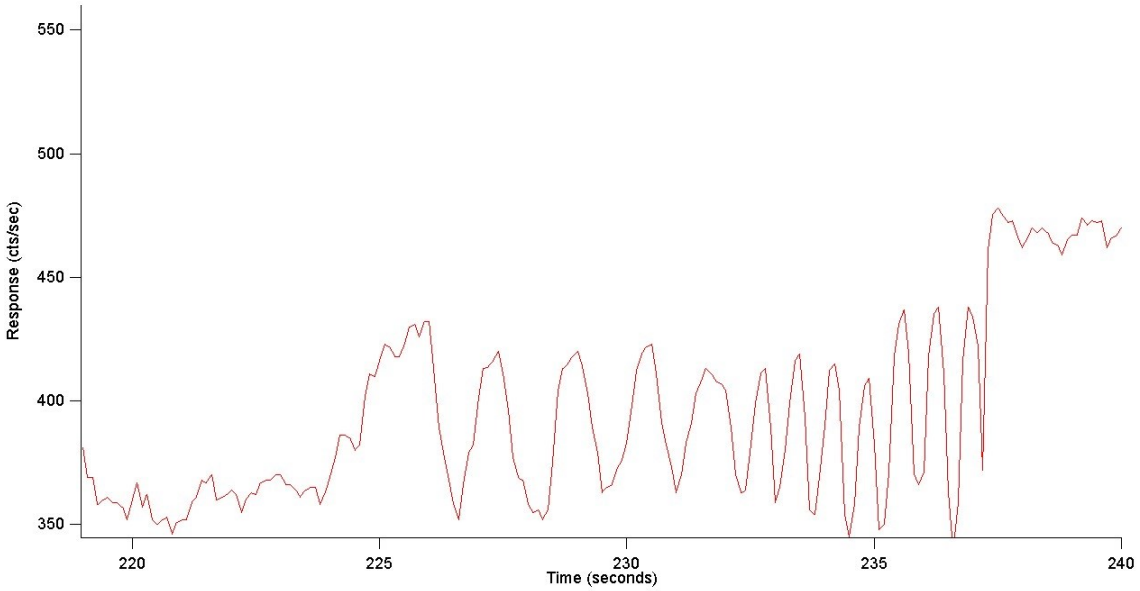

Figure 3.8 - 10 fM rhodamine 6G in droplets on a chip

The detection, while successful, for the 10 fM sample pointed out the limits of the system, as the stability of the droplets' detection began to fail due to the incredibly low concentration makeup of the droplets. This was most likely due to the detector missing the droplets due to their low level fluorescence. This data however was incredibly exciting since it proved to the researcher that the setup was ready for analysis. A system that allows for attomole sample loads gives the researcher an extremely powerful analytical scheme for ultratrace detection that eliminates detection limit as a point of concern.

Conclusion

The detection of sub-attomole sample loads in segmented flow microdroplets is highly attractive in the investigation of trace and ultratrace analysis. In order to detect these droplets an optimized system must be used to minimize noise from the instrument and background reflection from the chip itself while still yielding a high signal to noise

ratio. By obtaining the optimum values, in this case 10 mW power, vertical polarization, and an 800 micron pinhole diameter, the signal to noise of the system is maximized while the system noise is minimized. By varying only one of the variables at a time an optimized system can be achieved. The optimized system was then used to analyze Rhodamine 6G droplets. The chronograms display that after a short equilibration period, stable and reproducible droplets are formed and detected. Although the system has been optimized it becomes apparent that although the system has an incredible detection limit that the droplets themselves need to be altered in order for them to maintain stability at very low concentrations. The design of the chip, by adding a detection channel that is narrowed, allowed for more of the droplet to be detected and allowed for the lower detection limit. The system appears extremely attractive for the porting of a fluorogenic reaction system such as that of FQCA or NDA.

Chapter 4: FQCA as a Fluorescence Marker for Primary Amines

Background

Lipids and Lipidomics

Lipids are an important biochemical subspecies that are involved in many different areas of mammalian biology. Lipids are bioorganic hydrocarbon based molecules that are soluble in nonpolar solvents but are almost insoluble in water. Lipids have various biochemical duties including energy storage (fats and sterols such as cholesterol), cell makeup (lipid bilayers and micelles), and some are essential hormones (steroids and eicosanoids).[6] The quantitative study of lipids is a burgeoning field in bioanalytical chemistry. The reason lower detection limits are attractive to those studying lipids is that some are in trace (picomolar (10^{-12}) – nanomolar (10^{-9})) and even ultra-trace (femtomolar (10^{-15}) and below) concentrations in samples.[114-115]

The sample volumes are usually minute, for example, there is only about 140 mL of cerebrospinal fluid (CSF) in the average human body. The CSF is mostly water and contains very little cells, hence the clear and colorless nature. In an early study by Nagai and Kanfer[6], the concentration of lipids in 100 mL of CSF was calculated. Only 87.2 nanomoles of total organics were isolated. This 87.2 nmol was not just lipids, specifically cerebrosides, but also proteins and hexoses.[6] Other lipids such as endocannabinoids, like anandamide, are researched due to their possible drug effects and binding to natural cannabinoid receptors in the brain.[116-124] An area that is intriguing to us is primary fatty acid amides, or PFAMs. The PFAMs are a neutral lipid family that is

part of the fatty acyl group and have been shown to be in the CSF of cats, mice, and humans, omentum samples and as slip additives in plastics.[4, 14, 70, 125-131] Oleamide ($C18:1^9$) is a primary amide that demonstrates a variety of physiological effects. Intraperitioneal administration of oleamide into rats induces sleep and hypomotility and exhibits long-lasting hypothermic effects.[132] Oleamide has been found in human plasma and circulating levels of 35 nM and 56 nM have been reported in rat plasma as opposed to 156 nM in CSF.[14, 130, 133-134] Oleamide has been linked to GABA inhibition and binding to dopamine and 5-hydroxytriptamine (5-HT) receptors.[25, 126, 135-137] Recently, oleamide has been shown to inhibit voltage-gated Na+ channels at concentrations of 100 μM, concluding that oleamide acts similarly to anesthetics.[25, 132, 138] Oleamide has been shown to be a potent regional vasodilator and a modifier of gap junction in the heart and endothelial cells with a half-maximal effective concentration of 1.2 μM.[25] Another study of oleamide derivatives showed their possibility as prototypes for anticancer drugs due to their ability to suppress spontaneous metastasis in the BL6 line of melanoma cells at 10 mg/kg. [25, 139-140] Palmitolyethanolamide has been shown to interfere with inactivation of endocannabinoids, thus enhancing their actions at cannabinoid receptors.[141-142] These low concentration levels demand sensitive techniques at the trace and ultra-trace levels.

Fluorescence and Detection

In order to detect at trace and ultratrace levels a highly sensitive technique with low detection and quantification limits is needed. The most used identification technology utilized in lipid studies is mass spectrometry (MS) but laser induced fluorescence (LIF) detection is employed in situations where its increased sensitivity and

lower detection limits are necessary. Fluorescence is the excitation of an incident, or initial, photon and emission of a photon that varies in wavelength from the incident photon.[32] Fluorescence is a resonant effect in that there is a resonance lifetime between the excitation to an excited electronic state, its relaxation to a parallel vibrational state, the relaxation to its electronic excited state and then the emission of the shifted photon.[32] Fluorescence always deals with a Stokes, or red, shift.[33-36].

LIF is made possible by "tagging" the lipid with a fluorophor or a fluorogen, both of which are fluorescing compounds; the main difference between the two fluorescent types is their natural fluorescence. Fluorophores have a natural fluorescence, while fluorogens only fluoresce when they are bound to a specific molecule type. Some of the tags used in the amine studies include fluorescein isothiocyanate (FITC), 3-(p-carboxybenzoyl)-quinoline-2-carboxaldehyde (CBQCA), and 3-(2-Furoyl)-Quinoline-2-Carbaldehyde (FQCA). Fluorescein, a typical fluorophor, is widely used in many areas of research.[38] It has a strong excitation maximum at 488 nm and an emission peak at 512 nm. FQCA, a fluorogen, reacts with amines to produce a highly fluorescent aromatic complex (Scheme 4.1) that excites at 480 nm and emits at 590 nm.

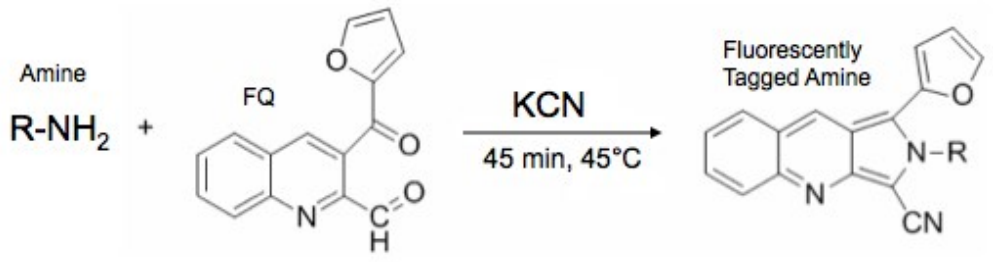

Scheme 4.1: Reaction of FQCA with primary amines yielding a fluorescent molecule.

The advantage of using FQCA is that, unlike FITC, it has a low native fluorescence and a large Stokes shift meaning that background fluorescence from the unreacted tag is

eliminated. FQCA, can self-react and create a fluorescent dimer which can cause background noise.[39] Another point of attractiveness is the large Stokes shift between excitation and emission wavelengths. The Stokes shift cuts down on the background scatter by detecting at a higher wavelength than the incident beam. This raises the signal to noise ratio, which allows for lower LOD. FQCA has been used for the analysis of amino acids and straight chain amines.[39-40] It has been used to achieve detection limits of 0.5 amol of oligosaccharides using on-column LIF.[39-40] The tag has been shown to bind to amines and not amides, which are difficult to tag. Derivatization of amides to amines has been shown by Feng et al.[42-43] using the reaction seen in Scheme 4.2.

Conversion of amides to amines

Unlike their primary amine chemical counterparts, such as amino acids, PFAMs are difficult to tag using conventional fluorophores. Previous work has shown a method using PIFA ((bis-[trifluoro]-acetoxy) iodo benzene) for the conversion of amides to amines.[42-43]

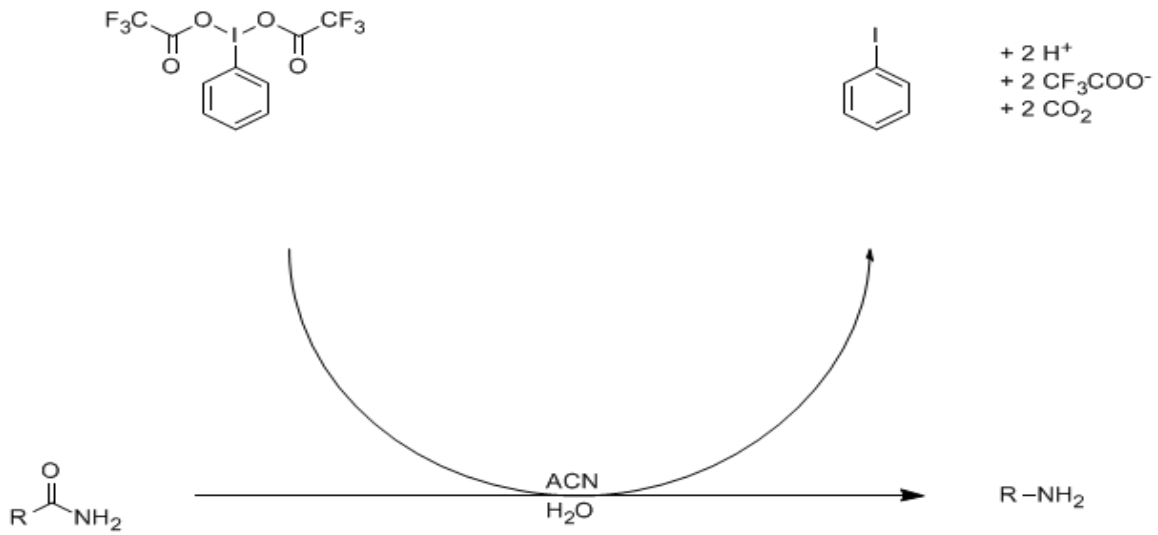

Scheme 4.2: Conversion of a primary amide (R-NH_2O) to a primary amine using PIFA. The reaction is a modified form of the Hofmann rearrangement.

The rearrangement would allow for tagging of the amino group that is left with FQ, an uncharged fluorescent tag that can be used at trace levels for detection of the PFAMs. A method using derivatized primary amines for HPLC separation coupled to fluorescence detection would prove beneficial and allow steps to be taken towards ultra-trace analysis.

Experimental

Reaction Of FQ With Primary Amines

In order to analyze the targeted primary amines, a highly reactive and tightly bound fluorogen was chosen in FQCA. A reaction protocol was needed in order to standardize the sample preparation and minimize error. Since FQCA was originally created to analyze protein and bioactive amines, a starting point for optimizing reaction conditions to maximize yield was provided by Invitrogen. This starting point was tested to give a baseline for optimizing the FQ-amine conditions.

Reactant Preparation Methodology

Weighing out and diluting pure amines, C10-C18 (95-99% purity, Fisher Scientific Pittsburgh, PA), in methanol (MeOH, HPLC grade, Fisher Scientific Pittsburgh, PA), made a stock solution of each of the primary amines. Based on the stock solution concentration, which varied due to limitations in precision weighing balances, a 10 mM working solution was made of each of the amines and a 10 mM total amine concentration solution was made that contained all five of the medium chain fatty amines.

A 10 mM solution of FQ (Invitrogen Grand Island, NY) is prepared by dissolving the 5 milligrams (mg) of the reagent in 2.0 milliliters (mL) of MeOH. The stock solution vial should then be capped and covered in aluminum foil, in order to minimize photo-degradation of the fluorophor. When not in use the covered vial is placed in a desiccator, which is then stored in the -20 ºC freezer. The stock must be thawed completely and then vortexed in order to fully mix the solution before usage.

A 200 milliMolar stock solution of potassium cyanide (KCN) is prepared by dissolving 20 mg of KCN in 1.5 mL of distilled and deionized water (ddH2O), the KCN is then diluted twenty fold to obtain a 10 mM working solution. A 500 µL aliquot of stock solution is diluted in 9.5 mL of ddH2O and is then vortexed. The working solution is then used for the fluorogen reaction.

Mix the chosen ratio, either 1:2:1 or 1:12:10 ratio, depending on which experiment is being performed, of the 10 mM amine mixture, 10 mM FQ solution, and 10 mM KCN solution in a brown vial. Allow the reaction to react for 40 minutes while the brown vial is submerged in a sand bath heated to 40 ºC. Once the reaction is completed it can be removed from the sand bath and it is then used for analysis or dried down for

long-term storage. The FQCA-amine product is actually stable enough that drying down is not required, which allows it to be repeatedly frozen and thawed when needed.

Liquid Chromatography With Fluorescence Detection

Initial experiments were conducted on a Waters 600 HPLC with fluorescence and UV detection. However due to the loss of sensitivity of the fluorescence detector, due to instrument age and cell size, it was quickly decided to use the Breeze HPLC/F system. The Breeze system features a Waters 1525 Binary LC pump. A 4.6 x 150 mm reverse-phase, XTerra®MS, C18, 5 μm column was chosen for the separation based on the previous work of Adams et al. and Carpenter et al. An isocratic mobile phase that was 100% MeOH at a flow rate of 0.8 mL/min was selected as a starting point for the analysis of converted amines. Detection was captured using the Waters 2475 multi-λ fluorescence detector. The excitation wavelength (λex) was set to 488 nm and the emission wavelength (λem) was set to 590 nm, corresponding to the emission and excitation maxima reported in the manufacturer information sheet provided by Invitrogen.

Calibration Curve Of Reacted Amines

In order to calculate the detection (S|N=3) and quantification (S|N=10) limits of the Breeze system a calibration curve was needed. A standard serial dilution was made of the reacted amines by diluting the amines in MeOH to the targeted concentration. The calibration curve concentration range spanned from 1 μM (1×10^{-6} M) down to 1 pM (1×10^{-12} M). The span was chosen based on the targeted concentration of the LIF setup to be used in later tests. The photon multiplier tube (PMT) detector used in LIF saturates at

higher concentration due to its high gain. The diluted reacted amines were loaded onto the LC column in 5 μL injections for analysis. In order to minimize error from late elution or over adsorption, the serial dilution was run in triplicate from low concentration to high and blanks, or runs without an analyte present, were run between each injection. The data was exported from the Breeze system and was analyzed using Igor Pro.

Purification Of Tagged Amine Standards

As part of a senior thesis in the department, Angela Jovanovich, was tasked with purifying a set of standards of FQCA reacted amines. The FQCA reaction was scaled up to provide her with tagged amines in solution. Angela would then be able to take the reaction mixture and hopefully purify out the reacted amine from the unreacted fluorophore. This is done to investigate whether it is possible to minimize side reaction products that occur when unreacted FQCA begins to quench the reacted product. Her work involved using a preparatory reverse phase LC with a sample collector to separate the reacted amines by carbon backbone. Her standard components were then analyzed by running the individual standards and a combined mixture using LC/fluorescence detection.

Results and Discussion

Reaction of FQCA with amines

FQCA was found to be a good fluorogen for amine detection. The fluorogen allowed for a dilution series to test the sensitivity of the Waters Breeze HPLC/Fluorescence system. A 10 micromolar (μM) solution was diluted to a 1 μM

working solution. The 1 µM working solution was used to make the two serial dilutions seen in Figure 4.1 and 4.2 below. One thing that was immediately noticed was a significant peak eluting at the dead volume, which was hypothesized to be FQCA that had reacted with itself. This finding would be the basis for the later work purifying the standards and also the testing of those standards by Mass Spectrometric analysis.

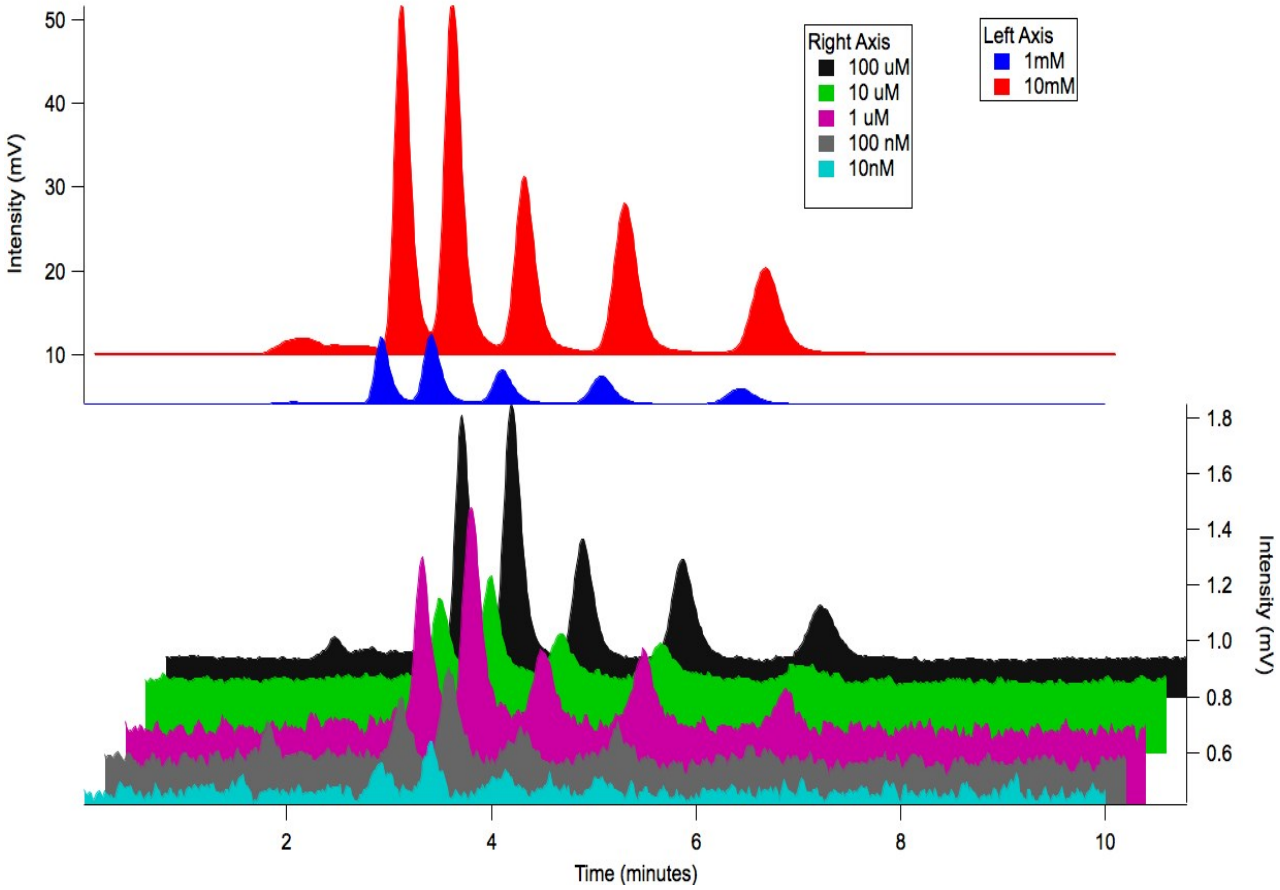

Figure 4.1 Dilution series from 1 micromolar FQCA reacted amines down to 25 nanomolar. The amines present in the solution were C10-18 primary, straight-chained amines.

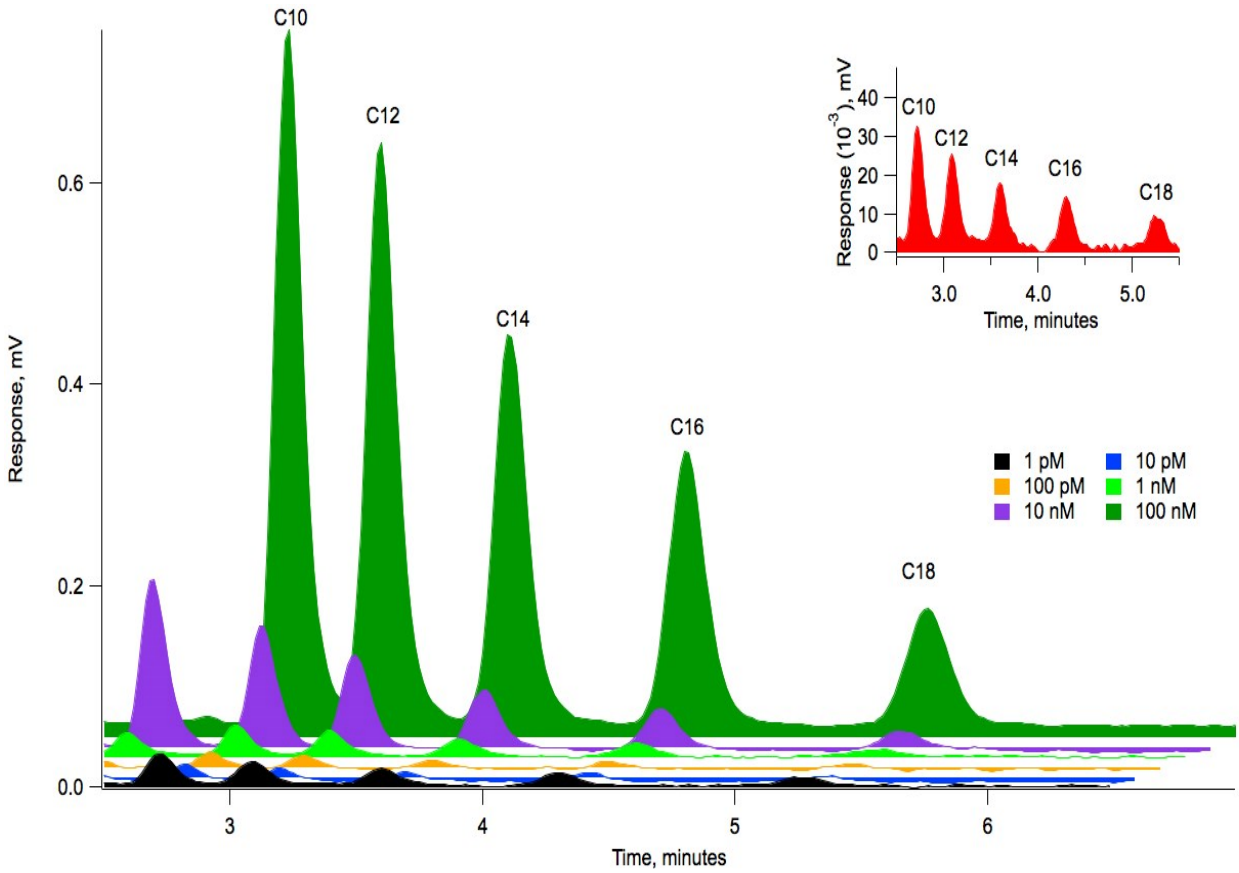

Figure 4.2 Dilution Series from 100 nanomolar to 1 picomolar of the amine mixture described in Figure 4.1. The 1 micromolar solution was depicted on the right axis. The inset depicts the 1 picomolar solution showing that the system is able to clearly see the vey low concentrations being analyzed.

Due to the large magnitude of our analysis (8 orders) calibration curve linearity breaks down at the extrema. However, as can be seen in the calibration curve below (Figure 4.3-6) a dual linearity does exist. In order to optimize linearity a multi-detector setup would be needed. Examples of this can be seen in Dovichi *et al.*[143-147] where the author pushed his system to more than 9 orders of magnitude dynamic range and yoctomole, which is about six molecules, detection limits.

Each of the standards was then purified using a preparatory LC with autosampler and fraction collector. The fractions were then analyzed as individual components and compared to the unpurified reaction product in order to identify the impurities present.

The calibration curves for these individual components can be seen in Figures 4.3 – 4.6. Each of these Figures shows a FQCA reacted amine from C10 – C16 respectively. C18 was found to be too difficult to perform a calibration curve on due to the lack of a significantly measurable reaction product. Adams et al. reported a similar finding using IR fluorescent tags and CE.[22] As anticipated the FQCA allows a fairly wide dynamic range for the analysis of the bioactive lipids. The linearity of the calibration curves opens the door for porting the reaction down to the microfluidic scale.

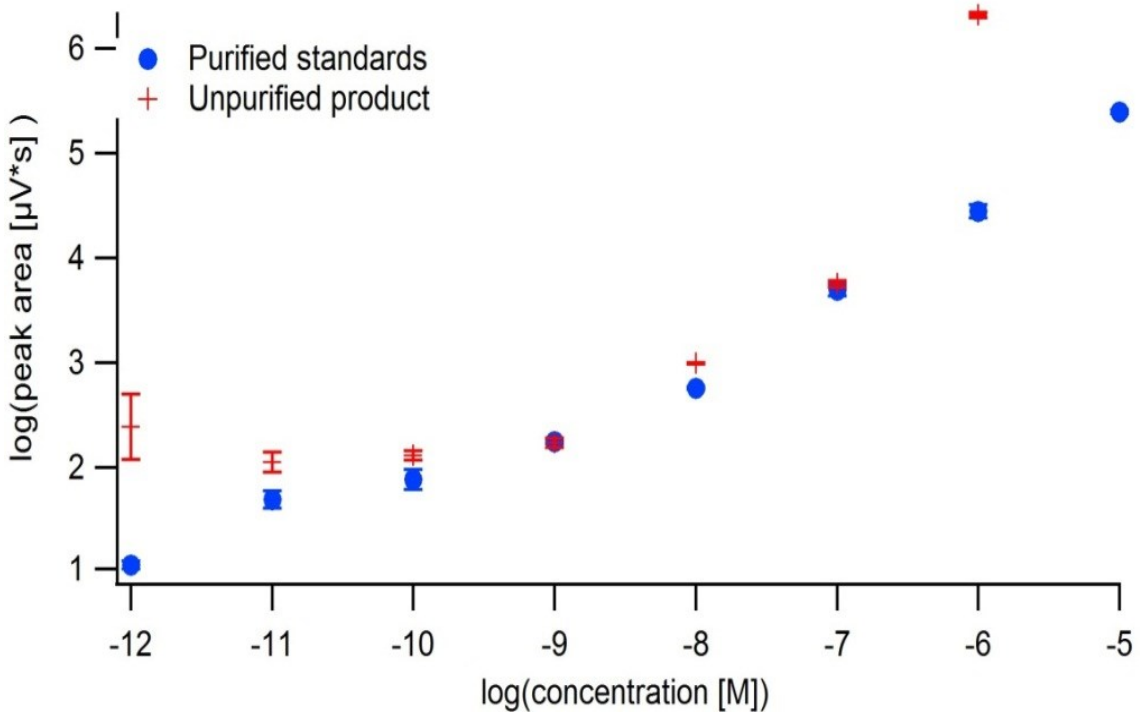

Figure 4.3 Calibration curve on both the purified and unpurified reaction product for C10 amine and FQCA

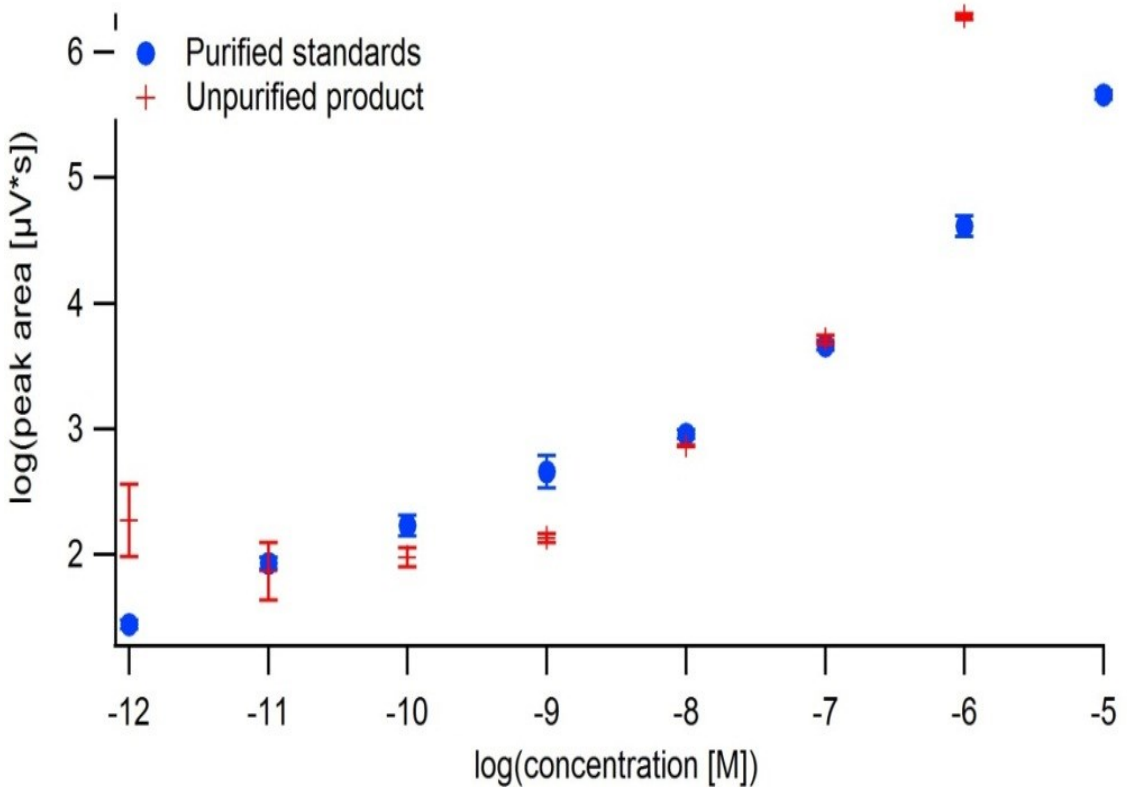

Figure 4.4 Calibration curve on both the purified and unpurified reaction product of C12 amine with FQCA

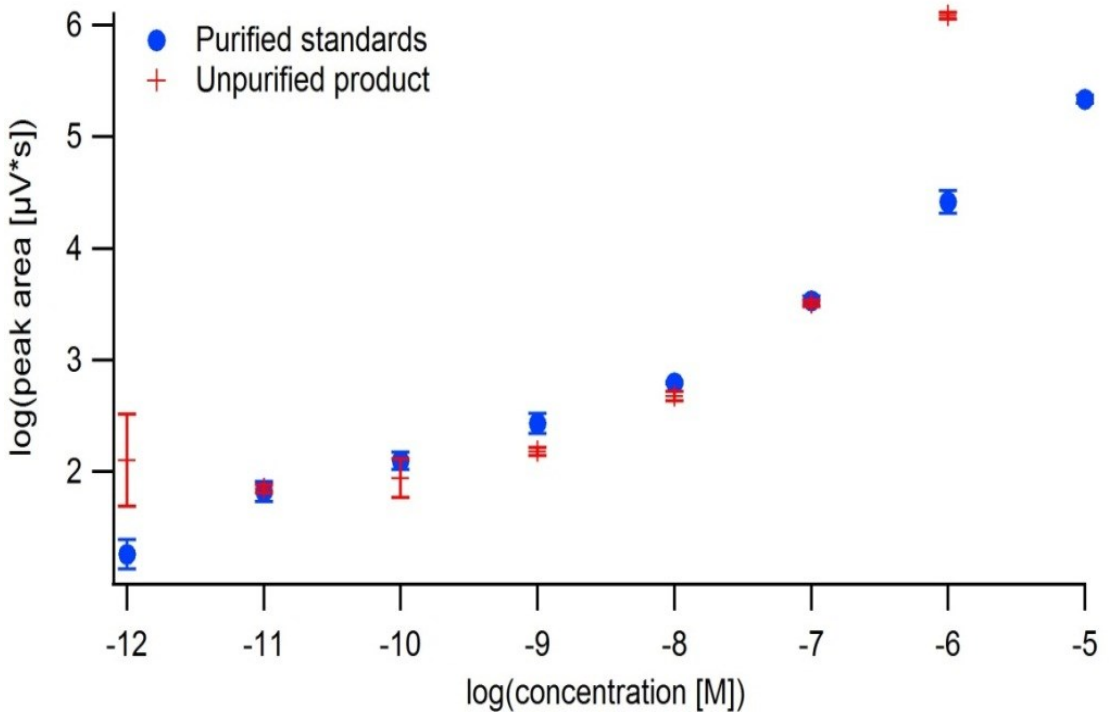

Figure 4.5 Calibration curve on both the purified and unpurified reaction products of C14 amine with FQCA

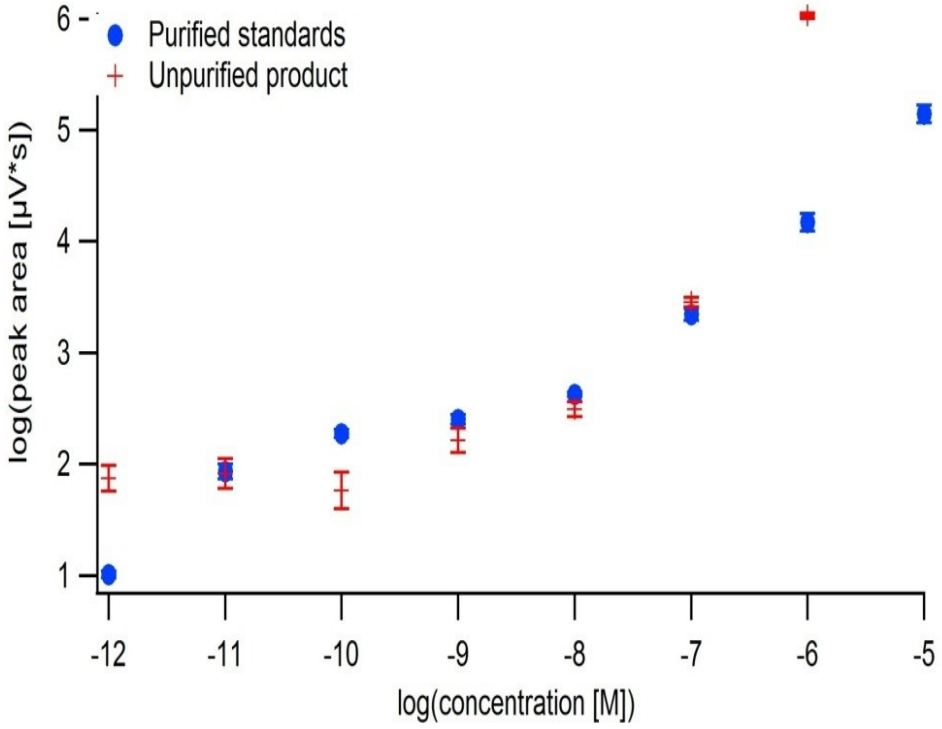

Figure 4.6 Calibration curves on both the purified and unpurified reaction products of C16 amine with FQCA

Following the purification of the standards, it was decided to examine the hypothesis that the leading elution peak was in fact some type of dimerization impurity of FQCA reacting with itself. The literature does not go past speculation on this.[39-40, 148] A sample of the eluted peak was captured using a prep LC's auto-fraction collector. These were then dried down and diluted in pure MeOH to make a stock solution for mass spectrometric analysis. The sample was given to Erin Divito to run on an Agilent electrospray ionization triple quadrupole mass spectrometer (ESI/TQMS). The TQMS would allow for the examination of the molecular structure if a mass peak was found. The spectrum that came back was incredibly convoluted and is not indicative towards any specific product. The lack of structural knowledge or even corroboration with a

hypothesis in the literature presents an interesting path for the researcher who uses FQCA.

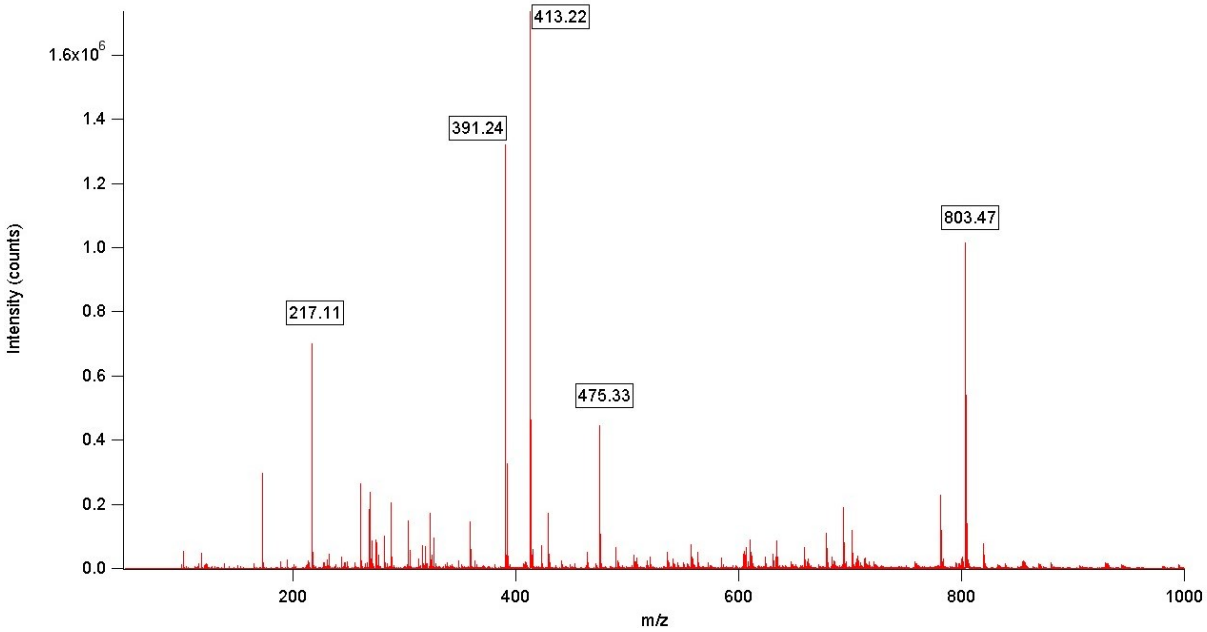

Figure 4.7 Mass Spectrum of unknown reacted FQCA derivative peak

Conclusions

FQCA is shown to be a very good fluorophor for the detection of amines. When the reaction was optimized it outperformed the reactivity reported by Invitrogen. Its Stokes shift and post-reaction increase in quantum efficiency allows for the minimization of noise from the excitation wavelength. It has a wide range of chemical reactivity and detection. Due to its two gain ranges, as long as the researcher maintains separate well-noted calibration curves, a wide range of concentrations can be analyzed using this method. Another very promising aspect of this methodology is that using the HPLC methods shown, detection of tagged amines have been shown as low as 1 pM and lower detection limits are possible. We were unable to push the limit of detection in this study due to the anticipation of moving the analysis to laser induced fluorescence, which would

allow the group to easily look at femtomolar solutions due to the overall sensitivity of LIF setups.

One large take away from this project was that the initial promise of FQCA was large and attractive; the actual usage kept the researcher from fully pushing the limits of the system. FQCA doesn't readily allow for a purified standard calibration curve. In order to attain the shown calibration curves, quite a bit of work and many failed trials and wasted product occurred and further tests were made incredibly difficult. A better fluorogen would be one that can be obtained more readily, in larger amounts, for a more affordable price. FQCA also deteriorates very quickly. It's excitation being in the visible light range means that it is more likely to photobleach when compared to other fluorogens. This and the hypothesized self-reacting potential means that standards and analytes alike can't be reacted and kept long term for future analysis. Once samples are created they must be used, at latest, within 24-48 hours of their reaction. The findings drove the researcher to examine a different fluorogen for analysis as described in the next chapter.

Further Work

The work performed on FQCA shows the attraction that it has as a fluorogen. It has an excitation that falls in the mainline of an Argon ion laser, reacts well with amine groups, and has a high quantum efficiency. While our group has decided to look past FQCA for our purposes, it can easily be adapted by other groups in Chemistry related disciplines from Biochemistry, for cellular staining, to Physical Chemistry, for kinetic studies.

Chapter 5: NDA as a Fluorogenic Tag for the Analysis of Primary Amines in HPLC and Microfluidics Analysis

Background

Fluorescence Detection

Fluorescence is the most sensitive analytical detection technique. A well-tuned laser induced fluorescence detection system can detect yoctomole (10^{-24}) sample load, beating mass spectrometry by at least 3 orders of magnitude. However, unlike mass spectrometry, which can be used for any molecule that can be ionized, fluorescence detection can only be used on molecules that fluoresce. Luckily science has adapted to this roadblock by developing fluorescent tags that can be reacted to non-fluorescing molecules. This allows researchers to analyze targeted molecules using this incredibly sensitive technique. One family of molecules that have been developed for the analysis of bioactive molecules is the ATTO-TAG family.[37],[149] One of these is FQCA, which was discussed previously. FQCA was found to have its limitations and it was desired to examine another potential fluorophor. The researchers decided on a common amino sugar and bioactive amine fluorogen, naphthalene-2,3-dicarboxaldehyde (NDA).[150-151] NDA is molecularly similar to FQCA with similar reactivity. It targets primary amine groups and reacts creating a conjugated pi-bond system as can be seen in the reaction scheme below (Scheme 5.1).

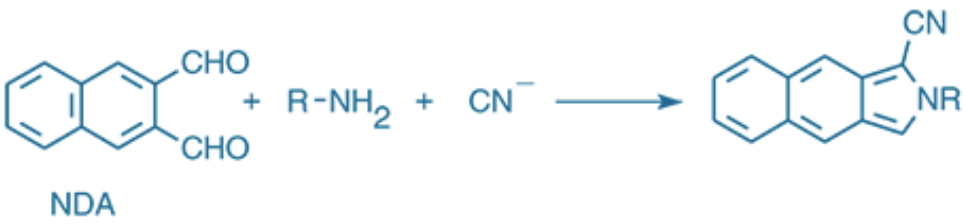

Scheme 5.1. Reaction of NDA with an amine in the presence of KCN to create a fluorescent molecule.

The attractiveness of NDA is that it has a large quantum efficiency enhancement post-reaction with primary amines, meaning that the reacted product will be incredibly fluorescent and very little background fluorescent will be expected from the unreacted fluorogen.[151-153] Unlike the other option for amino-reactivity, OPA, amine adducts of NDA have longer-wavelength spectral characteristics and greater sensitivity than the amine adducts of OPA.[154-156] The stability and detectability of the amine derivatives of NDA are also superior;[4] the detection of glycine with NDA and cyanide is reported to be 50-fold more sensitive than with OPA and 2-mercaptoethanol.[4-5] The limit for electrochemical detection of the NDA adduct of asparagine has been determined to be as low as 36 attomoles[157] (3.6×10^{-17} moles). An optimized procedure that uses NDA for amino acid analysis in microplates has also been examined.[158] NDA has use as a detection molecule for assays of HNO through binding with glutathione.[159] NDA also has a large Stokes shift with an excitation max at 405 nm and an emission max at 493 nm. The attractiveness of a molecule such as NDA is that it would allow for the analysis of ultratrace compounds on the microfluidic chips mentioned previously while unhindered by side-reaction product interferences.[156]

Experimental

HPLC of NDA Reacted Amines

Optimization of Gradient Conditions

In order to build a gradient a suitable percentage slope and time slope must be decided. For the separations a Waters 1525 Binary HPLC Pump using a reverse-phase, XTerra® MS, C18, 5 μm column with an initial isocratic flow of 100% MeOH at a flow rate of 0.8 mL/min was used. Detection was performed using the Waters 2475 Multi-λ fluorescence detector with an excitation wavelength (λ_{ex}) of 405 nm and an emission wavelength (λ_{em}) of 493 nm. Due to the need to separate the C10 and C12 reacted analytes in the chromatograph; a relatively simple gradient was needed. Several time scales were decided (Table 5.1) and an 80:20 MeOH:H_2O to 100:0 MeOH:H_2O solvent ramp was decided in order to allow all impurities and side-reaction products to elute prior to the reacted C10 amine.

Table 5.3 – Gradients for NDA Separations

Initial Time	Gradient Time
0 – 2 minutes at 80:20 MeOH:H_2O	2 – 4 minutes from 80:20 MeOH:H_20 to 100% MeOH
0 – 3 minutes at 80:20 MeOH:H_2O	3 – 5 minutes from 80:20 MeOH:H_20 to 100% MeOH
0 – 3 minutes at 80:20 MeOH:H_2O	3 – 6 minutes from 80:20 MeOH:H_20 to 100% MeOH
0 – 4 minutes at 80:20 MeOH:H_2O	4 – 8 minutes from 80:20 MeOH:H_20 to 100% MeOH

Comparison of NDA and FQ

In order to verify that the NDA fluorogen is appropriate for analysis a full sequence of tests must be undertaken to compare the two fluorogens. The first test that was performed was a fluorescence efficiency test. This is performed by taking identical reaction conditions and analytes and reacting both fluorogens and running them on the Waters Breeze system using an identical separation method. The only analysis difference, other than the fluorogen, is the detection wavelength due to their differing fluorescence. The results should be compared at the same concentration so as to directly compare the signal-to-noise ratio.

An additional test would be to test the lifetime of the reacted amines. FQCA has a very short experimental lifetime compared to NDA, as can be seen in Table 5.2, once it has been reacted with a targeted analyte.

Table 5.4: Fluorogens for Primary Amines Comparison

Fluorogen	Excitation λ	Emission λ	Quantum Yield	Experimental Lifetime
FQCA	488 nm	590 nm	Not Determined	24-48 hours
NDA	405 nm	493 nm	34%[158]	> 2 weeks

The FQCA product degrades and loses fluorescence within 48 hours. The literature on NDA does not report a similar issue as FQCA.[158] Therefore the amines are reacted with NDA per the following SOP and tested at several time increments; immediately after reaction, after 48 hours, after one week. Weighing out and diluting pure amines, C10-C18 (95-99% purity, Fisher Scientific Pittsburgh, PA), in methanol (MeOH, HPLC grade, Fisher Scientific Pittsburgh, PA), made a stock solution of varying

concentrations for each of the primary amines. Based on the stock solution concentration, which varied due to limitations in precision weighing balances, a 10 mM working solution was made of each of the amines and a 10 mM total amine concentration solution was made that contained all five of the medium chain fatty amines.

A 10 mM solution of NDA (Invitrogen Grand Island, NY) was prepared by dissolving the 5 milligrams (mg) of the reagent in 2.0 milliliters (mL) of MeOH in a brown glass vial. The stock solution vial should then be capped and covered in aluminum foil, in order absolutely minimize any light exposure so no photo-degradation of the fluorophor can occur. When not in use the covered vial is placed in a desiccator, which is then stored in a -20 ºC freezer. The stock must be thawed completely and then vortexed in order to fully mix the solution before usage.

A 200 milliMolar stock solution of potassium cyanide (KCN) is prepared by dissolving 20 mg of KCN in 1.5 mL of distilled and deionized water (ddH2O), the KCN is then diluted twenty fold to obtain a 10 mM working solution. A 500 µL aliquot of stock solution is diluted in 9.5 mL of ddH2O and is then vortexed. The working solution is then used for the fluorogen reaction.

For the ratio based experiments, the chosen volumetric ratios depending on which experiment is being performed, were mixed of the 10 mM amine mixture, 10 mM FQ solution, and 10 mM KCN solution in a brown vial (to minimize light exposure). Allow the reaction to react for 40 minutes while the brown vial is submerged in a sand bath heated to 40 ºC. Once the reaction is completed it can be removed from the sand bath and it is then used for analysis or dried down for long-term storage. Unlike the FQCA-amine product, the NDA-amine product is actually stable enough that drying down is not

required, which allows it to be repeatedly frozen and thawed when needed. The reacted products are kept in at least a -20 ºC freezer but ideally would be kept in a -80ºC freezer. If positive results are found, the reacted products will be kept and re-tested at longer time increments.

Optimization of Reaction Conditions

Once the NDA fluorogen has been compared to FQCA an optimization of the reaction conditions will be performed. The ratios used for FQCA (1:10:12 amine:KCN:fluorogen) may not be the optimum conditions for NDA. Several concentration ratios will be tested starting at 1:1:1 and will go up to 1:40:48 the ratios are chosen based on recommendations from the supplier (Invitrogen) and multiples of these ratios. The various reactions will then be run on the Waters Breeze system and then compared.

Calibration Curve

Once the reaction and analysis conditions have been optimized NDA will be evaluated to check for linearity of the NDA reactant over a wide detection range. The hope is that, unlike FQCA, the NDA allows for a wide linear response over the entire detection range of the HPLC/F and μF/LIF. The logarithmic value of the peak areas will be plotted over the logarithmic value of the concentration.

Examination of Impurities

In order to evaluate the impurities, their source was examined. The first part of the analysis will be to run three reactions and compare their products by using HPLC/F. The second part of the analysis is to then analyze the impurities by mass spectrometry to

see whether their mass spectrum matches hypothetical side-reaction products. The mass spectrometric analysis was conducted using an Agilent triple quad mass spectrometer. The spectra were then plotted using IgorPro software.

Droplet Tests

Once the bulk reaction work has been validated and tested, droplet verification can be performed. Like FQCA the NDA reactions will be performed on similar PDMS microchips and analyzed using laser induced fluorescence. NDA, however, has much different excitation and emission wavelengths when compared to FQCA. NDA excites at 405 nm and emits at 493 nm as compared to the 488 and 590 nm excitation and emission maxima of FQCA. This difference caused the researcher to construct a laser induced fluorescence system for NDA using a solid-state diode blue-violet laser. This setup was calibrated and optimized the same way as the argon ion laser as described in chapter 2 of this dissertation. The NDA was then tested on chip for droplet formation at several concentrations. An ultimate detection limit in the picoMolar range is sought so a calibration curve was then run on-chip to test for linearity over the detection scheme.

Results and Discussion

Optimization of Gradient Conditions

Once the test mixture was created, four HPLC runs were set up using an 80:20 methanol:water (MeOH:H_2O) to 100% methanol. The fifth run was a completely isocratic run at 100% MeOH.

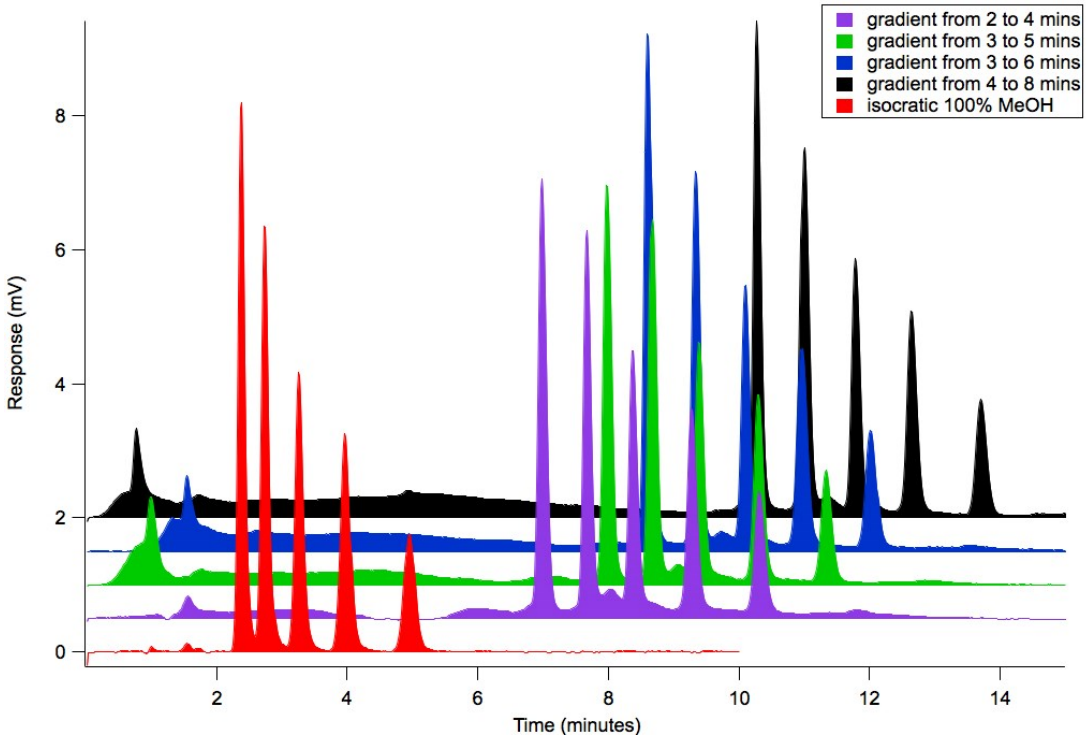

Figure 5.1 Investigation of gradient elution of NDA reacted amines.

As can be seen in Figure 5.1 the isocratic run gave the best elution times, however C10 and C12's peaks overlapping made it less than ideal. This will make it difficult to accurately measure their peak areas. After testing several quick gradients to help aid in baseline separation of the C10 and C12 peaks without causing band broadening on the C16 and C18 peaks, it was decided to use the gradient that ramped from 80:20 to 100:0 MeOH: H_2O from 2-4 minutes, which allowed for baseline separation between the C10 and C12 peaks. This gave baseline resolution while also maintaining the peak shape at higher chain length.

Comparison of NDA and FQ

Upon selecting the gradient method for NDA a direct comparison was needed between FQCA and NDA. In order to verify that NDA is an optimal fluorogen two equivalent reactions were run, one with FQCA and one with NDA. Their resulting

reacted products were run isocratically (i.e. not using the gradient tested above) on the Waters Breeze and their resulting spectra were analyzed using Igor Pro. Immediately apparent was that the NDA actually saturated the detector at the 100 µM concentration used for the tests. The NDA standard was then diluted to 10 µM and retested.

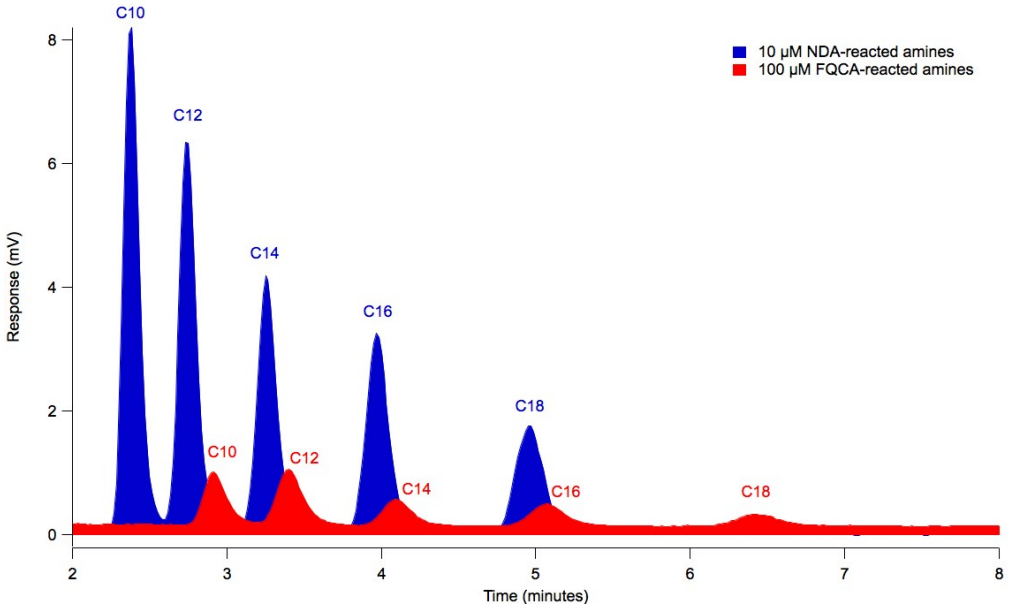

Figure 5.2 Comparison of reacted FQCA with NDA.

As can be seen in Figure 5.2, even at a concentration 10 x lower than the FQCA reacted amines, the NDA presents much cleaner, more intense and faster eluting peaks. These results show that NDA has incredible promise as a highly sensitive fluorescent tag. The fluorescent byproducts of the NDA reaction had incredible signal-to-noise ratios, which were examined more in-depth at low concentrations.

The next test that was examined was whether the NDA-reacted amines would last longer than the 48 hours seen with FQCA. The researcher found the initial testing specifications of the 48-hour window was far too conservative. The testing specifications were altered to test the solution immediately post-reaction, one week after reaction and two weeks after reaction.

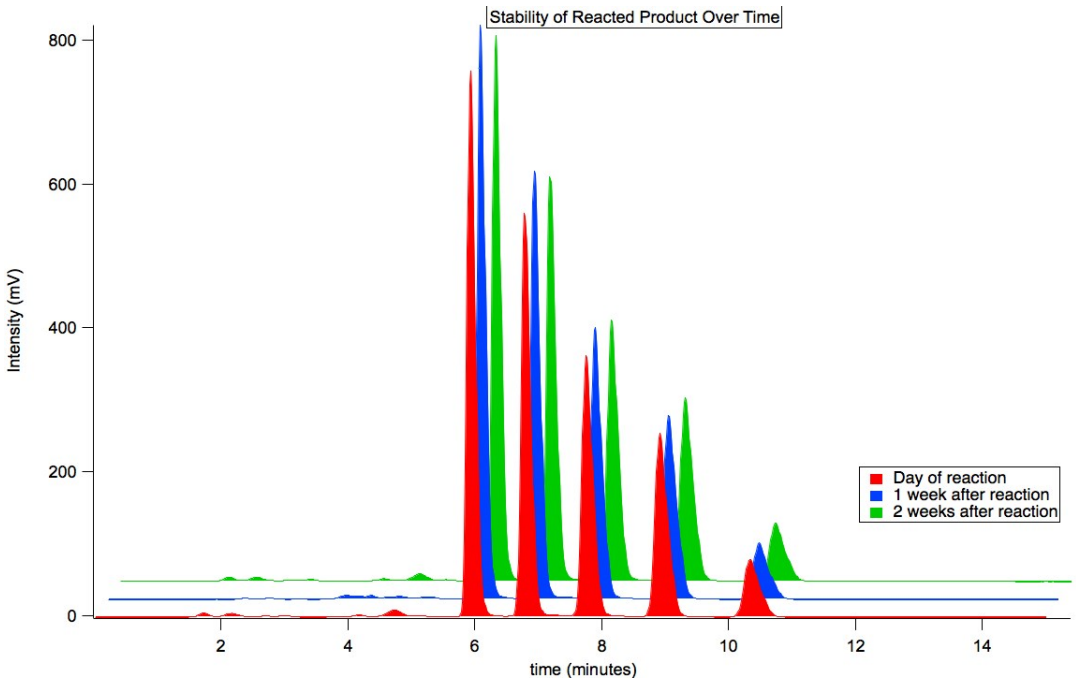

Figure 5.3 Stability of reacted product over time

The stability study showed that the reacted products are stable over many weeks. This allows for the researcher to create standards and have confidence that those standards will still be able to be analyzed later on. This longevity can allow commercial and medical researchers to prepare a large amount of reacted samples, instead of small freshly reacted batches, and due to the lack of impurities and no evidence of side products those researchers can be confident in their reproducibility and statistical significance while allowing for minimization of sample preparation over time. Currently researchers in fluorescence detection have to worry about their samples photobleaching and degrading and thus make new samples every time they make a calibration curve.

Optimization of Reaction Conditions

Once it was decided that NDA would be the reactant of choice the reaction conditions were optimized to verify that they were the best conditions for NDA. Several reactions were created using different ratios of the unreacted fluorogen to potassium cyanide to

amine. The ratios were chosen using manufacturer recommended ratios (which were specified for cell staining, amino sugars, and electrophoresis) and multiples of the FQCA ratio due to its analogous reaction pathway. The following ratios were chosen:

- 1:2:2
- 1:2.5:3
- 1:5:6
- 1:10:12
- 1:15:18
- 1:20:24
- 1:25:30
- 1:30:36
- 1:35:42
- 1:40:48

The reacted products were then run on the Breeze HPLC/F and the resulting spectra were compared for their fluorescent intensity while looking for the absence of impurity peaks. Figure 5.4 A&B shows the results of each of the reacted product separations.

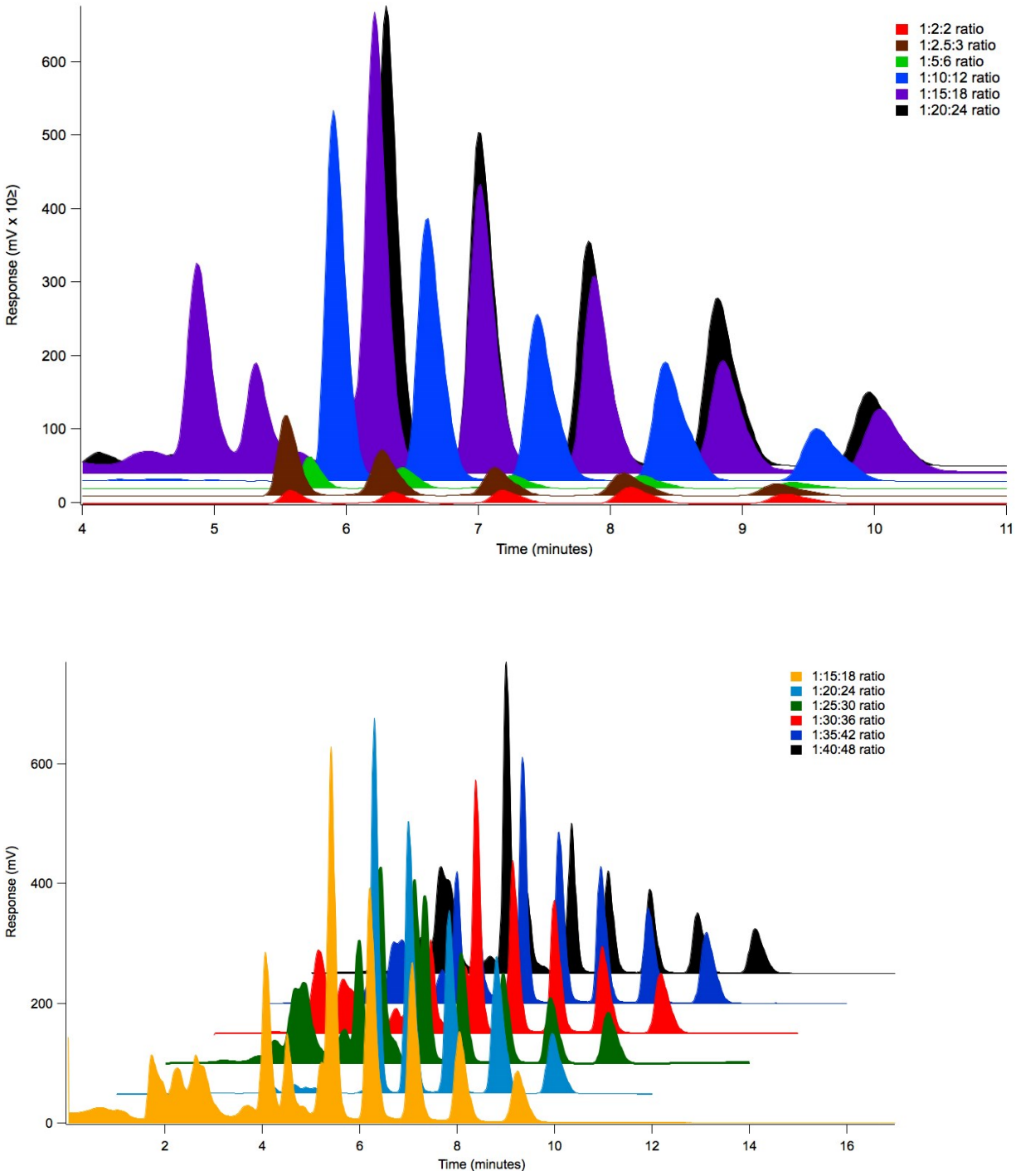

Figure 5.4 Varied concentration ratios for NDA and amine reaction. (A) Shows the lower reactant ratios and (B) shows the higher reactant ratios.

The initial results of the analysis brought forth an interesting observation. The intensity and quantum yield of the NDA outperforms the other fluorogens of its class

once optimized. Manufacturer's literature pointed towards a 1:1:1 ratio for the fluorogen reactions. [1,2] As seen in Chapter 4 and in the data above that reaction ratio is far from ideal let alone good enough to be called optimal. This is probably due to the main use of the ATTO-TAG reagents (FQ and NDA's commercial name) as a cell tag where a high amount of the reagent and KCN would change the nature of the biochemistry trying to be observed. The 1:10:12 ratio that was the optimum for the FQCA reaction was found to be less than optimal for the analogous NDA reaction ratio. The 1:20:24 reaction was found to not only give the most intense spectra, it also had an absence of the impurities that are seen in some of the other reactions with different ratios of the reactants. These impurities need to be avoided in order to push detection limits when the reactions are occurring in a droplet.

Calibration Curve

The bulk reaction mixtures were run through a standard serial dilution calibration curve in order to test of linearity before moving to the droplet phase. The serial dilution started with a 100 μM base reaction that was then diluted over 4 orders of magnitude. These were run on the Breeze system and their peak areas plotted for linearity.

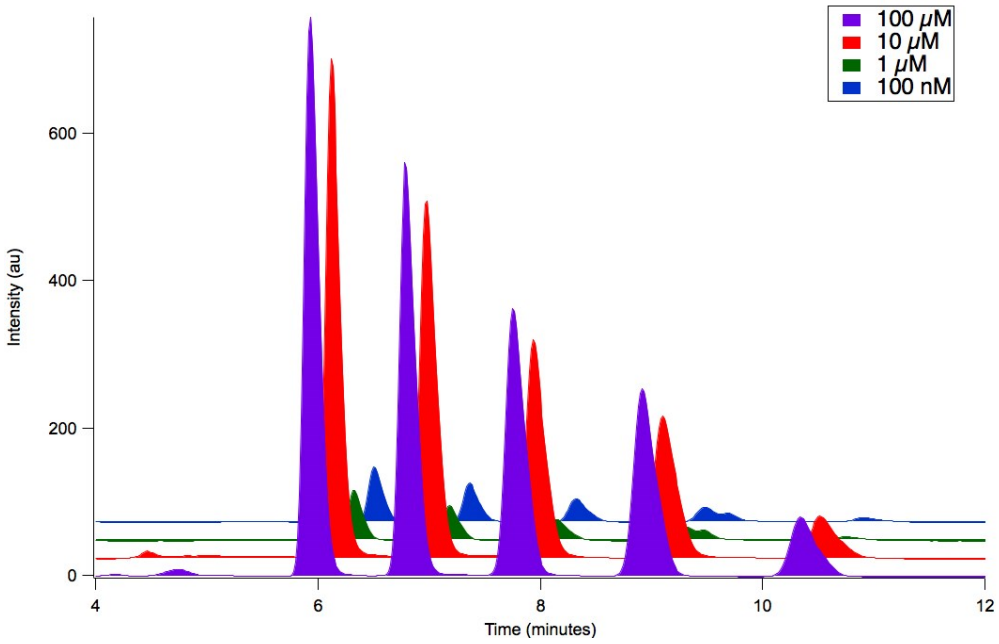

Figure 5.5 NDA-reacted amines calibration curve

The products, even from the very dilute reactions, show very clean spectra on the Breeze. This gives the confidence to take the NDA reacted amines onto the microfluidic chip for detection.

Examination of Impurities

Impurity peaks were found in low concentration reactions during the analytical scale analyses at several of the reaction ratios. To discover the nature of these peaks, mixtures were tested without the amine. This was hoped to give further information on the impurities as seen in the FQCA. In the absence of an amine in the reaction mixture it is hypothesized that the NDA reacts with itself and creates a di-NDA complex.

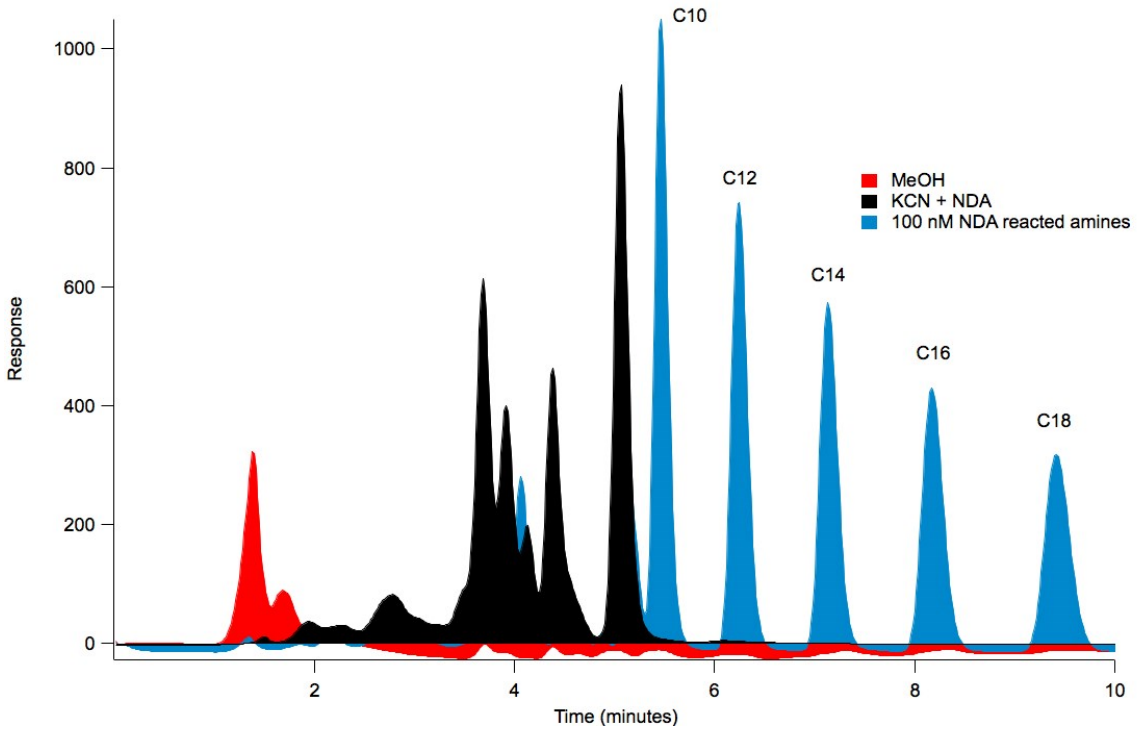

Figure 5.6 Components of the NDA reaction for comparison of impurities

Impurities were separated and purified using prep-LC. The resulting fractions were dried down and reconstituted in 100% MeOH for MS analysis. The mass spectral analysis, as with the FQCA, was inconclusive. It was theorized that there are several side-reactions that could be co-eluting and causing the noisy MS spectra. Since the department did not have access to an MS system that was also coupled to a fluorescence detector it was decided to move forward with the droplet analyses since these peaks are seen in incredibly trace amounts in the 1:20:24 ratio analyses.

Droplet Formation and Detection

After a brief stabilization period (~ 5-10 seconds) droplets can be seen maintaining their average peak area and intensity. Several concentrations were tested to look at the dynamic range of the system. Figure 5.7 shows 1 µM NDA-reacted amines

giving an incredibly strong response, averaging 1.4 Megacounts, which is actually pushing the upper limit, 2 Megacounts, of the detector.

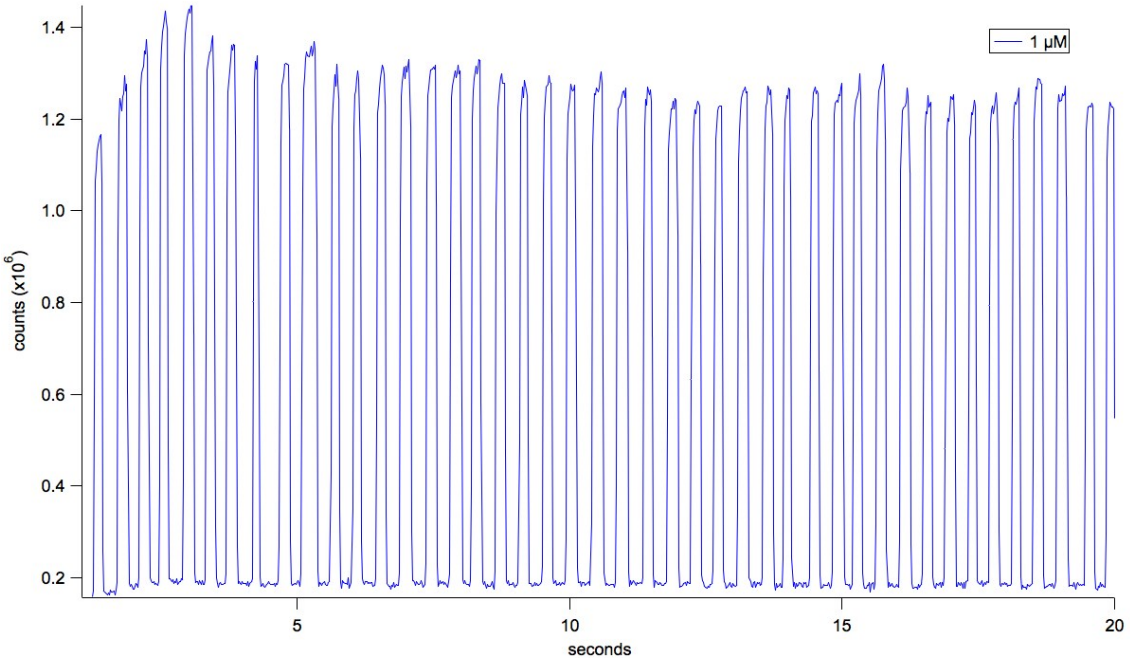

Figure 5.7 1 µM NDA-reacted amine droplets suspended in fluorinated oil.

The next concentration level tested was 10 nM, which shows an average response of 200 kilocounts. This was incredibly promising for our work since we were hoping to hit the low picomolar range and the S/N detection limit (standard is 3 for DL and 10 for QL). It should be noted that we can see the initial "pump on" pulse at the beginning of the spectrum. We found that the reaction was completed before it traversed the detection region and further strengthened reducing the number of turns from 80 to 12 on the chips.

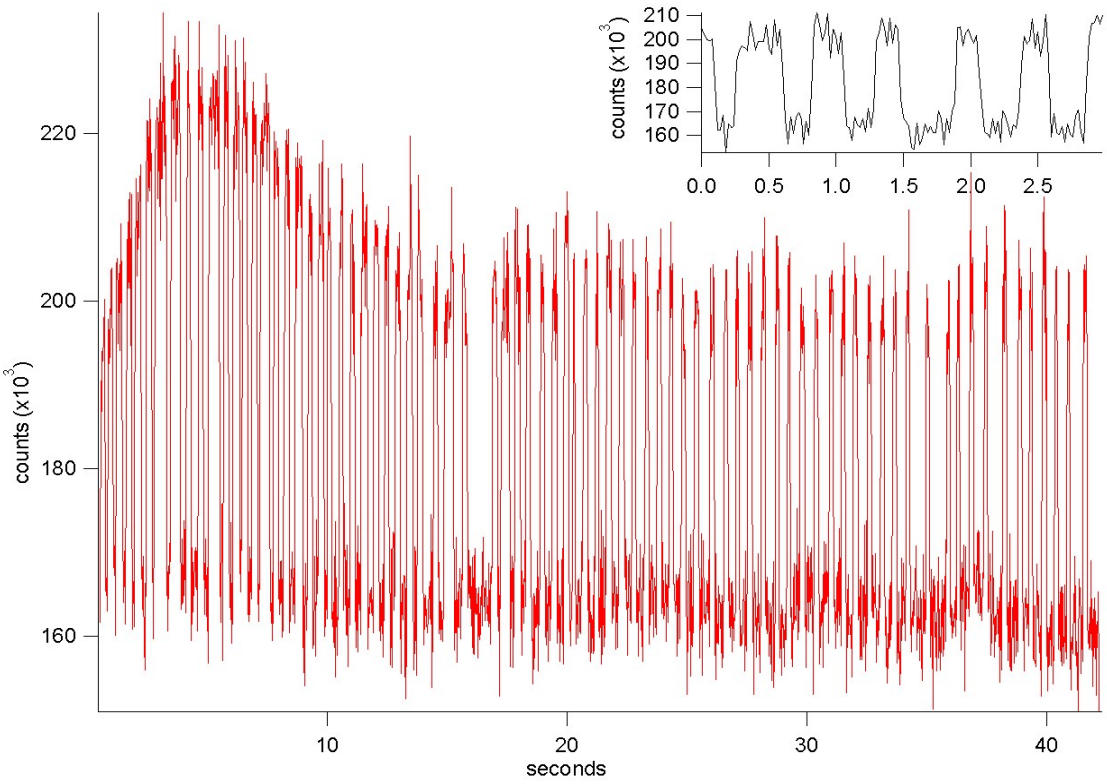

Figure 5.8 10 nM NDA reacted amine droplets. Inset: individual peak details.

Finally we diluted the sample further and ran the system again. For the droplet chronograph seen in Figure 5.9, the NDA-reacted amine concentration is 10 pM. The average response comes in at 3000 counts. The inset in the Figure shows the peak shape in more detail. For all of these chronographs, the collection bin-width was set to 75 msec to allow for detail of the droplet width while still allowing for collection over at least 1 minute of total detection run time.

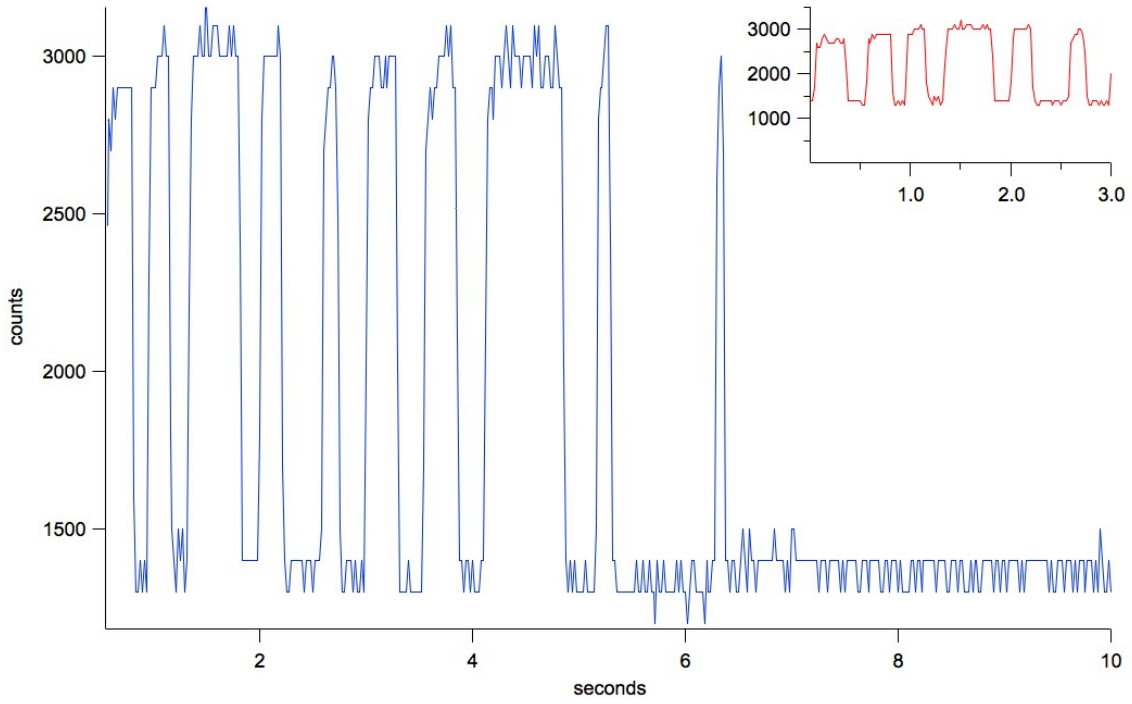

Figure 5.9 10 pM NDA droplets on the microfluidic chip detection platform. Inset: Individual peak detail

Droplet Calibration Curve

Optimized detection settings were used to maximize signal to noise ratio. Average sample load in the 10 pM droplets is 170 femtomoles. At a signal to noise ratio of 95 the system is still about 30x above its detection limit. Calibration gives evidence of a lower detection limit, around 7-10 femtomoles, than expected.

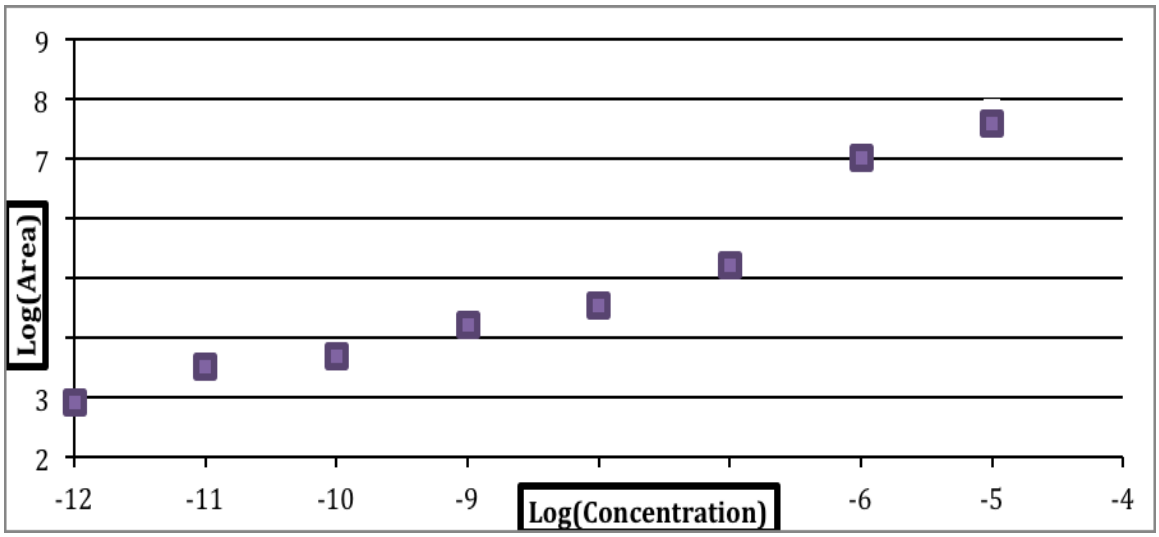

Figure 5.10 Calibration Curve of NDA reacted amines on a microfluidic-LIF platform.

The calibration curve really exposed the potential of the microfluidic chip setup. The researcher was able to detect down to the femtomolar level while still being above the detection limit of the system. This is evidence that carefully choosing a fluorogen and detection scheme can allow for the analysis of ultra trace quantities in a very reproducible and analytical way. Although the dynamic range of the system is impressive at 7 orders of magnitude, the system may be able to be reconFigured with additional detector elements to allow an even broader dynamic range, up to 9 orders of magnitude, as shown by Dovichi et al.[145] Expanding the dynamic range is only attractive if bulk amines (microMolar and higher concentrations) would be in the analysis system. The direction of this work was looking specifically at trace analysis and focused on linearity and detection of the low level concentrations.

Conclusions

Both NDA and FQ provide the opportunity for sensitive analysis due to their large Stokes shift and their increase in quantum efficiency. NDA is more readily obtained than FQ making for a more attractive fluorogen.

Microdroplets have allowed for a minimization of waste while also allowing for a maximization of signal-to-noise ratio at low concentrations. A method for the derivatization of primary fatty amines with NDA has been demonstrated at the analytical and microfluidic scales. Detection limits in the sub-femtomolar concentration region have been achieved and impurities present at low concentrations have been investigated. As seen in the droplet studies a new and separate laser setup was constructed to detect the NDA droplets due to the differences in excitation/emission wavelengths from FQ.

In comparison to the detection limits and reproducibility that is shown with our analysis of NDA-reacted-fatty-amines, recent work by He *et al.*[160] studying Sphingosine-1-phosphate (S1P) (a signaling lipid that regulates numerous cellular processes) explored a parallel analysis using NDA for HPLC/fluorescence analysis. Their detection limit using S1P standards was 20.9 fmol (12.6 nM), and the limit of quantification (LOQ) was 69.6 fmol (41.7 nM). [160]

He *et al.* studies also included quantifying the S1P levels in plasma from human, horse, and mouse. The mean values of S1P being 0.45 in humans, 0.25 in horses, and 1.23 μM in mice. Their results bolster the sensitivity and utility of NDA as a lipid fluorogen.

Further strengthening the use of NDA as a lipid analysis tool is work done by Hao et al. using NDA on a microfluidic chip as a way to label glutathione in mice

hepatocyte[161]. They report a much higher detection level than as seen in He et al. or this work, as they are looking at the milliMolar region and found detection limits in the tens of micromolar region. Our method delivers an even more sensitive detection scheme allowing for sub-femtomole detection.

Future Works

The attractiveness of this project is incredible. As part of the project progresses under Andrew Davic as he expands on the NDA reaction on-chip, a researcher could take a different direction and use this setup and couple it to a separation technique such as liquid chromatography (LC) in order to react the small sample loads from the column and analyze them. We would ideally take the SPE chip seen in chapter 2 and couple it with the segmented flow chip in order to do it all on-chip. Once that was functioning and validated it would be incredibly interesting to add a cell profusion area where you could stress certain cells, such as N18TG2 cells from mice or bovine omentum cells, separate targeted molecules using the SPE chip technology and then run it into the segmented flow for LIF analysis. This could be adapted onto a chip that would be at biggest 3”x3”, which was our starting chip size just for the segmented flow. Another interesting direction to take this is to include a droplet separation chip after the segmented flow that runs into a nanoESI chip. This would allow for both nondestructive and sensitive LIF analysis along with the structural analysis of mass spectrometry.

Works Cited

1. Slashme, Raman Scattering. Creative Commons attribution - Share Alike 3.0: 2007.

2. Nelson, D. L., Cox, M.M., *Lehninger's Principles of Biochemistry*. 4th ed.; W.H. Freeman & Co.: New York, NY, 2002.

3. Fahy, E.; Subramaniam, S.; Brown, H. A.; Glass, C. K.; Merrill, A. H.; Murphy, R. C.; Raetz, C. R. H.; Russell, D. W.; Seyama, Y.; Shaw, W.; Shimizu, T.; Spener, F.; van Meer, G.; VanNieuwenhze, M. S.; White, S. H.; Witztum, J. L.; Dennis, E. A., A comprehensive classification system for lipids. *Journal of Lipid Research* **2005,** *46* (5), 839-861.

4. Guan, X.; Cravatt, B. F.; Ehring, G. R.; Hall, J. E.; Boger, D. L.; Lerner, R. A.; Gilula, N. B., The Sleep-inducing Lipid Oleamide Deconvolutes Gap Junction Communication and Calcium Wave Transmission in Glial Cells. *Journal of Cell Biology* **1997,** *139* (7), 1785-1792.

5. HuidobroToro, J. P.; Harris, R. A., Brain lipids that induce sleep are novel modulators of 5-hydroxytryptamine receptors. *Proceedings of the National Academy of Sciences of the United States of America* **1996,** *93* (15), 8078-8082.

6. Nagai, Y.; Kanfer, J. N., Composition of human cerebrospinal fluid cerebroside. 1971; Vol. 12, pp 143-148.

7. Nakamura, T.; Toyomizu, M., Fatty acid amide in fishes. *Nippon Suisan Gakkaishi* **1970,** *36* (6), 631-7.

8. Nakamura, T.; Toyomizu, M., Gas chromatographic analysis of fatty acid amides in visceral lipid of fin whale. *Nippon Suisan Gakkaishi* **1970,** *36* (2), 192-4.

9. Tan, W.; Yeung, E. S., Monitoring the Reactions of Single Enzyme Molecules and Single Metal Ions. *Analytical Chemistry* **1997,** *69* (20), 4242-4248.

10. Boue, S. M.; Cole, R. B., Confirmation of the structure of lipid A from Enterobacter agglomerans by electrospray ionization tandem mass spectrometry. *Journal of Mass Spectrometry* **2000,** *35* (3), 361-368.

11. Cravatt, B. F.; Lichtman, A. H., The enzymatic inactivation of the fatty acid amide class of signaling lipids. *Chemistry and Physics of Lipids* **2002,** *121* (1-2), 135-148.

12. van der Stelt, M.; Nieuwenhuizen, W. F.; Veldink, G. A.; Vliegenthart, J. F. G., Dioxygenation of N-linoleoyl Amides by Soybean Lipoxygenase-1. *FEBS Letters* **1997,** *411*, 287-290.

13. van der Stelt, M.; Paoletti, A. M.; Maccarrone, M.; Nieuwenhuizen, W. F.; Bagetta, G.; Veldink, G. A.; Finazzi Agro, A.; Vliegenthart, J. F. G., The effect of hydroxylation of linoleoyl amides on their cannabinomimetic properties. *FEBS Letters* **1997,** *415* (3), 313-316.

14. Arafat, E. S.; Trimble, J. W.; Andersen, R. N.; Dass, C.; Desiderio, D. M., Identification of Fatty Acid Amides in Human Plasma. *Life Sciences* **1989,** *45*, 1679-1687.

15. Cartier, R.; Brunette, I.; Hashimoto, K.; Borne, W. M.; Schaff, H., V., Angiogenic Factor: A Possible Mechanism for Neovascularization Produced by Omental Pedicles. *Journal of Thorascic and Cardiovascular Surgery* **1990,** *99* (2), 264-268.

16. Huo, D.; Lu, Y.; Kingston, H. M., Determination and Correction of Analytical Biases and Study on Chemical Mechanisms in the Analysis of Cr(IV) in Soil Samples Using EPA Protocols. *Environmental Science and Technology* **1998,** *32* (21), 3418-3423.

17. Liu, Y.-C.; Wu, S.-N., Block of erg current by linoleoylamide, a sleep-inducing agent, in pituitary GH3 cells. *European Journal of Pharmacology* **2003,** *458* (1-2), 37-47.

18. Lo, J. M., A simple method for sample application in chromatography. *Journal of Chemical Education* **1982,** *59*, 66.

19. Mitchell, C. A.; Davies, M. J.; Grounds, M. D.; McGeachie, J. K.; Crawford, G. J.; Hong, Y.; Chirila, T., Enhancement of Neovascularization in Regenerating Skeletal Muscle by the Sustained Release of Erucamide from a Polymer Matrix. *Journal of Biomaterials Applications* **1996,** *10* (Jan), 230-249.

20. Wakamatsu, K.; Masaki, T.; Itoh, F.; Kondo, K.; Sudo, K., Isolation of Fatty Acid Amide as an Angiogenic Principle from Bovine Mesentery. *Biochemical and Biophysical Research Communications* **1990,** *168* (2), 423-429.

21. Corey, E. J.; Cashman, J. R.; Kantner, S. S.; Wright, S. W., Rationally Designed, Potent Competitive Inhibitors of Leukotriene Biosynthesis. *Journal of the American Chemical Society* **1984,** *106*, 1503-1504.

22. Morisseau, C.; Newman, J. W.; Dowdy, D. L.; Goodrow, M. H.; Hammock, B. D., Inhibition of Microsomal Epoxide Hydrolases by Ureas, Amides, and Amines. *Chemical Research in Toxicology* **2001,** *14* (4), 409-415.

23. Watanabe, T.; Hammock, B. D., Rapid Determination of Soluble Epoxide Hydrolase Inhibitors in Rat Hepatic Microsomes by High-Performance Liquid Chromatography with Electrospray Tandem Mass Spectrometry. *Analytical Biochemistry* **2001,** *299* (2), 227-234.

24. Cravatt, B. F.; Prospero-Garcia, O.; Siuzdak, G.; Giang, D. K.; Henriksen, S. J.; Gilula, N. B.; Boger, D. L.; Lerner, R. A., The Chemistry and Biology of 9(Z)-Octadecenamide (Oleamide): A Sleep-inducing Lipid. In *Sleep and Sleep Disorders: From Molecule to Behavior*, Hayaishi, O.; Inoué, S., Eds. Academic Press: New York, 1997; pp 29-45.

25. Hiley, C. R.; Hoi, P. M., Oleamide: A fatty acid amide signaling molecule in the cardiovascular system ? *Cardiovascular Drug Reviews* **2007,** *25* (1), 46-60.

26. Mechoulam, R.; Ben-Shabat, S., From gan-zi-gun-nu to anandamide and 2-arachidonoylglycerol: the ongoing story of cannabis. *Nat. Prod. Rep.* **1999,** *16* (2), 131-143.

27. Mendelson, W. B.; Basile, A. S., The hypnotic actions of the fatty acid amide, oleamide. *Neuropsychopharmacology* **2001,** *25* (S5), S36-S39.

28. Schmid, H. H. O.; Schmid, P. C.; Kuwae, T., Pathways and mechanisms of anandamide biosynthesis mammalian systems. *Essent. Fatty Acids Eicosanoids, Invited Pap. Int. Congr., 4th* **1998**, 363-371.

29. Hedlund, P. B.; Carson, M. J.; Sutcliffe, J. G.; Thomas, E. A., Allosteric regulation by oleamide of the binding properties of 5-hydroxytryptamine7 receptors. *Biochem. Pharmacol.* **1999,** *58* (11), 1807-1813.

30. Murillo-Rodriguez, E.; Giordano, M.; Cabeza, R.; Henriksen, S. J.; Mendez Diaz, M.; Navarro, L.; Prospero-Garcia, O., Oleamide modulates memory in rats. *Neuroscience Letters* **2001,** *313* (1-2), 61-64.

31. Hibbeln, J. R.; Makino, K. K., Omega-3 fats in depressive disorders and violence: The context of evolution and cardiovascular health. In *Brain Lipids and Disorders in Biological Psychiatry*, Skinner, E. R., Ed. Elsevier Science: Amsterdam, 2002; pp 67-111.

32. Skoog, D. A., Holler, F.J., and Crouch, S.R., *Principle of Instrumental Analysis*. 6th ed.; Thomson Brooks/Cole: Belmont, CA, 2007; p 1039.

33. Mathies, R. A.; Peck, K.; Stryer, L., Optimization of High-Sensitivity Fluorescence Detection. *Analytical Chemistry* **1990,** *62* (17), 1786-1791.

34. Piepmeier, E. H., *Analytical Applications of Lasers*. Wiley-Interscience: New York, 1986; Vol. 87.

35. Omenetto, N., *Analytical Laser Spectroscopy*. John Wiley & Sons: NY, 1979; Vol. 50.

36. Demtroder, W., *Laser Spectroscopy. Basic Concepts and Instrumentation*. Corr. 3rd printing ed.; Springer-Verlag: Berlin, 1981; Vol. 5.

37. Technologies, L., Molecular Probes Handbook. 2010.

38. Beale, S. C.; Savage, J. C.; Wiesler, D.; Wietstock, S. M.; Novotny, M., Fluorescence Reagents for High-Sensitivity Chromatographic Measurements of Primary Amines. *Analytical Chemistry* **1988,** *60* (17), 1765-1769.

39. Beale, S. C.; Hsieh, Y.-Z.; Wiesler, D.; Novotny, M., Application of 3-(2-Furoyl)quinoline-2-carbaldehyde as a Fluorogenic Reagent for the Analysis of Primary Amines by Liquid Chromatography with Laser-induced Fluorescence Detection. *Journal of Chromatography* **1990,** *499*, 579-587.

40. Craig, D. B.; Dovichi, N. J., Multiple Labeling of Proteins. *Analytical Chemistry* **1998,** *70* (13), 2493-2494.

41. Craig, D. B.; Arriaga, E.; Wong, J. C. Y.; Lu, H.; Dovichi, N. J., Life and Death of a Single Enzyme Molecule. *Analytical Chemistry* **1998,** *70* (1), 39A-43A.

42. Feng, L.; Johnson, M. E., Selective Fluorescence Derivatization and Capillary Electrophoretic Separation of Amidated Amino Acids. *Journal of Chromatography A* **1999,** *832*, 211-224.

43. Feng, L. Selective Derivatization and Capillary Electrophoresis Separation of a-Amidated Amino Acids. MS, Duquesne University, Pittsburgh, PA, 1998.

44. Dittrich, P. S.; Tachikawa, K.; Manz, A., Micro total analysis systems. Latest advancements and trends. *Analytical Chemistry* **2006,** *78* (12), 3887-3907.

45. Figeys, D.; Pinto, D., Lab-on-a-chip: A revolution in biological and medical sciences. *Analytical Chemistry* **2000,** *72* (9), 330A-335A.

46. Lee, S.; Jeong, W.; Beebe, D. J., Microfluidic valve with cored glass microneedle for microinjection. *Lab on a Chip* **2003,** *3* (3), 164-167.

47. McClain, M. A.; Culbertson, C. T.; Jacobson, S. C.; Allbritton, N. L.; Sims, C. E.; Ramsey, J. M., Microfluidic devices for the high-throughput chemical analysis of cells. *Analytical Chemistry* **2003,** *75* (21), 5646-5655.

48. Braun, R. M.; Beyder, A.; Xu, J.; Wood, M. C.; Ewing, A. G.; Winograd, N., Spatially resolved detection of attomole quantities of organic molecules localized in picoliter vials using time-of-flight secondary ion mass spectrometry. *Analytical Chemistry* **1999,** *71* (16), 3318-3324.

49. Litborn, E.; Emmer, A.; Roeraade, J., Parallel reactions in open chip-based nanovials with continuous compensation for solvent evaporation. *Electrophoresis* **2000,** *21* (1), 91-99.

50. Litborn, E.; Roeraade, J., Liquid lid for biochemical reactions in chip-based nanovials. *Journal of Chromatography B* **2000,** *745* (1), 137-147.

51. Licklider, L.; Kuhr, W. G.; Lacey, M. P.; Keough, T.; Purdon, M. P.; Takigiku, R., On-Line Microreactors/Capillary Electrophoresis/Mass Spectrometry for the Analysis of Proteins and Peptides. *Analytical Chemistry* **1995,** *67* (22), 4170-4177.

52. Fletcher, P. D. I.; Haswell, S. J.; Pombo-Villar, E.; Warrington, B. H.; Watts, P.; Wong, S. Y. F.; Zhang, X., Micro reactors: principles and applications in organic synthesis. *Tetrahedron* **2002,** *58* (24), 4735-4757.

53. Fletcher, P. D. I.; Haswell, S. J.; Zhang, X., Electrical currents and liquid flow rates in micro-reactors. *Lab on a Chip* **2001,** *1* (2), 115-121.

54. Haswell, S. J.; Middleton, R. J.; O'Sullivan, B.; Skelton, V.; Watts, P.; Styring, P., The application of micro reactors to synthetic chemistry. *Chemical Communications (Cambridge, United Kingdom)* **2001,** (5), 391-398.

55. Watts, P.; Wiles, C.; Haswell, S. J.; Pombo-Villar, E.; Styring, P., The synthesis of peptides using micro reactors. *Chemical Communications (Cambridge, United Kingdom)* **2001,** (11), 990-991.

56. Ottino, J. M., Mixing and Chemical-Reactions - a Tutorial. *Chemical Engineering Science* **1994,** *49* (24A), 4005-4027.

57. Beebe, D. J.; Mensing, G. A.; Walker, G. M., Physics and applications of microfluidics in biology. *Annual Review of Biomedical Engineering* **2002,** *4*, 261-286.

58. Stroock, A. D.; Dertinger, S. K. W.; Ajdari, A.; Mezic, I.; Stone, H. A.; Whitesides, G. M., Chaotic mixer for microchannels. *Science* **2002,** *295* (5555), 647-651.

59. Helen Song, J. D. T. R. F. I., A Microfluidic System for Controlling Reaction Networks in Time. 2003; Vol. 42, pp 768-772.

60. Song, H.; Chen, D. L.; Ismagilov, R. F., Reactions in droplets in microfluidic channels. *Angew. Chem., Int. Ed. FIELD Full Journal Title:Angewandte Chemie, International Edition* **2006,** *45* (44), 7336-7356.

61. Teh, S.-Y.; Lin, R.; Hung, L.-H.; Lee, A. P., Droplet microfluidics. *Lab on a Chip* **2008,** *8* (2), 198-220.

62. Johnson, M. E.; Landers, J. P., Fundamentals and Practice for Ultrasensitive Laser-Induced Fluorescence Detection in Micro-Analytical Systems. *Electrophoresis* **2004**, in press.

63. Tice, J. D.; Song, H.; Lyon, A. D.; Ismagilov, R. F., Formation of droplets and mixing in multiphase microfluidics at low values of the Reynolds and the capillary numbers. *Langmuir* **2003,** *19* (22), 9127-9133.

64. Zhang, L.; Krylov, S. N.; Hu, S.; Dovichi, N. J., Methyl-.beta.-cyclodextrin modified micellar electrokinetic capillary chromatography with laser-induced

fluorescence for separation and detection of phospholipids. *J. Chromatogr., A* **2000,** *894* (1-2), 129-134.

65. Nie, Z. H.; Li, W.; Seo, M.; Xu, S. Q.; Kumacheva, E., Janus and ternary particles generated by microfluidic synthesis: Design, synthesis, and self-assembly. *Journal of the American Chemical Society* **2006,** *128* (29), 9408-9412.

66. Shepherd, R. F.; Conrad, J. C.; Rhodes, S. K.; Link, D. R.; Marquez, M.; Weitz, D. A.; Lewis, J. A., Microfluidic assembly of homogeneous and janus colloid-filled hydrogel granules. *Langmuir* **2006,** *22* (21), 8618-8622.

67. Xu, S. Q.; Nie, Z. H.; Seo, M.; Lewis, P.; Kumacheva, E.; Stone, H. A.; Garstecki, P.; Weibel, D. B.; Gitlin, I.; Whitesides, G. M., Generation of monodisperse particles by using microfluidics: Control over size, shape, and composition. *Angew. Chem.-Int. Edit.* **2005,** *44* (5), 724-728.

68. deMello, A. J., Control and detection of chemical reactions in microfluidic systems. *Nature* **2006,** *442* (7101), 394-402.

69. Janasek, D.; Franzke, J.; Manz, A., Scaling and the design of miniaturized chemical-analysis systems. *Nature* **2006,** *442* (7101), 374-380.

70. Guan, X. J.; Cravatt, B. F.; Ehring, C. R.; Hall, J. E.; Boger, D. L.; Lerner, R. A.; Gilula, N. B., The sleep-inducing lipid oleamide deconvolutes gap junction communication and calcium wave transmission in glial cells. *Journal of Cell Biology* **1997,** *139* (7), 1785-1792.

71. Gutnikov, G., Fatty-Acid Profiles of Lipid Samples. *Journal of Chromatography B-Biomedical Applications* **1995,** *671* (1-2), 71-89.

72. Jacobson, S. C.; Hergenröder, R.; Koutny, L. B.; Ramsey, J. M., High-Speed Separations on a Microchip. *Analytical Chemistry* **1994,** *66* (7), 1114-1118.

73. Fischer-Frühholz, S., The Handling of Nanoliter Samples on a Chip. *American Laboratory* **1998,** *30* (4), 46-51.

74. Footz, T.; Wunsam, S.; Kulak, S.; Crabtree, H. J.; Glerum, D. M.; Backhouse, C. J., Sample purification on a microfluidic device. *Electrophoresis* **2001,** *22* (18), 3868-3875.

75. Fu, A. Y.; Chou, H.-P.; Spence, C.; Arnold, F. H.; Quake, S. R., An integrated microfabricated cell sorter. *Analytical Chemistry* **2002,** *74* (11), 2451-2457.

76. Dittrich, P. S.; Schwille, P., An integrated microfluidic system for reaction, high-sensitivity detection, and sorting of fluorescent cells and particles. *Anal. Chem. FIELD Full Journal Title:Analytical Chemistry* **2003,** *75* (21), 5767-5774.

77. Karlsson, R.; Karlsson, A.; Orwar, O., A Nanofluidic Switching Device. *Journal of the American Chemical Society* **2003,** *125* (28), 8442-8443.

78. Liu, Y.; Garcia, C. D.; Henry, C. S., Recent progress in the development of mu TAS for clinical analysis. *Analyst* **2003,** *128* (8), 1002-1008.

79. El-Ali, J.; Sorger, P. K.; Jensen, K. F., Cells on chips. *Nature* **2006,** *442* (7101), 403-411.

80. Whitesides, G. M., The origins and the future of microfluidics. *Nature* **2006,** *442* (7101), 368-373.

81. Wirth, M. J., Separation Media for Microchips. *Analytical Chemistry* **2007,** *79* (3), 801-808.

82. Miller, E. M.; Wheeler, A. R., A Digital Microfluidic Approach to Homogeneous Enzyme Assays. *Anal. Chem. (Washington, DC, U. S.) FIELD Full Journal Title:Analytical Chemistry (Washington, DC, United States)* **2008,** *80* (5), 1614-1619.

83. Figeys, D.; Pino, D., Lab-on-a-chip: A revolution in biological and medical sciences. *Analytical Chemistry* **2000,** *72* (9), 330A-335A.

84. Lee, J. N.; Park, C.; Whitesides, G. M., Solvent compatibility of poly(dimethylsiloxane)-based microfluidic devices. *Analytical Chemistry* **2003,** *75* (23), 6544-6554.

85. Duffy, D. C.; McDonald, J. C.; Schueller, O. J. A.; Whitesides, G. M., Rapid Prototyping of Microfluidic Systems in Poly(dimethylsiloxane). *Analytical Chemistry* **1998,** *70* (23), 4974-4984.

86. Bean, W. R. a. K., *Semiconductor Integrated Circuit Processing Technology*. Addison-Wesley: Reading, MA, 1990.

87. Jaeger, R., *Introduction to Microelectronic Fabrication*. Addison-Wesley: Reading, MA, 1993.

88. Tech, G. Virtual Clean Room: Photolithography. http://www.ece.gatech.edu/research/labs/vc/theory/photolith.html.

89. Telic Recommended Process for Telic Photomask Blanks. http://www.telic2000.com/.

90. Roper, M. G.; Shackman, J. G.; Dahlgren, G. M.; Kennedy, R. T., Microfluidic chip for continuous monitoring of hormone secretion from live cells using an electrophoresis-based immunoassay. *Analytical Chemistry* **2003,** *75* (18), 4711-4717.

91. Sun, T.; Pawlowski, S.; Johnson, M. E., Highly Efficient Microscale Purification of Glycerophospholipids by Microfluidic Cell Lysis and Lipid Extraction for Lipidomics Profiling. *Analytical Chemistry* **2011,** *83* (17), 6628-6634.

92. Basu, P. J., Mitchell, *The Integrated Approach to Chemistry Laboratory: Selected Experiments*. Destech Publishing: 2009; p 122.

93. Wen, J.; Guillo, C.; Ferrance, J. P.; Landers, J. P., Microfluidic-Based DNA Purification in a Two-Stage, Dual-Phase Microchip Containing a Reversed-Phase and a Photopolymerized Monolith. 2007; Vol. 79, pp 6135-6142.

94. Sun, Y.; Lim, C. S.; Liu, A. Q.; Ayi, T. C.; Yap, P. H., Design, simulation and experiment of electroosmotic microfluidic chip for cell sorting. *Sensors and Actuators, A: Physical* **2007,** *A133* (2), 340-348.

95. Petersson, F.; Aberg, L.; Sward-Nilsson, A. M.; Laurell, T., Free Flow Acoustophoresis: Microfluidic-Based Mode of Particle and Cell Separation. 2007; Vol. 79, pp 5117-5123.

96. Hellman, A. N.; Rau, K. R.; Yoon, H. H.; Bae, S.; Palmer, J. F.; Phillips, K. S.; Allbritton, N. L.; Venugopalan, V., Laser-Induced Mixing in Microfluidic Channels. 2007.

97. Chen, X.; Cui, D. F.; Liu, C. C.; Li, H.; Chen, J., Continuous flow microfluidic device for cell separation, cell lysis and DNA purification. *Analytica Chimica Acta* **2007,** *584* (2), 237-243.

98. Pihl, J.; Sinclair, J.; Karlsson, M.; Orwar, O., Microfluidics for cell-based assays. *Materials Today* **2005,** *8* (12), 46-51.

99. Wu, H.; Wheeler, A.; Zare, R. N., Chemical cytometry on a picoliter-scale integrated microfluidic chip. *Proceedings of the National Academy of Sciences of the United States of America* **2004,** *101* (35), 12809-12813.

100. Sato, K.; Hibara, A.; Tokeshi, M.; Hisamoto, H.; Kitamori, T., Microchip-based chemical and biochemical analysis systems. *Advanced Drug Delivery Reviews* **2003,** *55* (3), 379-391.

101. Ramsey, J. D.; Jacobson, S. C.; Culbertson, C. T.; Ramsey, J. M., High-efficiency, two-dimensional separations of protein digests on microfluidic devices. *Analytical Chemistry* **2003,** *75* (15), 3758-3764.

102. Beard, N. P.; Edel, J. B.; deMello, A. J., Integrated on-chip derivatization and electrophoresis for the rapid analysis of biogenic amines. *Electrophoresis* **2004,** *25* (14), 2363-2373.

103. Gast, F. U.; Dittrich, P. S.; Schwille, P.; Weigel, M.; Mertig, M.; Opitz, J.; Queitsch, U.; Diez, S.; Lincoln, B.; Wottawah, F.; Schinkinger, S.; Guck, J.; Kaes, J.;

Smolinski, J.; Salchert, K.; Werner, C.; Duschl, C.; Jaeger, M. S.; Uhlig, K.; Geggier, P.; Howitz, S., The microscopy cell (MicCell), a versatile modular flowthrough system for cell biology, biomaterial research, and nanotechnology. *Microfluidics and Nanofluidics* **2006,** *2* (1), 21-36.

104. Beer, N. R.; Hindson, B. J.; Wheeler, E. K.; Hall, S. B.; Rose, K. A.; Kennedy, I. M.; Colston, B. W., On-Chip, Real-Time, Single-Copy Polymerase Chain Reaction in Picoliter Droplets. 2007.

105. Song, H.; Bringer, M. R.; Tice, J. D.; Gerdts, C. J.; Ismagilov, R. F., Experimental test of scaling of mixing by chaotic advection in droplets moving through microfluidic channels. *Appl. Phys. Lett. FIELD Full Journal Title:Applied Physics Letters* **2003,** *83* (22), 4664-4666.

106. Song, H.; Ismagilov, R. F., Millisecond kinetics on a microfluidic chip using nanoliters of reagents. *J. Am. Chem. Soc. FIELD Full Journal Title:Journal of the American Chemical Society* **2003,** *125* (47), 14613-14619.

107. Song, H.; Tice, J. D.; Ismagilov, R. F., A Microfluidic System for Controlling Reaction Networks in Time. *Angewante Chemie International Edition* **2003,** *42* (7), 768-772.

108. Teh, S. Y.; Lin, R.; Hung, L. H.; Lee, A. P., Droplet microfluidics. *Lab on a Chip* **2008,** *8* (2), 198-220.

109. Vickers, J. A.; Caulum, M. M.; Henry, C. S., Generation of hydrophilic poly(dimethylsiloxane) for high-performance microchip electrophoresis. *Analytical Chemistry* **2006,** *78* (21), 7446-7452.

110. Mulvaney, S. P.; Cole, C. L.; Kniller, M. D.; Malito, M.; Tamanaha, C. R.; Rife, J. C.; Stanton, M. W.; Whitman, L. J., Rapid, femtomolar bioassays in complex matrices combining microfluidics and magnetoelectronics. *Biosens. Bioelectron. FIELD Full Journal Title:Biosensors & Bioelectronics* **2007,** *23* (2), 191-200.

111. Noblitt, S. D.; Kraly, J. R.; VanBuren, J. M.; Hering, S. V.; Collett, J. L.; Henry, C. S., Integrated membrane filters for minimizing hydrodynamic flow and filtering in microfluidic devices. *Analytical Chemistry* **2007,** *79* (16), 6249-6254.

112. Whitmore, C. D.; Essaka D Fau - Dovichi, N. J.; Dovichi, N. J., Six orders of magnitude dynamic range in capillary electrophoresis with ultrasensitive laser-induced fluorescence detection. (1873-3573 (Electronic)).

113. Ramsay, L. M.; Dickerson, J. A.; Dada, O.; Dovichi, N. J., Femtomolar Concentration Detection Limit and Zeptomole Mass Detection Limit for Protein Separation by Capillary Isoelectric Focusing and Laser-Induced Fluorescence Detection. *Analytical Chemistry* **2009,** *81* (5), 1741-1746.

114. Britz-McKibbin, P.; Markuszewski, M. J.; Iyanagi, T.; Matsuda, K.; Nishioka, T.; Terabe, S., Picomolar analysis of flavins in biological samples by dynamic pH junction-sweeping capillary electrophoresis with laser-induced fluorescence detection. *Analytical Biochemistry* **2003,** *313* (1), 89-96.

115. Britz-McKibbin, P.; Terabe, S., On-line preconcentration strategies for trace analysis of metabolites by capillary electrophoresis. *Journal of Chromatography, A* **2003,** *1000* (1-2), 917-934.

116. Ben-Shabat, S.; Fride, E.; Sheskin, T.; Tamiri, T.; Rhee, M.-H.; Vogel, Z.; Bisogno, T.; De Petrocellis, L.; Di Marzo, V.; Mechoulam, R., An entourage effect: inactive endogenous fatty acid glycerol esters enhance 2-arachidonoyl-glycerol cannabinoid activity. *Eur. J. Pharmacol.* **1998,** *353* (1), 23-31.

117. Di Marzo, V., 'Endocannabinoids' and other fatty acid derivatives with cannabimimetic properties: biochemistry and possible physiopathological relevance. *Biochimica et Biophysica Acta* **1998,** *1392* (2-3), 153-175.

118. Di Marzo, V., Biosynthesis and inactivation of endocannabinoids: relevance to their proposed role as neuromodulators. *Life Sci.* **1999,** *65* (6/7), 645-655.

119. De Petrocellis, L.; Melck, D.; Bisogno, T.; Di Marzo, V., Endocannabinoids and fatty acid amides in cancer, inflammation and related disorders. *Chemistry and Physics of Lipids* **2000,** *108* (1-2), 191-209.

120. Walker, J. M.; Krey, J. F.; Chu, C. J.; Huang, S. M., Endocannabinoids and related fatty acid derivatives in pain modulation. *Chemistry and Physics of Lipids* **2002,** *121* (1-2), 159-172.

121. Burstein, S. H.; Huang, S. M.; Petros, T. J.; Rossetti, R. G.; Walker, J. M.; Zurier, R. B., Regulation of anandamide tissue levels by N-arachidonylglycine. *Biochemical Pharmacology* **2002,** *64* (7), 1147-1150.

122. Kozak, K. R.; Crews, B. C.; Morrow, J. D.; Wang, L.-H.; Ma, Y. H.; Weinander, R.; Jakobsson, P.-J.; Marnett, L. J., Metabolism of the Endocannabinoids, 2-Arachidonylglycerol and Anandamide, into Prostaglandin, Thromboxane, and Prostacyclin Glycerol Esters and Ethanolamides. *Journal of Biological Chemistry* **2002,** *277* (47), 44877-44885.

123. Di Marzo, V.; Bisogno, T.; De Petrocellis, L.; Melck, D.; Martin, B. R., Cannabimimetic fatty acid derivatives: the anandamide family and other "endocannabinoids". *Current Medicinal Chemistry* **1999,** *6* (8), 721-744.

124. Fezza, F.; Dillwith, J. W.; Bisogno, T.; Tucker, J. S.; Di Marzo, V.; Sauer, J. R., Endocannabinoids and related fatty acid amides, and their regulation, in the salivary glands of the lone star tick. *Biochimica et Biophysica Acta* **2003,** *1633* (1), 61-67.

125. Cravatt, B. F.; Prospero-Garcia, O.; Suizdak, G.; Gilula, N. B.; Henriksen, S. J.; Boger, D. L.; Lerner, R. A., Chemical Characterization of a Family of Brain Lipids That Induce Sleep. *Science* **1995,** *268* (09Jun), 1506-1509.

126. Huidobro-Toro, J. P.; Harris, R. A., Brain Lipids That Induce Sleep are Novel Modulators of 5-hydroxytryptamine Receptors. *Proceedings of the National Academy of Sciences of the USA* **1996,** *93*, 3.

127. Lerner, R. A.; Siuzdak, G.; Prospero-Garcia, O.; Henriksen, S. J.; Boger, D. L.; Cravatt, B. F., Cerebrodiene: A Brain Lipid Isolated from Sleep-deprived Cats. *Proceedings of the National Academy of Sciences of the USA* **1994,** *91*, 9505-9508.

128. Bisogno, T.; Sepe, N.; De Petrocellis, L.; Mechoulam, R.; Di Marzo, V., The Sleep Inducing Factor Oleamide Is Produced by Mouse Neuroblastoma Cells. *Biochemical and Biophysical Research Communications* **1997,** *239* (2), 473-479.

129. Bezuglov, V. V.; Bobrov, M. Y.; Archakov, A. V., Bioactive Amides of Fatty Acids. *Biochemistry (Moscow)* **1998,** *63* (1), 22-30.

130. Ritenour-Rodgers, K. J.; Driscoll, W. J.; Merkler, K. A.; Merkler, D. J.; Mueller, G. P., Induction of Peptidylglycine a-Amidating Monooxygenase in $N_{18}TG_2$ Cells: A Model for Studying Oleamide Biosynthesis. *Biochemical and Biophysical Research Communications* **2000,** *267* (2), 521-526.

131. Stewart, J. M.; Boudreau, N. M.; Blakely, J. A.; Storey, K. B., A comparison of oleamide in the brains of hibernating and non-hibernating Richardson's ground squirrel (Spermophilus richardsonii) and its inability to bind to brain fatty acid binding protein. *Journal of Thermal Biology* **2002,** *27* (4), 309-315.

132. Nicholson, R. A.; Zheng, J.; Ganellin, C. R.; Verdon, B.; Lees, G., Anesthetic-like interaction of the sleep-inducing lipid oleamide with voltage-gated sodium channels in mammalian brain. *Anesthesiology* **2001,** *94* (1), 120-128.

133. Hanus, L. O.; Fales, H. M.; Spande, T. F.; Basile, A. S., A Gas Chromatographic-Mass Spectral Assay for the Quantitative Determination of Oleamide in Biological Fluids. *Analytical Biochemistry* **1999,** *270* (1), 159-166.

134. Hanus, L.; Gopher, A.; Almog, S.; Mechoulam, R., Two New Unsaturated Fatty Acid Ethanolamides in Brain That Bind to the Cannabinoid Receptor. *Journal of Medicinal Chemistry* **1993,** *36*, 3032-3034.

135. Verdon, B.; Zheng, J.; Nicholson, R. A.; Ganellin, C. R.; Lees, G., Stereoselective modulatory actions of oleamide on GABAA receptors and voltage-gated Na+ channels in vitro: a putative endogenous ligand for depressant drug sites in CNS. *Br. J. Pharmacol.* **2000,** *129* (2), 283-290.

136. Lees, G.; Edwards, M. D.; Hassoni, A. A.; Ganellin, C. R.; Galanakis, D., Modulation of GABAA receptors and inhibitory synaptic currents by the endogenous

CNS sleep regulator cis-9,10-octadecenoamide (cOA). *Br. J. Pharmacol.* **1998,** *124* (5), 873-882.

137. Laposky, A. D.; Homanics, G. E.; Basile, A.; Mendelson, W. B., Deletion of the GABAA receptor b3 subunit eliminates the hypnotic actions of oleamide in mice. *NeuroReport* **2001,** *12* (18), 4143-4147.

138. Irmisch, G.; Schlafke, D.; Gierow, W.; Herpertz, S.; Richter, J., Fatty acids and sleep in depressed inpatients. *Prostaglandins Leukotrienes and Essential Fatty Acids* **2007,** *76* (1), 1-7.

139. Kanao, Y.; Ohba, Y.; Kita, Y.; Nojima, H., Oleamide derivatives potently inhibit the spontaneous metastasis of mouse melanoma BL6 cells. *Clinical & Experimental Metastasis* **2007,** *24* (4), 307-307.

140. Ohba, Y.; Kanao, Y.; Morita, N.; Fujii, E.; Hohrai, M.; Takatsuji, M.; Hirose, H.; Miura, D.; Watari, A.; Yutsudo, M.; Zhao, H.; Yabuta, N.; Ito, A.; Kita, Y.; Nojima, H., Oleamide derivatives suppress the spontaneous metastasis by inhibiting connexin 26. *International Journal of Cancer* **2007,** *121* (1), 47-54.

141. Fowler, C. J.; Jonsson, K. O.; Tiger, G., Fatty acid amide hydrolase: biochemistry, pharmacology, and therapeutic possibilities for an enzyme hydrolyzing anandamide, 2-arachidonoylglycerol, palmitoylethanolamide, and oleamide. *Biochemical Pharmacology* **2001,** *62* (5), 517-526.

142. Bezuglov, V.; Bobrov, M.; Gretskaya, N.; Gonchar, A.; Zinchenko, G.; Melck, D.; Bisogno, T.; Di Marzo, V.; Kuklev, D.; Rossi, J. C.; Vidal, J. P.; Durand, T., Synthesis and biological evaluation of novel amides of polyunsaturated fatty acids with dopamine. *Bioorganic & Medicinal Chemistry Letters* **2001,** *11* (4), 447-449.

143. Chen, D. Y.; Adelhelm, K.; Cheng, X. L.; Dovichi, N. J., A simple laser-induced fluorescence detector for sulforhodamine 101 in a capillary electrophoresis system: Detection limits of 10 yoctomoles or six molecules. *Analyst (Cambridge, United Kingdom)* **1994,** *119* (2), 349-52.

144. Cheng, Y. F.; Dovichi, N. J., Subattomole amino acid analysis by laser-induced fluorescence: the sheath flow cuvette meets capillary zone electrophoresis. In *Laser Techniques in Luminescence Spectroscopy*, Vo Dinh, T.; Eastwood, D., Eds. ASTM: 1990; Vol. 1066, p 151.

145. Dada, O. O.; Essaka, D. C.; Hindsgaul, O.; Palcic, M. M.; Prendergast, J.; Schnaar, R. L.; Dovichi, N. J., Nine Orders of Magnitude Dynamic Range: Picomolar to Millimolar Concentration Measurement in Capillary Electrophoresis with Laser Induced Fluorescence Detection Employing Cascaded Avalanche Photodiode Photon Counters. *Analytical Chemistry* **2011,** *83* (7), 2748-2753.

146. Waldron, K. C.; Dovichi, N. J., Sub-Femtomole Determination of Phenylthiohydantoin-Amino Acids: Capillary Electrophoresis and Thermooptical Detection. *Analytical Chemistry* **1992,** *64* (13), 1396-1399.

147. Wu, S.; Dovichi, N. J., High-sensitivity fluorescence detector for fluorescein isothiocyanate derivatives of amino acids separated by capillary zone electrophoresis. *Journal of Chromatography* **1989,** *480*, 141-155.

148. Lee, I. H.; Pinto, D.; Arriaga, E. A.; Zhang, Z.; Dovichi, N. J., Picomolar Analysis of Proteins Using Electrophoretically Mediated Microanalysis and Capillary Electrophoresis with Laser lnduced Fluorescence Detection. *Analytical Chemistry* **1998,** *70* (21), 4546-4548.

149. Chen, D. Y.; Dovichi, N. J., Yoctomole detection limit by laser-induced fluorescence in capillary electrophoresis. *Journal of Chromatography, B: Biomedical Sciences and Applications* **1994,** *657* (2), 265-9.

150. Kettler, C. N.; Sepaniak, M. J., Pulsed-Laser Photothermal Refraction Detection in Capillary Liquid Chromatography. *Analytical Chemistry* **1987,** *59*, 1733-1736.

151. De Montigny, P.; Stobaugh, J. F.; Givens, R. S.; Carlson, R. G.; Srinivasachar, K.; Sternson, L. A.; Higuchi, T., Naphthalene-2,3-dicarboxyaldehyde/cyanide ion: a rationally designed fluorogenic reagent for primary amines. *Analytical Chemistry* **1987,** *59* (8), 1096-1101.

152. Sano, A.; Takezawa, M.; Takitani, S., Spectrofluorimetric determination of cyanide in blodd and urine with naphthalene-2,3-dialdehyde and taurine. *Analytica Chimica Acta* **1989,** *225* (0), 351-358.

153. Sano, A.; Takimoto N Fau - Takitani, S.; Takitani, S., High-performance liquid chromatographic determination of cyanide in human red blood cells by pre-column fluorescence derivatization.

154. Roach Mc Fau - Harmony, M. D.; Harmony, M. D., Determination of amino acids at subfemtomole levels by high-performance liquid chromatography with laser-induced fluorescence detection. (0003-2700 (Print)).

155. Ndube, N.; van der Westhuizen, L.; Green, I. R.; Shephard, G. S., HPLC determination of fumonisin mycotoxins in maize: A comparative study of naphthalene-2,3-dicarboxaldehyde and o-phthaldialdehyde derivatization reagents for fluorescence and diode array detection. *Journal of Chromatography B* **2011,** *879* (23), 2239-2243.

156. Givens, R. S.; Jencen, D. A.; Riley, C. M.; Stobaugh, J. F.; Chokshi, H.; Hanaoka, N., Chemiluminescence: A sensitive and versatile method for analyte detection. *Journal of Pharmaceutical and Biomedical Analysis* **1990,** *8* (6), 477-491.

157. Kennedy, R.; Oates, M.; Cooper, B.; Nickerson, B.; Jorgenson, J., Microcolumn separations and the analysis of single cells. *Science* **1989,** *246* (4926), 57-63.

158. Bantan-Polak, T.; Kassai, M.; Grant, K. B., A Comparison of Fluorescamine and Naphthalene-2,3-dicarboxaldehyde Fluorogenic Reagents for Microplate-Based Detection of Amino Acids. *Analytical Biochemistry* **2001,** *297* (2), 128-136.

159. Johnson, G. M.; Chozinski, T. J.; Salmon, D. J.; Moghaddam, A. D.; Chen, H. C.; Miranda, K. M., Quantitative Detection of Nitroxyl Upon Trapping with Glutathione and Labeling with a Specific Fluorogenic Reagent. *Free Radical Biology and Medicine* **2013,** *63* (0), 476-484.

160. He, X.; Huang, C.-L.; Schuchman, E. H., Quantitative analysis of sphingosine-1-phosphate by HPLC after napthalene-2,3-dicarboxaldehyde (NDA) derivatization. *Journal of Chromatography B* **2009,** *877* (10), 983-990.

161. Hao, M.; Liu, R.; Zhang, H.; Li, Y.; Jing, M., Detection of glutathione within single mice hepatocytes using microfluidic chips coupled with a laser-induced fluorescence system. *Spectrochimica Acta Part A: Molecular and Biomolecular Spectroscopy* **2014,** *125* (0), 7-11.